

LIBRARY OF CONGRESS

NEW YORK

1917

1-2

1-2

1-2

LIBRARY OF CONGRESS

JKA  
703  
66.1  
MPN  
LIBRARY



703  
66.1  
MPN

REPORT ON GEOLOGICAL SURVEY

OF

ANTA GORDA

BRAZIL

JICA LIBRARY



1030080(4)

PHASE IV

MAY 1984

JAPAN INTERNATIONAL COOPERATION AGENCY

METAL MINING AGENCY OF JAPAN

国際協力事業団	
受入 月日 '84.6.28	703
登録No. 10441	66.1
	MPN

マイクロ  
フィシニ作文

## PREFACE

The government of Japan, in response to the request of the Government of the Federative Republic of Brazil, decided to conduct collaborative mineral exploration in Anta Gorda area in southern Brazil and entrusted its execution to Japan International Cooperation Agency (JICA) and Metal Mining Agency of Japan (MMAJ).

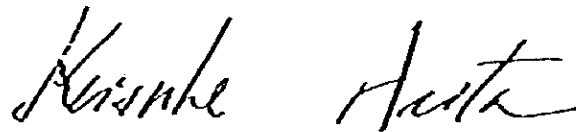
Between 26 August, 1983 and 7 February, 1984, Metal Mining Agency of Japan dispatched a survey team headed by Mr. Tsuyoshi SUZUKI to conduct geological survey, geophysical survey and drilling survey of the Phase IV of the project.

The survey had been accomplished under close cooperation with the Government of the Federative Republic of Brazil and its various authorities.

This report is a compilation of the survey of the Phase IV, and after the completion of the project the consolidated report will be submitted to the Government of the Federative Republic of Brazil.

We wish to express our appreciation to all of the organizations and members who bore the responsibility for the project; the Government of the Federative Republic of Brazil Departamento Nacional da Produção Mineral, and other authorities and the Embassy of Japan in Brazil.

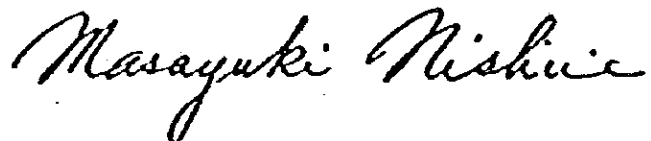
March 1984



Keisuke Arita

President

Japan International Cooperation Agency



Masayuki Nishiie

President

Metal Mining Agency of Japan

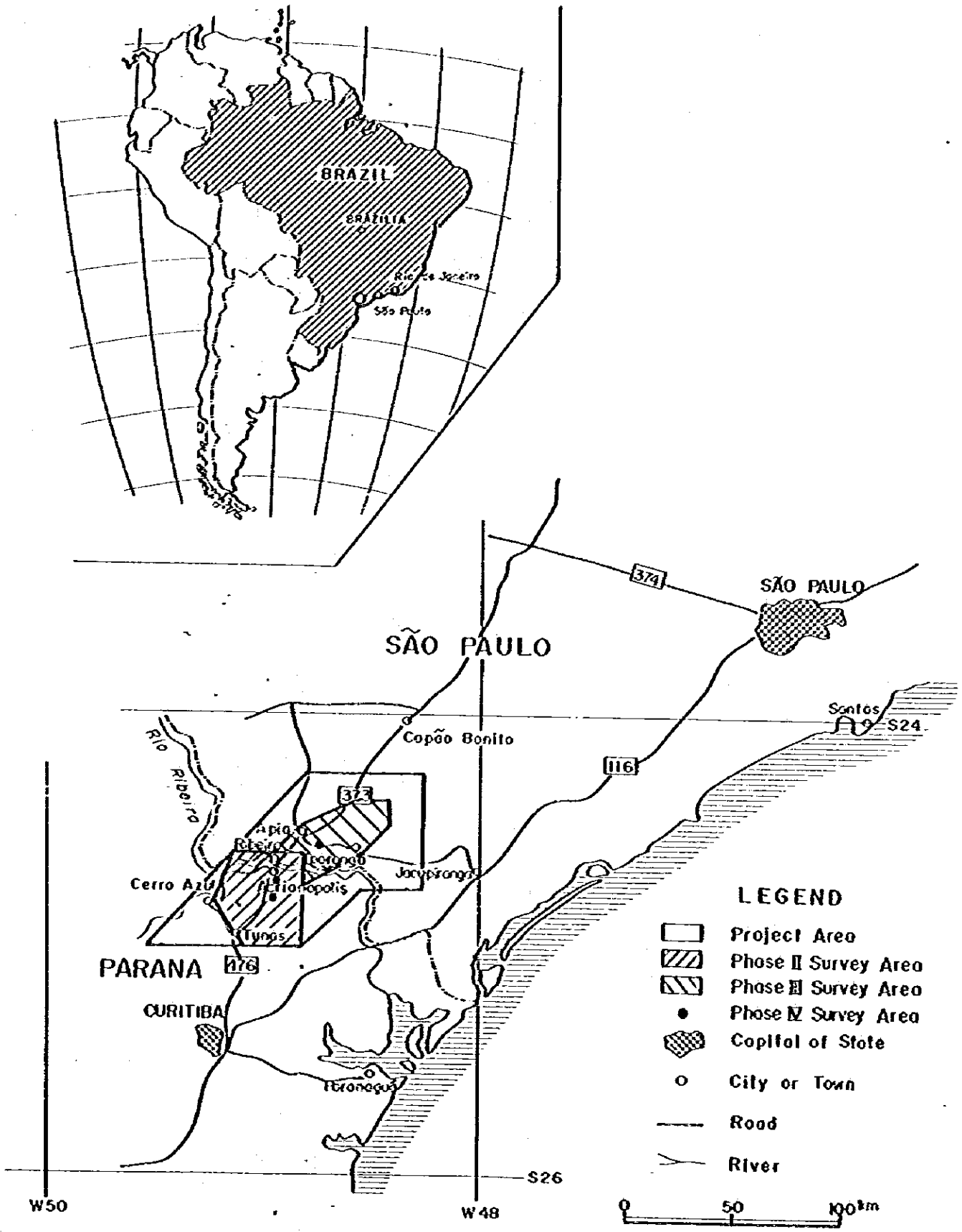
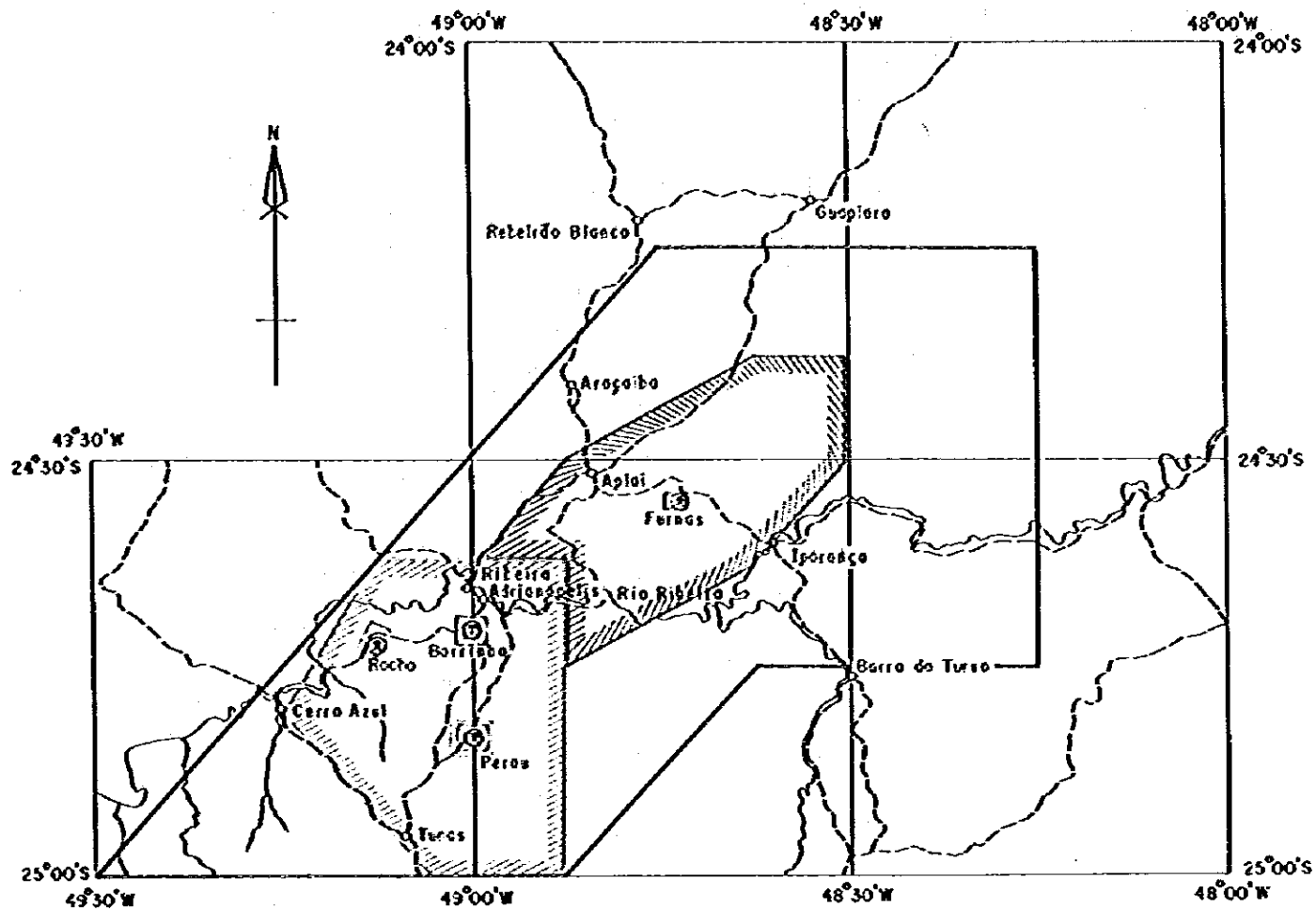
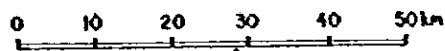


Fig. 1 Location Map of the Project Area



**LEGEND**

- |  |                         |  |              |
|--|-------------------------|--|--------------|
|  | Phase I Surveyed Area   |  | City or Town |
|  | Phase II Surveyed Area  |  | Road         |
|  | Phase III Surveyed Area |  | River        |
|  | Phase IV Surveyed Area  |  |              |



**Fig. 2 Location Map of the Surveyed Area**

## CONTENTS

Preface

Location Map of the Project Area

Contents

Abstract

### GENERAL REMARKS

<b>Chapter 1</b>	<b>Introduction</b> .....	<b>1</b>
<b>1-1</b>	<b>Purpose and Scope of the Survey</b> .....	<b>1</b>
<b>1-2</b>	<b>Substance of the Survey</b> .....	<b>2</b>
<b>1-3</b>	<b>Organization of the Survey Team</b> .....	<b>2</b>
<b>1-4</b>	<b>Previous Surveys</b> .....	<b>3</b>
<b>1-5</b>	<b>Reference</b> .....	<b>5</b>
<b>Chapter 2</b>	<b>Comprehensive Investigation</b> .....	<b>7</b>
<b>2-1</b>	<b>Geological Survey (Fumas Area)</b> .....	<b>7</b>
<b>2-1-1</b>	<b>Geology</b> .....	<b>7</b>
<b>2-1-2</b>	<b>Ore Deposits</b> .....	<b>7</b>
<b>2-2</b>	<b>Geophysical Survey</b> .....	<b>8</b>
<b>2-3</b>	<b>Drilling Survey</b> .....	<b>10</b>
<b>2-3-1</b>	<b>Perau Area</b> .....	<b>10</b>
<b>2-3-2</b>	<b>Barrinha Area</b> .....	<b>10</b>
<b>Chapter 3</b>	<b>Conclusion and Recommendation</b> .....	<b>12</b>
<b>3-1</b>	<b>Conclusion</b> .....	<b>12</b>
<b>3-2</b>	<b>Recommendation</b> .....	<b>12</b>



## PARTICULARS

### PART I GEOLOGICAL SURVEY

<b>Chapter 1</b>	<b>Geology</b> .....	<b>14</b>
1-1	Summary of Geology .....	14
1-2	Stratigraphy .....	14
1-2-1	AHIL <sub>2</sub> Member .....	14
1-2-2	AHIS <sub>2</sub> Member .....	15
1-2-3	AHIL <sub>3</sub> Member .....	16
1-2-4	AHIS <sub>3</sub> Member .....	19
1-3	Metamorphism .....	20
1-4	Geologic Structure .....	20
<b>Chapter 2</b>	<b>Ore Deposit</b> .....	<b>22</b>
2-1	Summary of the Ore Deposit .....	22
2-2	Shape and Scale of Ore Deposit .....	22
2-3	Assemblage of Ore Minerals .....	23
2-4	Result of Analysis of Ore .....	25
2-5	Relationship between Geologic Structure and Ore Deposits .....	26
2-6	Relationship between Geologic Structure and Result of Geophysical Survey .....	26
2-7	Future Exploration .....	27

### PART II GEOPHYSICAL SURVEY

<b>Chapter 1</b>	<b>Outline of Survey</b> .....	<b>28</b>
1-1	Purpose of Survey .....	28
1-2	Survey Area .....	28
1-3	Survey Period .....	28
<b>Chapter 2</b>	<b>SIP and IP Methods</b> .....	<b>29</b>
2-1	Survey Method .....	29
2-1-1	Method of Measurement .....	29
2-1-2	Survey Line .....	29
2-1-3	Procedure for Data Analysis .....	30
2-2	Results of SIP Method .....	31

2-2-1	Pseudosection .....	31
2-2-2	Laboratory Measurement .....	33
2-3	Results of IP Method .....	34
2-3-1	Pseudosection .....	35
2-3-2	Plan Map .....	35
2-3-3	In-Situ Measurement .....	36
2-3-4	Model Simulation .....	37
2-4	Relation of Results with Geology .....	37
2-5	Summary .....	38

### PART III DRILLING SURVEY

<b>Chapter 1</b>	<b>Summary of Drilling .....</b>	<b>40</b>
1-1	Purpose of Survey .....	40
1-2	Summary of Operation .....	40
1-3	Logging and Analysis Work .....	41
<b>Chapter 2</b>	<b>Diamond Drilling Work .....</b>	<b>42</b>
2-1	Access Road for Transporting Equipment and Materials .....	42
2-2	Location of Drill Holes .....	42
2-3	Preparation Work .....	42
2-4	Drilling Work .....	43
2-5	Measurement of Drill Holes .....	46
<b>Chapter 3</b>	<b>Geology and Mineralization of Drill Holes .....</b>	<b>49</b>
3-1	AG-04 .....	49
3-2	AG-05 .....	50
3-3	AG-06 .....	51
3-4	AG-B1 .....	52
3-5	AG-B2 .....	53
<b>Chapter 4</b>	<b>Discussion of Drilling Survey .....</b>	<b>55</b>
4-1	Perau Area .....	55
4-2	Barrinha Area .....	56

### APPENDICES

## LIST OF ILLUSTRATIONS

- Fig. 1                    Location Map of the Project Area
- Fig. 2                    Location Map of the Surveyed Area
- Fig. 1-1                 Geological Map and Geological Profile of Furnas Area
- Fig. 1-2                 Generarized Stratigraphic Columnar Section in Furnas Area
- Fig. 1-3                 Principal Stress Field Analysis of Fracture and Strain Ellipsoid of Planar Schistosity Plane of Furnas Area
- Fig. 1-4                 Geological Sketch of Trench, Open Pit and Underground in Furnas Area
- Fig. 1-5                 Geotectonic Profile of Phase III Surveyed Area
- Fig. II-1                Location Map of IP & SIP Survey Lines
- Fig. II-2                Schematic Diagram of SIP Measurement
- Fig. II-3                Flow Chart of IP & SIP Data Analysis
- Fig. II-4                SIP Pseudosection of Apparent Resistivity [0.125 Hz] (Line-FA, FD, FI)
- Fig. II-5                SIP Pseudosection of Raw Phase [0.125 Hz] (Line-FA, FD, FI)
- Fig. II-6                SIP Pseudosection of 3-Point Decoupled Phase [0.125-0.375-0.625 Hz] (Line-FA, FD, FI)
- Fig. II-7                SIP Pseudosection of Percent Frequency Effect [0.125-1.0 Hz] (Line-FA, FD, FI)
- Fig. II-8                Classification of Phase Spectral Type
- Fig. II-9-1~3            Phase Spectrum (Line-FA, FD, FI)
- Fig. II-10-1~3         Magnitude Spectrum (Line-FA, FD, FI)
- Fig. II-11-1~3         Cole-Cole Diagram (Line-FA, FD, FI)
- Fig. II-12               Location Map of Collected Rock Samples
- Fig. II-13               Block Diagram for Laboratory Measurement
- Fig. II-14               Typical Phase Spectral Type of Dolomite
- Fig. II-15               Typical Phase Spectral Type of Limestone
- Fig. II-16               Typical Phase Spectral Type of Sericite Schist
- Fig. II-17-1~11        IP Pseudosection (Line-FA~FK)
- Fig. II-18-1            Correlation of PFE (0.3 - 3.0 Hz) with PFE (0.375 - 3.0 Hz)
- Fig. II-18-2            Correlation of AR (0.125 Hz) with AR (3.0 Hz)
- Fig. II-19-1~3         Plan Map of Apparent Resistivity [N=1, 3, 5]
- Fig. II-20-1~3         Plan Map of Percent Frequency Effect [N=1, 3, 5]

Fig. II-21	Pseudosection of Percent Frequency Effect in Test Lines (T-1, T-2, T-3)
Fig. II-22-1~2	Model Simulation (Line-FA, FD)
Fig. II-23	Example of Prism Model for IP Response
Fig. II-24	Interpretation Map in Furnas Area
Fig. III-1	Location Map of the Drilling Holes
Fig. III-2-1~5	Progress Record of Diamond Drilling
Fig. III-3-1	Geological Profile for AG-04 and AG-03
Fig. III-3-2	Geological Profile for AG-05, AG-01 and AG-02
Fig. III-3-3	Geological Profile for AG-06
Fig. III-3-4	Geological Profile for AG-06, AG-01 and AG-04
Fig. III-3-5	Geological Profile for AG-B1
Fig. III-3-6	Geological Profile for AG-B2
Table I-1	Assay Results of Ores of Furnas Area
Table II-1	Specification and Instruments
Table II-2	List of Survey Lines
Table II-3	Results of Laboratory Measurement in Rock Samples
Table II-4	Ranges of PFE and AR
Table II-5	Results of In-Situ Measurement
Photo A-1	Microphotograph of Thin Section
Photo A-2	Microphotograph of Polished Section
Table A-1	List of Mines and Showings in Furnas Area
Table A-2	Microscopic Observations (Thin Section) (Geological Survey)
Table A-3-1	Microscopic Observations (Polished Section) (Geological Survey)
Table A-3-2	Microscopic Observations (Polished Section) (Logging Core)
Table A-4	Assay Results of Drilling Core
Fig. A-1	Raw Phase Pseudosection of Each Frequency (Line-FA, FD, FI)
Plate I-1	Geological Map and Geological Profile of Furnas Area (1:10,000)
Plate I-2	Location Map of the Rock and Ore Samples of Furnas Area (1:10,000)
Plate I-3	Distribution Map of the Mines and Showings in Furnas Area (1:10,000)
Plate III-1~3	Columnar Section of Core Logs in Perau Area (1:200)
Plate III-2~2	Columnar Section of Core Logs in Barrinha Area (1:200)

## ABSTRACT

The geological survey in the Anta Gorda region in the Federative Republic of Brazil was initiated by basic geological survey in Phase I (the first year) and the detail of survey was successively raised, having resulted in to discover a new ore deposit in the Perau area in the third year. On the other hand, because it was made clear that the survey of detail was to be needed in the Barrinha area as well as the Furnas area, the period of survey was extended for one year to continue it in Phase IV (the fourth year).

In Phase IV, detailed geological survey and geophysical survey in the Furnas area and drill survey in the Perau area and the Barrinha area were performed.

### 1. Geological Survey

As the result of the survey, the meta-sedimentary rocks and carbonate rocks in the Precambrian Açungui formation which constitute the geology of the Furnas area were subdivided and detailed stratigraphy was established, which resulted in to make clear the position of ore-bearing horizon.

The geologic structure of the surveyed area is positioned in the middle of the Serra Manduri anticline and the Calabouço syncline, showing homoclinal structure with general strike of  $N60^{\circ}E$  and general dip of  $45^{\circ}NW$ .

The host rocks of the Furnas deposit are limestone and dolomite in the lower part of the  $AlHL_3$  member, and the ore deposits are vein-type (to irregular massive-type and pipe-like-type) silver bearing lead deposit emplaced along the fractures of NE–SW system and E–W system being harmonious with the bedding plane, forming the ore shoots at the interesection of the fractures of those two systems.

Although some showings were newly discovered in the ore-bearing horizon, the geophysical survey (IP and SIP methods) resulted in to detect no anomalous zone to indicate the existence of notable ore deposit.

It is thought therefore that the detailed survey and geochemical survey are effective for the future exploration in the area including the surrounding part.

### 2. Geophysical Survey

As the result of geophysical survey (IP and SIP), the apparent resistivity shows a pattern well reflecting the geologic structure.

Although the IP anomalous zones were detected along the beds in the hanging wall and

footwall of the ore-bearing horizon, no marked anomalous zone was detected within the ore-bearing horizon.

The reason of no anomaly being detected is thought that a scale of ore deposit would be so small and a current flow from the surface be interrupted by the ore-bearing horizon with an unporizable and compact rock.

### **3. Drill Survey**

The drill survey of Phase IV was conducted in the Perau area and the Barrinha area.

As the result of drill survey in the Perau area, the conditions of the surrounding part of the stratiform lead and zinc deposit discovered in Phase III was made clear, especially the north-western limit and the southern limit of the deposit were confirmed.

As the result of drill survey in the Barrinha area, the relationship between the SIP anomalous zone to the southeast of the Quatro deposit and the IP anomalous zone in the northeastern part of the surveyed area, and the geologic structure as well as the area to be explored in future, were made clear.

## GENERAL REMARKS

## CHAPTER 1 INTRODUCTION

### I-1 Purpose and Scope of the Survey

The natural resources development collaborative mineral exploration in the Federative Republic of Brazil was started in 1980 by the Metal Mining Agency of Japan (MMAJ) as the request of the Japan International Cooperation Agency (JICA).

In October, 1980, the MMAJ agreed a Scope of Work in relation to the project with Departamento Nacional Da Produção Mineral (DNPM).

Many small lead ore deposits have been found in two states of São Paulo and Parana in the southeastern part of Brazil and various studies have been conducted in the past, but as yet there is still no widespread acceptance about the relationship between mineralization and geologic structure or igneous activity as well as the ore genesis.

In the survey of JICA and MMAJ, the basic survey was started in the first year, and the survey have been gradually raised the accuracy year by year to clarify the geologic structure and the genesis of ore deposits, and in the third year, a new ore deposit was discovered in the west of the Perau deposit.

Based on the Scope of Work, preliminary geological survey was conducted in the first year in the area of 5,800 km<sup>2</sup> to establish the stratigraphy and to clarify the relation of the geologic structure and mineralization.

In the survey of the second year, semidetailed geological survey was carried out over the extent of 1,200 km<sup>2</sup> in the southern part of the area, southern side of Rio Ribeira, located in Parana State. The detailed survey of the Perau mine and the Rocha mine conducted to clarify the situation of emplacement of the ore deposits as well as their characters.

In the survey of Phase III, geological survey (semidetailed survey) was conducted for the area of 1,000 square kilometers in the northern area (the area belonging to São Paulo State on the northern side of Rio Ribeira) to make geological positioning of the ore deposits, and at the same time, the occurrence of latent ore deposit in the Perau area selected on the basis of the result of survey of Phase III and the promising areas in the Barrinha area warranted for future exploration were made clear.

In the survey of this year, Phase IV, it was purposed to know the conditions of occurrence of ore deposit particularly in three promising areas such as Perau, Barrinha and Fumas among the areas of high possibility of ore occurrence selected as the result of the survey performed from Phase I to Phase III, and to evaluate them.



## 1-2 Substance of the Survey

In the survey of Phase IV, the drill survey in the two areas of Perau and Barrinha, the geological survey (detailed survey) and geophysical survey (IP and SIP) in the Furnas area were conducted.

### (1) Geological Survey (Furnas Area)

Geological survey (detailed survey) was carried out for the area of 10 square kilometers and a geological map (scale 1 : 10,000) was produced.

### (2) Geophysical Survey (Furnas Area)

IP electrical survey (15 km) and SIP electrical survey (4.5 km) were carried out for the target of vein-type to pipe-shaped lead deposits emplaced in limestone to dolomite.

The survey of this time was conducted by three Japanese and two Brazilian engineers.

### (3) Drill Survey

Three holes were drilled in the Perau area with the total length of 931.6 meters (220 m in Hole AG-04, 361.60 m in Hole AG-05 and 350 m in Hole AG-06), Two holes were drilled in the Barrinha area with the total length of 600 meters (300 m in Hole AG-Bland 300 m in Hole AG-B2).

## 1-3 Organization of the Survey Team

The members engaged for the planning and the field survey were as mentioned below.

### 1-3-1 Planning and Negotiation

#### (1) Japanese Counterparts

Toru Miura	MMAJ
Kisou Tsuruoka	JICA
Ken Nakayama	MMAJ
Hideyuki Ueda	MMAJ
Ken Nakayama	MMAJ
Tsunekazu Ajiki	MMAJ (Rio de Janeiro)
Hideyuki Ueda	MMAJ

#### (2) Brazilian Counterparts

Carlos Oiti Berbert	DNPM
Kiomar Oguino	DNPM
Luiz Eraldo de Mattos	DNPM
Fernando Batolla Junior	DNPM

### 1-3-2 Field Survey Team

#### (1) Japanese Counterparts

##### Team leader

Tsuyoshi Suzuki                      Bishimetal Exploration Co., Ltd. (BEC)

##### Geological Survey

Norio Ikeda                              BEC

##### Geophysical survey

Tomio Tanaka                            BEC

Toshimasa Tajima                      BEC

Masatane Kato                          BEC

#### (2) Brazilian Counterparts

##### Team leader

Elias Carneiro Daitx                    CPRM

##### Geological Survey

José Carlos Garcia Ferreira          CPRM

### 1-4 Previous Surveys

The geology of the area under study has been investigated by many people, and it is apparent that Pre-Cambrian age rocks, a principle part of the area, are well distributed throughout the area.

Cordani and Bittencourt (1967) have obtained calibrated results of radiometric age as 3,000 -- 450 m.y., and described that orogenic movements took place several times in the period.

For the petrological and stratigraphical studies, Bigarella and Salamuni (1956), Marini et al. (1967), Fuck et al. (1971), Ebert (1971), Coutinho (1971), and DNPM/CPRM (1972), have all attempted to define the geological stratigraphy.

For the studies of mineral deposits, Melcher (1968), has reported on the ore deposits in the limestone of the Açungui group.

Barbosa (1956), thought that the origins of the ore deposits of the area have to do with hypogene deposits, which are related to granite. However, Melcher (1968) and others have proposed differing viewpoints from their studies on the Pb radiometric age.

For the regional geological map of the survey area and its surrounds, the DNPM's compiled map in scale (1/1,000,000) Curitiba (1974), the DNPM-CPRM produced 1/100,000 geological map for Projeto Leste do Parana and the SUDELPA-CPRM produced 1/50,000 geological map for Projeto Sudelpa in the province of São Paulo in 1974 were widely used. As for surveys

done in recent years *Project\**, which was carried out between 1978-- 1979 by the CPRM on a request by the DNPM, studied the geology and ore deposits of the Perau and Rocha areas. In 1980, their report, including a 1/25,000 geologic map, was published. Also, the MMAJ carried out the first year survey of the collaborative mineral exploration of the Anta Gorda area from January to April 1980 on a request by the JICA. In their report, the classification of the geologic stratigraphy followed basically the 1/1,000,000 Curitiba maps (1974) dividing the Açungui Formation I, II and III. According to the same report, the lead ore deposits of the area are classified to the bedded ore deposits of Perau type and in the fissure filling deposits of Rocha type. It also describes that the Perau type is distributed Açungui Formation I while Rocha type is distributed in the limestone of Açungui Formation III.

---

\* *Integração e Detalhe Geológico no Vale do Ribeira*

## 1-5 References

- (1) De Almeida, F.F.M., Hasui, Y., De Brito Neves, B.B. and Fuck, R.A. --1981-- Brazilian structural provinces: an introduction, *Earth-Sci. Rev.*, 17: 1-29.
- (2) AMARAL, G.; CORDANI, U.G.; KAWASHITA, K & REYNOLDS, J.H. --1966-- Potassium-argon dates of basaltic rocks from Southern Brazil, *Geoch. Cosmoch. Acta*, v. 30, pp. 159-189.
- (3) AMARAL, G. et al. --1967-- Potassium Argon Ages of Alkaline rocks from Southern Brazil. *Geoch. Cosmoch. Acta*, v. 31, n.2., pp. 117-142.
- (4) BARBOSA, A.F. --1956-- Algumas observações sobre a jazida de chumbo de Pannels, Estado do Paraná. *Bol. Soc. Bras. Geologia*, 5(2): 51-76.
- (5) BATOLLA Jr., F., HAMA, M. and LOPES Jr., I --1977-- Idades radiométricas Rb/Sr e K/Ar em rochas cristalinas Pré-Brasílicas da região leste do Estado do Paraná. *Atas 1º simpósio Regional de Geologia*, São Paulo, pp. 324-337.
- (6) BATOLLA Jr., F., SILVA, A.T.S.F. da and ALGARTE, J.P. --1981-- o Pre-Cambriano da região sul-sudeste do Estado de São Paulo e este-nordeste do Estado do Paraná *Atas 3º Simpósio Regional de Geologia*, Curitiba, pp. 94-108.
- (7) BIGARELLA, J.J. & SALAMUNI, R. --1956-- Estudos Preliminares na Série Açungui. V-Estruturas organógenas nos dolomitas da Formação Capirú (Estado do Paraná). *Dusenja*, Curitiba, VIII(6): 317-323.
- (8) CORDANI, U.G. and BITTENCOURT, I. --1957-- Determinações de idade potássio-argônio em rochas do Grupo Açungui. *Anais 21º Congresso Brasileiro de Geologia*, Curitiba, pp. 218-233.
- (9) CORDANI, U.G. and KAWASHITA, K. --1971-- Estudo geocronológico pelo método Rb-Sr, de rochas graníticas intrusivas no Grupo Açungui. *Anais 25º Congresso Brasileiro Geologia*, São Paulo, v.1, pp. 105-110.
- (10) D.N.P.M. --1974-- Carta Geológica do Brazil ao Milionésimo Folha Curitiba -- SG22.
- (11) DNPM/CPRM --1977-- Projeto Leste do Paraná. São Paulo, 14v, inédito
- (12) DNPM/CPRM --1978-- Projeto Geoquímica no Vale do Ribeira. São Paulo, 8v., inédito.
- (13) DNPM/CPRM --1981-- Projeto Integração e Detalhe Geológico no Vale do Ribeira. São Paulo, 15v. inédito.
- (14) EBERT, H. --1971-- observações sobre a litologia e sub-divisão do "Grupo Setuva" no Estado do Paraná, com sugestões à tectônica geral do "Geossinclínio Açungui". *Anais 25º Congresso Brasileiro de Geologia*, São Paulo, v.1, pp. 131-146.

- (15) FUCH, R.A., MARINI, O.J., TREIN, E. and MURATORI, A. –1971– Geologia do Leste paranaense. Anais 25º Congresso Brasileiro Geologia, São Paulo, v.1, pp. 121–130.
- (16) JICA/MMAJ –1981– On Geological Survey of Anta Gorda Brazil, Phase I.
- (17) JICA/MMAJ –1982– On Geological Survey of Anta Gorda Brazil, Phase II.
- (18) JICA/MMAJ –1983– On Geological Survey of Anta Gorda Brazil, Phase III.
- (19) KAEFER, L.Q. and ALGARTE, J.P. –1972– Projeto sudeste do Estado de São Paulo. Folha de Itararé SG–22–X–B. Relatório Geológico Preliminar, DNPM/CPRM, São Paulo, v.1, 181p., 1972 (inédito).
- (20) MARINI, O.J., TREIN, E. and FUCH, R.A. –1967– O Grupo Açungui no Estado do Paraná. Bol. Paran. Geoci., Curitiba, nº 23–25, pp. 43–103.
- (21) MELCHER, G.C. –1968– Contribuição ao conhecimento do distrito mineral do Ribeira do Iguape, Estados de São Paulo e Paraná. Tese Livre Doc. Geol., ESE. Politécnica USP, São Paulo, 122p., (inédito).
- (22) ODAN, Y., FLEISCHER, R. and ESPOURTEILLE, F. –1978– Geologia da mina de chumbo de Panelas – Adrianópolis –PR. Anais 30º Congresso Brasileiro Geologia, Recife, v4, pp. 1545–1552.
- (23) SUDELPA/DPRM –1975– Projeto Sudelpa. São Paulo, 18v., inédito
- (24) Gerald W.H (1977); Numerical IP Modeling, Induced Polarization for Exploration Geologists and Geophysicists, The University of Arizona
- (25) Hallof P.C. (1964, 1967); A Comparison of the Various Parameter Employed in the Variable Frequency Induced Polarization Method
- (26) Kaku H. (1966); On the Coupling Effect in the Induced Polarization Method Butsuri Tanko, 19 (405)
- (27) Pelton W.H., Ward S.H., Hallof P.G., Sill W.R. and Nelson P.H. (1977); Mineral Discrimination and Removal of Induced Coupling with Multi-frequency IP, Metal Mining Agency of Japan, 1980 – 1982  
Report on Research and Development Survey for Mineral Resources -- Spectral IP
- (28) Sumner J.S. (1976); Principles of Induced Polarization for Geophysical Exploration
- (29) Wait J.R. (1958); Discussions on a Theoretical Study of Induced Electrical Polarization, Geophysics, 23

## CHAPTER 2 COMPREHENSIVE INVESTIGATION

### 2-1 Geological Survey (Furnas Area)

#### 2-1-1 Geology

Geology of the survey area consists of meta-sedimentary rocks (S) and carbonate rocks (L) of the Precambrian Açungui III formation, and these are subdivided into the members such as AIHL<sub>2</sub>, AIHS<sub>2</sub>, AIHL<sub>3</sub>, and AIHS<sub>3</sub> from the base upward.

The AIHL<sub>2</sub> member mainly consists of dark gray fine-grained limestone, while the AIHS<sub>2</sub> member mainly consists of gray to yellowish brown quartz-sericite schist with filmy graphite, intercalated with fine-grained meta-sandstone.

The AIHL<sub>3</sub> member is mainly composed of limestone, intercalated with pelitic dolomite, quartz-sericite schist and meta-sandstone and is subdivided into the lower, middle and upper parts.

The Furnas deposit is emplaced in limestone and dolomite of the lower part of AIHL<sub>3</sub>, and the lithological unit which contains the ore bearing horizon continues up to the western and eastern end of the survey area.

In the survey of this time, several showings were newly confirmed in the same horizon in the southwestern part of the known Furnas deposit.

AIHS<sub>3</sub> consists of meta-quartz sandstone.

Regionally, the area is located between the Serra Manduri anticline and the Calabouço syncline, the first order, and the homoclinal structure with the general strike of N60°E and general dip of 45°NW are shown. Any large-scale fault and fold structures can not be found in the area.

#### 2-1-2 Ore Deposit

In the Furnas mine in operation at present, the traces of numerous open pits and trenches are observed, and several galleries are found. The known showings and other several showings newly confirmed this time are also distributed to the southwest of the aboves.

The ore deposits consist of vein-type, irregular massive to pipe-like type, silver bearing lead deposits emplaced in the fractures of NE-SW system consistent with the bedding plane of limestone (AIHL<sub>3</sub>lsA) and dolomite (AIHL<sub>3</sub>dola<sub>1</sub>.A<sub>2</sub>) in the lower part of the AIHL<sub>3</sub> member and the fractures of E-W system dipping steeply. The ore deposits show the shape of pipe or chimney with frequent swells and pinches, and the bonanza is formed at the intersection of the fractures of the above two systems. Although a unit ore body is small on a scale, the three places (the zone on the eastern side of Laranjeiras, the adjacent area of Santo Antônio and

Trés Bocas) where plural ore bodies are concentrated were extracted in the known ore deposits.

Ore minerals consist mainly of galena and cerussite, accompanied by pyrite and small amount of chalcopyrite and sphalerite. Hematite and goethite are found in abundance near the surface.

The assay result of ore (Pb,Zn,Cu,Ag) showed that lead and silver was high in grade, that zinc was small in amount as a whole though locally high in grade, and that copper is very small in amount.

In respect of the relationship between the geologic structure and ore deposit, the ore bearing fractures were formed simultaneously by lateral pressure of NW–SE system with formation of fold structure of NE–SW system.

Taking in account the geology and ore deposit above mentioned, geophysical survey (IP,SIP) were carried out in the surrounding part of Santo Antonio and the area containing the Três Bocas showings which had not been tested below the surface. However, no notable FE anomaly was detected. The reasons for this are likely that the ore deposits are small on a scale, that the country rock is unpolarizable and high resistivity and also that small-scale anomalies in the ore bearing horizon are difficult to be detected because of presence of the beds showing strong IP-effect in both the hanging wall and footwall.

For the future exploration, it seems to be effective to extract the mineralized zone by soil geochemical survey on a grid or rock geochemical survey, since the ore bearing horizon of the area has been defined. Moreover, a detailed geological survey is to be desired because it was made clear that the geology of the ore horizon extends toward the southwest and northeast beyond the boundary of the survey area.

## 2-2 Geophysical Survey

The Spectral Induced Polarization (SIP) and Induced Polarization (IP) methods were performed to clarify the possible existence of the ore deposits in the Furnas area.

Ten IP and three SIP survey lines with 1.5 km line length each were set perpendicular to the geological structure. the results are summarized below:

(1) The distribution of apparent resistivity, which shows high-low-high-medium on each line, fits closely with the geological structure, and the portion of the apparent resistivity change indicates the contact of formation.

(2) Two distinct anomalous zones were revealed between No.3 and No.8, and between No.12 and No.14 on each line. The former shows a complicated contour pattern suggesting the existence of many anomalous sources, and the phase spectrum gradually increases with frequency between 0.125 Hz and 8 Hz. The latter shows the anomaly pattern caused by an unit body and the phase spectrum linealy increases with frequency.

(3) The source of the former is thought to be caused by the pyrite dissemination in dolomite and graphite interbedded with limestone. The source of latter is seen to be caused by film-shaped graphite in schist.

(4) These two anomalies dip southward and are considered to continue to outside of the survey area at northeast-southwest direction along the geological structure..

(5) The reason, an anomaly was not detected in the horizon of ore deposit, are as follows:

The horizon is unpolarizable and high resistivity rock, and a scale of deposit is so small for detection.

Nevertheless, if there exists a wide range of mineralization and a large scale of deposit, an anomaly will be detectable.



## 2-3 Drilling Survey

In the drill survey of Phase IV, three holes (931.6 m) in the Perau area and two holes (600 m) in the Barrinha area, five holes (1,531.6 m) in total, were drilled. As the result, the conditions of the surrounding area of the stratiform lead and zinc deposit, discovered in Phase III, was made clear in the Perau area, and the relationship between the IP and SIP anomalous zones and the geologic structure was made clear in the Barrinha area.

### 2-3-1 Perau Area

The Perau area is dominantly underlain by the metamorphic rocks belonging to the Precambrian Açungui I formation. In this survey, mica schist, amphibolite, carbonate schist, graphite schist and limestone were mainly drilled.

The ore deposit is a stratiform deposit emplaced in the carbonate schist, and the main ore minerals are barite, galena, sphalerite, pyrite and pyrrhotite.

Core recovery was more than 95%, and almost 100% in the ore horizon.

The assay result of the ore intersections of the holes is as follows:

Hole	Depth (m)	Length (m)	Pb%	Zn %	Cu ppm	Ag ppm
AG-04	196.95 ~ 197.15	0.20	1.60	0.46	330	26
AG-04	199.80 ~ 199.90	0.10	8.00	0.03	18	200
AG-04	200.65 ~ 200.75	0.10	4.50	1.60	30	100
AG-05	354.65 ~ 355.65	1.00	2.50	2.90	100	75
AG-05	357.85 ~ 358.35	0.50	4.90	2.80	160	185
AG-06	327.55 ~ 328.05	0.50	2.20	0.04	22	38
AG-06	328.60 ~ 239.40	0.80	1.80	4.40	70	38
AG-06	330.15 ~ 330.60	0.45	1.30	1.10	30	38

As the result of survey, it was made clear that the vicinities of Hole AG-04 and AG-06 was shown to be the southern and the northwestern limits of the ore deposit respectively and that the size of deposit reduces toward Hole AG-05.

### 2-3-2 Barrinha Area

In the Barrinha area, carbonate rocks ( $AlHIL_2$ ) and mica schists ( $AlHS_2$ ) are distributed showing a complicated folding. The known deposit of the Barrinha mine is vein-type to irregular massive silver bearing lead deposit, which is concentrated from the axial part to the limb of the

fold structure.

As the result of drilling of two holes of AG-B1 and AG-B1S through the SIP anomaly in the southern part of Quatro and AG-B2 through the IP anomaly in the northeastern part of the area, complicated geologic structure and the exploration targets for future were studied.

The geologic structure in the vicinity of Hole AG-B1 in the southeastern part of Quatro shows a steep fold structure, and the hole drilled mainly in mica schist. Because of thick soil and presence of silicified zone and quartz veins directly below the soil, the apparent resistivity is shown high contrast.

Hole AG-B1S drilled mica schist, carbonate schist and dolomite to limestone, and pyrite zone was observed in dolomite to limestone. This pyrite zone is situated in the same horizon of the Quatro deposit, and seems to have caused the IP effect.

Although in Hole AG-B2 in the northeastern part of the area drilled mica schist, siliceous schist and graphitic mica schist, neither limestone nor mineralized zone was found. Dolomite to limestone with pyrite-galena mineralized zone was encountered in Hole S-9 of the Barrinha mine.

In the geologic structure in the vicinity of Hole AG-B2 a fault is assumed to be present between the holes AG-B2 and S-9. The IP anomalous zone detected in the surrounding area of these holes seems to be a combination of IP effect caused by pyrite-galena mineralized zone and graphitic mica schist together with pyrite contained in it.

## CHAPTER 3 CONCLUSION AND RECOMMENDATION

### 3-1 Conclusion

In the survey of Phase IV, detailed geological survey and geophysical survey (IP and SIP) in the Furnas area and drill survey in the Perau area and the Barrinha area were conducted.

#### (1) Furnas Area

As the result of geological survey, detailed stratigraphy was established, the ore bearing horizon of the Furnas deposit was clarified, and the mineral showings were newly discovered in the same horizon.

As the result of geophysical survey, no marked anomalous zone was detected in the ore bearing horizon, because the horizon is an unpolarizable and high resistivity rock, and a scale of deposit is too small to detect.

#### (2) Perau Area

As the result of drill survey, the continuity of the stratiform lead and zinc deposit discovered in Phase III was made clear. Also it became clear that the ore deposit extends in approximate direction of NE-SW and that the vicinities of holes AG-04 and AG-06 were the southern limit and the northwestern limit respectively.

#### (3) Barrinha Area

As the result of drill survey, the relationship between the geologic structure in the southeastern part of the Quatro deposit and the northeastern part of the area and the anomalous zone detected by geophysical survey (SIP and IP) conducted in Phase III as well as the new areas for future exploration were made clear.

### 3-2 Recommendation

Although the technological collaboration project by Japanese government is to be completed by the end of fiscal 1983, the following items will be proposed for the Brazil side to continue the survey in future.

#### (1) Furnas Area

An effort is to be made to discover new ore deposit by detailed geochemical survey (soil and rock), trenching and drilling because detection of geophysical (IP, SIP) anomalies in the ore bearing horizon was proved to be difficult.

Since it was made clear that the ore bearing horizon extended beyond the area of survey of this time, it is necessary to trace and investigate it.

It is desirable to conduct a detailed survey, underground survey, on ore fractures in the

known ore deposit and to make clear the "chute" of ore shoots of every ore body to lead to performance of prospecting in the lower extension.

**(2) Perau Area**

It will be necessary to confirm the whole aspect of the stratiform lead and zinc deposit by carrying out the drill survey in the areas to the north and to the northeast of Hole AG-02 continuously to follow the drill survey so far conducted. Moreover, fill-in drill holes with an interval of 30 to 50 meters are to be necessary between the exploration holes for evaluation of the ore deposit.

**(3) Barrinha Area**

Since there is a possibility of occurrence of Quatro-type lead deposit in the pyrite zone in limestone in the southern part of the Quatro deposit, it is necessary to trace the horizon by drilling. Especially it is desirable to carry out drill survey from the adjacent area of Hole AG-B1S to the vicinity of No.10-point on the I-line. In the northern part and the northeastern part of the area, it is to be desired to make drill survey for the mineralized zone in limestone distributed on the southern side of the fault encountered in Hole AG-B2.

PARTICULARS  
PART I GEOLOGICAL SURVEY

## CHAPTER I GEOLOGY

### 1-1 Summary of Geology

Regionally, geology of the surrounding area of the survey area consists of metamorphic rocks of the Precambrian Açungui group, which have been intruded by basic rocks and granitic rocks of Brazilian Orogeny (750 ~ 500 Ma.) and diabasic dykes of Jurassic to Cretaceous.

The Açungui group is divided into the Açungui I, II and III formations, and the Açungui III formation is further subdivided into four members such as AIII<sub>1</sub>-AIII<sub>4</sub> by the combination of carbonate rocks (L) and meta-sedimentary non-carbonate rocks (S) (JICA-MMAJ, 1983).

Among these, Açungui III is distributed in the survey area. The Açungui III formation in the survey area is composed of, from the lower upward, the AIII<sub>2</sub> member consisting of limestone and dolomite, AIII<sub>3</sub> member consisting of sericite schist and meta-sandstone, AIII<sub>1</sub> member consisting of limestone, dolomite and sericite schist and the AIII<sub>4</sub> member consisting of meta-quartz sandstone.

As for the regional geologic structure, the faults and folds of NE-SW system seems to have been formed in Brazilian Orogeny, but large-scale one can not be observed in the survey area.

Fig. 1-1 and Plate 1-1 show the geological maps and Fig. 1-2 shows general geological columnar section.

### 1-2 Stratigraphy

Geology of the survey area consists of the members such as AIII<sub>2</sub>, AIII<sub>3</sub>, AIII<sub>1</sub>, and AIII<sub>4</sub> of the Açungui III formation mentioned above.

#### 1-2-1 AIII<sub>2</sub> Member

##### Distribution and Thickness

The member is distributed in a narrow zone in the direction of NE-SW in the southern peripheral part of the survey area. Although the thickness is more than 280 meters, the member is widely distributed in the Lageado area to the south of the survey area, where the thickness of 750 meters is shown.

##### Rock Facies

The member consists mainly of gray to dark gray fine-grained limestone (NI-06) interbedded with thin layers of calcareous dolomite (NI-35, JG-14) and sericite schist. A small

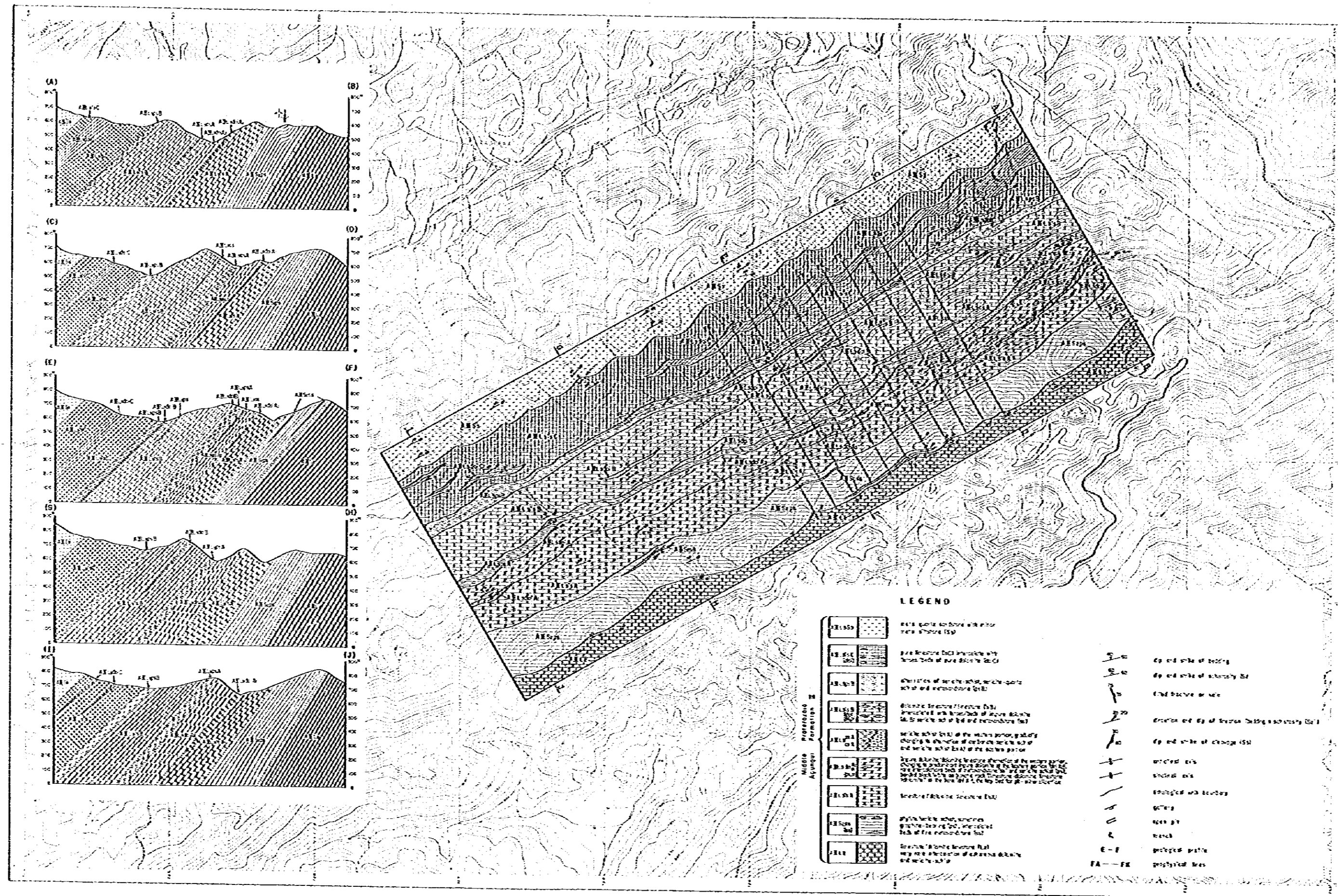


Fig. 1-1 Geological Map and Geological Profile of Furnas Area

Formation	Columnar Section	Lithology	Thickness (m)
Açungui Formation III	AIII5s	meta quartz sandstone with meta siltstone (AIII5s)	220 ±
	AIII5d1C	dolomite	350
	AIII5s1C	limestone	450
	AIII5psB	alteration of sericite schist, sericite-quartz schist and meta sandstone	980
	AIII5d1B	dolomite	30 65
	AIII5ps	intercalation of sericite schist	230
	AIII5s1B	limestone	340
	AIII5ss	intercalation of meta quartz sandstone	1090
	AIII5psA	sericite schist alteration of carbonate schist ~ carbonate phyllite and sericite schist	40 60
	AIII5d1A2	dolomite with Fe pyrite	110
	AIII5d1A1	banded white dolomite and black limestone	185
	AIII5s1A	limestone with dolomitic part	100 200
	AIII5zss	intercalation of sericite-quartz schist ~ meta sandstone	150
	AIII5zps	sericite schist ~ phyllite	260
	AIII2	limestone with dolomitic part, very rare sericite schist	280 ±

Fig. 1-2 Generalized Stratigraphic Columnar Section in Furnas Area



amount of fine-grained pyrite dissemination is locally observed.

The result of microscopic observation of the typical rock is as follows:

**Fine-grained crystalline limestone (NI-06)**

**Locality :** Along São Paulo State Highway 165

**Texture :** Granoblastic

**Constituent minerals :**

Calcite (95%)  $\gg$  quartz + muscovite (5%) > plagioclase, biotite, opaque minerals, chlorite, epidote

Calcite occurs as abundant crystals with distinct cleavage less than 0.1 mm across, which have been well sorted.

Muscovite is 0.15 x 0.02 mm in maximum, and partly shows preferred orientation.

Quartz is 0.2 mm across in maximum, and wavy extinction can be observed.

**Calcareous dolomite (JG-14)**

**Locality :** Southeastern end of the area

**Texture :** Granoblastic, lepidoblastic

**Constituent minerals :**

Dolomite (50%) > calcite (25%)  $\gg$  quartz (10%), muscovite (10%) > biotite, opaque minerals, zircon

Dolomite is 0.08 mm across in average, and is not so well sorted.

Quartz is 0.3 mm across in maximum, and 0.08 mm across in average. Lenticular aggregate 0.5 mm across composed of quartz and opaque minerals is observed.

Muscovite shows a notable preferred orientation.

## **1-2-2 AHIS<sub>2</sub> Member**

### **Distribution and Thickness**

The member is distributed in the southern part of the survey area being put between the AHIL<sub>2</sub> member and the AHIL<sub>3</sub> member. The thickness is 150 m at the central part, which increases toward the both direction becoming 240 to 260 m. The member conformably overlies the lower AHIL<sub>2</sub> member in the lower reaches of Furnas creek.

### **Rock Facies**

The member is composed mainly of gray to yellowish brown graphite-bearing sericite schist (AHIS<sub>2</sub>ps) (NI-29, JG-10) intercalated with thin layers of reddish brown to pink sericite-quartz schist to fine-grained meta-sandstone (AHIS<sub>2</sub>ss) (JG-09). Crystals of chloritoid 2 mm across and fine-grained pyrite dissemination are observed in sericite schist in the lower

reaches of Furnas creek

The result of microscopic observation of the typical rock is as follows:

**Chlorite-quartz sericite schist (NI-29)**

**Locality :** lower reaches of Furnas creek.

**Texture :** lepidoblastic

**Constituent minerals :**

Quartz, sericite, chlorite > opaque minerals > plagioclase, muscovite, tourmaline, zircon, apatite, graphite, epidote

Minerals less than 0.1 mm in size are dominant in general, but sericitized plagioclase 1 mm across and tourmaline 0.2 mm across are observed.

Quartz shows the granular aggregate, and chlorite fills the interstices of sericite crystals.

Film-like graphite is observed.

**Sericite-quartz schist (JG-09)**

**Locality :** point at FE-13.7

**Texture :** lepidoblastic

**Constituent minerals :**

quartz > muscovite, opaque minerals, sericite, chlorite > biotite, epidote

Quartz is 0.08 to 0.2 mm across, showing wavy extinction.

Chlorite fills the interstices of sericite grains.

Secondary limonite occurs in abundance in general.

**1-2-3 AIII<sub>3</sub> Member**

**Distribution and Thickness**

The member is widely distributed in the central part of the survey area. The thickness is 980 m in the northeastern part, which increases toward the southwest to reach 1,090 m, while it is 1,045 m at the southwestern end. It is considered that the member conformably overlies the lower AIII<sub>2</sub> member (JICA, MMAJ, 1981 - 1983).

**Rock Facies**

The member consists mainly of limestone (AIII<sub>3</sub>ls) interbedded with dolomite (AIII<sub>3</sub>dol) and graphite-bearing sericite schist (AIII<sub>3</sub>ps), and very small amount of meta-quartz sandstone (AIII<sub>3</sub>ss). The member is further divided into three parts such as the lower (A), middle (B) and upper (C) bordered by the two layers of sericite schist (AIII<sub>3</sub>psA, AIII<sub>3</sub>psB) showing a relatively good continuity at each boundary. That is, these are, from the base upward, AIII<sub>3</sub>lsA, AIII<sub>3</sub>dolA<sub>1</sub>, AIII<sub>3</sub>dolA<sub>2</sub>, AIII<sub>3</sub>psA, AIII<sub>3</sub>lsB, AIII<sub>3</sub>dolB, AIII<sub>3</sub>psB, AIII<sub>3</sub>lsC and

### **AHLL<sub>3</sub>dolC.**

AHLL<sub>3</sub>ls A (JG-12), AHLL<sub>3</sub>lsB and AHLL<sub>3</sub>lsC (JG-01) are dark gray, fine-grained and relatively well bedded limestone to dolomitic limestone, being intercalated with the layers of sericite schist and meta-quartz sandstone several centimeters to several meters thick. In limestone of AHLL<sub>3</sub>lsA, a horizon with dominant amount of dolomite extends from the São Manoel showing east of the survey area toward the southwest for about 100 m and pyrite dissemination is observed in it. The rock of the same horizon as the above found almost in the central part of the survey area shows a rock facies of pale gray siliceous dolomite (NI-43). Among AHLL<sub>3</sub>lsB, NI-13 is dolomitic limestone with a banded pattern of black and white, but the banded texture is not so distinct as compared with AHLL<sub>3</sub>dolA<sub>1</sub>.

AHLL<sub>3</sub>dolA<sub>1</sub> is black and white banded dolomite to dolomitic limestone (NI-28), which is observed discontinuously from the Maxial portal at the eastern end of the survey area to the western end of the area. AHLL<sub>3</sub>dolA<sub>2</sub> consists mainly of gray to dark gray pelitic dolomite (NI-08, 20, 37) accompanied by pyrite in the eastern half and dolomitic limestone increases in the western half. It is intercalated with sericite schist and meta-quartz sandstone.

AHLL<sub>3</sub>dolB shows a rock facies similar to that of AHLL<sub>3</sub>dolA<sub>2</sub>, in which pyrite dissemination is sometimes observed (NI-55). AHLL<sub>3</sub>dolC is gray medium-grained dolomite to calcareous dolomite, in which network veins of white dolomite are observed, and brecciated texture is partly shown. Dolomite is generally massive as compared with limestone, in which bedding is indistinct, being dominant with fractures.

AHLL<sub>3</sub>psA consists of alternating beds of dark gray carbonate-sericite schist to carbonate phyllite and brown sericite schist (NI-54) in the eastern half of the area of its distribution, while the western half consists of gray to brown sericite schist (NI-36). AHLL<sub>3</sub>psB is alternating beds of purplish gray sericite schist and yellowish brown sericite-quartz schist (NI-56), intercalated with graphite schist on a little western side of the central part. AHLL<sub>3</sub>ss is gray to brown, fine to medium-grained meta-quartz sandstone (NI-46, 50).

Among the geology in the above, the Furnas deposit is emplaced in AHLL<sub>3</sub>ls A, AHLL<sub>3</sub>dolA<sub>1</sub> and AHLL<sub>3</sub>dolA<sub>2</sub>. AHLL<sub>3</sub>dolA<sub>1</sub> is effective as the key bed of the ore horizon and psA is effective as the key bed to indicate the hanging wall of the ore horizon.

The result of microscopic observation of typical rocks is as follows:

**Limestone (JG-12) : AHLL<sub>3</sub>lsA**

**Locality : FI-11.5**

**Texture : granoblastic**

**Constituent minerals :**

Calcite (85%) ≫ dolomite (5%) > quartz (4%) > muscovite (1%) > plagioclase, opaque minerals

Calcite is observed as the crystals with distinct cleavages 0.2 mm across in average, having been well sorted.

Quartz is 0.2 mm across in maximum and shows wavy extinction.

Black and white banded crystalline dolomitic limestone : AHIL<sub>3</sub>dolA<sub>1</sub>

Locality : Maxial

Texture : porphyroblastic

Constituent minerals :

Calcite (50%) > dolomite (30%) > quartz (10%) > muscovite (5%) > plagioclase, opaque minerals

The black part consists of dolomite and calcite 0.03 mm across in average, having been well sorted. Quartz and plagioclase are contained about seven percent for each.

In the white part, quartz (0.05 mm across, 10%), muscovite (0.1 mm >, 10%) and dolomite (0.01 – 0.03 mm across) irregularly fill the interstices of dolomite crystals which is 0.1 mm across in maximum and poorly sorted.

The boundary between the black part and white part is distinct, and fine-grained opaque minerals are observed there.

Fine-grained pelitic dolomite (NI-08) : AHIL<sub>3</sub>dolA<sub>2</sub>

Locality : São Paulo State Highway 165

Texture : lepidoblastic

Constituent minerals :

Dolomite (65%) ≫ quartz (10 -- 20%) > muscovite (10%) > opaque minerals

Dolomite is 0.1 mm in maximum, having been sorted moderately.

Quartz crystals are generally less than 0.1 mm, containing coarse crystals (1.4 x 0.7 mm in maximum), having been poorly sorted. The content is generally 10% reaching up to 20%.

Muscovite is less than 0.1 mm and shows preferred orientation.

Fine-grained opaque minerals are observed throughout the rock.

Quartz-sericite schist (NI-54) : AHIL<sub>3</sub>psA

Locality : São Paulo State Highway 165

Texture : lepidoblastic

Constituent minerals :

sericite, quartz > opaque minerals > zircon, chlorite

Minerals less than 0.1 mm across are arranged in a lepidoblastic texture in general.

The characteristic of each mineral is similar to that of NI-29.

Vein-like vesicles are observed, and they are likely to be the trace of leaching out of calcite vein.

**Alternating beds of sericite and sericite-quartz schist (NI-56): AIII<sub>3</sub>psB**

Locality : São Paulo State Highway 165

Texture : Lepidoblastic

Constituent minerals :

Sericite, quartz > opaque minerals > muscovite, zircon, chlorite

It is observed in the section that almost colorless sericite-quartz schist is interbedded between reddish brown sericite schist. The size of minerals is less than 0.1 mm, in which the latter is a little coarser, sometimes showing crenulation.

**Dolomite (JG-06) : AIII<sub>3</sub>dolC**

Locality : northwestern end

Texture : granoblastic

Constituent minerals :

dolomite (85%) >> calcite (5%), opaque minerals

The greater part of the sample consist of poorly sorted dolomite 0.04 to 0.4 mm.

**1-2-4 AHS<sub>3</sub> Member**

Distribution and Thickness

The member is distributed in a zone in the northern periphery of the survey area. The thickness is more than 220 m in the area, which reaches up to 900 m when Serra Boa Vista north of the survey area is included. Although the relation between the member and the underlying AIII<sub>3</sub> can not directly be observed, it has been considered to be conformable (JICA, MMAJ, 1983).

Rock Facies

The member consists mainly of meta-quartz sandstone (NI-03, JG-07) intercalated with thin layers of metasiltstone (NI-04).

The former is grayish brown to pinkish gray, fine to medium-grained rock and the bedding is generally distinct. The later occurs as intercalated thin layers 5 to 20 cm thick (3 m in maximum) in meta-quartz sandstone.

The result of microscopic observation of the typical rocks is as follows:

**Meta-quartz sandstone (NI-03)**

Locality : São Paulo State Highway 165

Texture : blastopsammitic

Constituent minerals :

Quartz > muscovite > opaque minerals, tourmaline, sphene, chlorite, epidote

Quartz is 4 mm across in maximum and 0.3 to 0.6 mm across in average, showing wavy extinction.

Muscovite irregularly fills the interstices of the quartz grains.

The texture of sandstone remains in the rock.

#### Metasiltstone (NI-04)

Locality : São Paulo State Highway 165

Texture : blastoclastic

Constituent minerals :

quartz > sericite, opaque minerals, tourmaline, chlorite > muscovite, zircon, epidote, calcite

The rock consists of minerals less than 0.1 mm across, partly containing subangular pebble of metasiltstone 0.2 to 0.5 mm across. The zones in which quartz shows a mosaic texture is also observed.

### 1-3 Metamorphism

The metamorphic rocks in the survey area consist of schists and phyllites formed in Brazilian Orogeny derived from psammitic and pelitic sediments. The metamorphic grade is low, showing mineral assemblage of graphite-sericite-muscovite. The carbonatic rocks are mainly recrystallized to a mosaic granoblastic of calcite or dolomite where sericite or quartz minerals are present, and sometimes planar orientation can be observed.

### 1-4 Geologic Structure

The survey area is positioned, from the standpoint of regional geologic structure, in the middle of the Calabouço syncline and the Serra Manduri anticline of the NE-SW system (JICA, MMAJ, 1983).

The formations distributed in the survey area show an homoclinal structure with general strike of N60°E and general dip of 45°NW. Although the minor fold structure is observed in several places on the surface, the structures to be specially mentioned such as complicated folds and faults are not observed. Faults and vein fracture of NE-SW to E-W systems are observed in the underground of the Furnas mine.

The Furnas deposit is mainly emplaced in the fractures of NE-SW system which are consistent with the bedding plane and the steeply dipping fracture of E-W system. The bonanzas

have been formed at the intersection of the two fracture systems.

As the result of analysis of the field of the principal stress, in the survey of this year, as was made in Phase III, for the conjugate set of the two fracture systems above mentioned, the relation of which is observed on the surface and in the underground that the one cut the other in one place and vice versa in other place, a direction was obtained as the maximum principal stress axis compressional which ascends in very low angle toward the northwest from the southeastern lower side (Fig. I-3). That is, a lateral compression of NW-SE system was obtained as the stress direction, which is well consistent with the result of survey in Phase II and Phase III.

The schistosity planes ( $S_1$ ,  $S_2$ ) and the cleavage ( $S_3$ ) are notably observed in the sericite schist in the survey area. Two planes of schistosity are observed; the one strikes  $N40^\circ$  to  $70^\circ E$  and dips  $25^\circ$  to  $60^\circ$  NW ( $S_1$ ), and the other strikes  $N60^\circ$  to  $80^\circ W$  and dips  $20^\circ$  to  $25^\circ$  NE ( $S_2$ ). The cleavage plane is of a microfold cleavage ( $S_3$ ) striking  $N20^\circ$  to  $30^\circ E$  and dipping  $70^\circ$  to  $80^\circ E$ , cutting  $S_1$  and  $S_2$ .

Among these, strain ellipsoid of  $S_1$  supports the result of analysis of principal stress field mentioned above. Thus the schistosity plane  $S_1$  and the fractures in which the ore deposits have been emplaced are thought to have been formed in the same stress field (Fig. I-3).

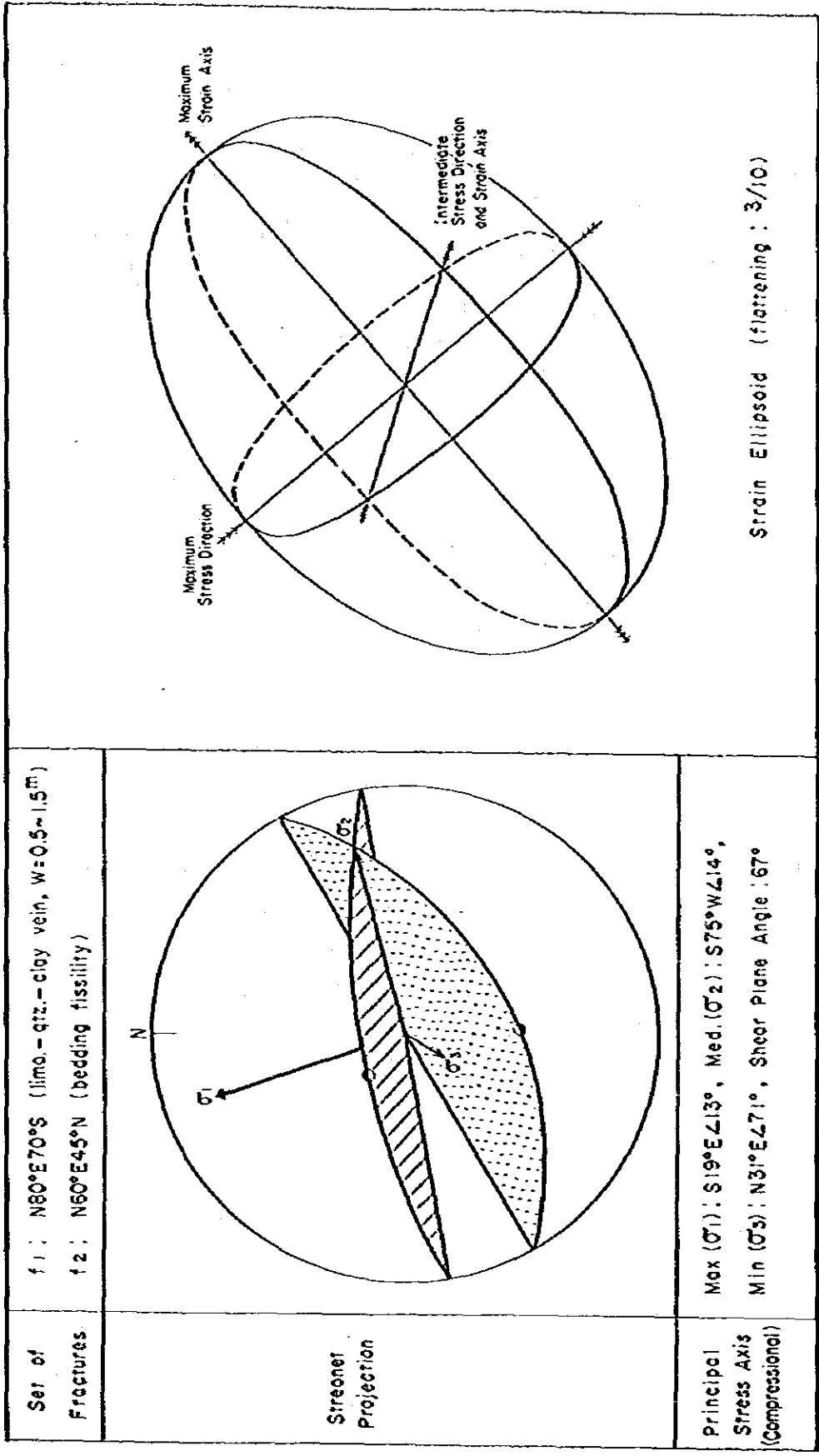


Fig. I-3 Principal Stress Field Analysis of Fracture and Strain Ellipsoid of Schistosity Plane of Furnas Area



## CHAPTER 2 ORE DEPOSIT

### 2-1 Summary of the Ore Deposit

The ore deposits in the project area are roughly divided into two types such as the Perau type stratiform lead and zinc deposit emplaced in limestone to calc-silicate rocks of the Açungui I formation in consistent with the bedding plane and the Rocha type silver bearing lead deposit emplaced in carbonate rocks of the Açungui III formation in a form of vein or irregular massive body.

Among these, the Furnas deposit situated in the survey area belongs to the latter.

The Furnas mine is situated along the São Paulo State Highway 165 about 17 km to the east of Apiai. At the mine, the operation is being carried out mainly for exploration and mining in the Santa Barbara 2 tunnel and the production of crude ore consists of 20 t of sulphide ore (50% in Pb) and 150 t of oxide ore (15% in Pb) per month.

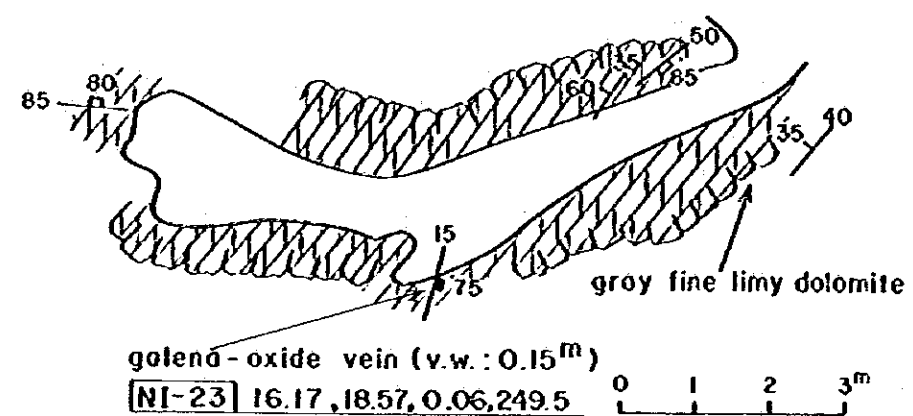
The trace of numerous open pits or trenches is found on the surface, and the main ones are concentrated along the ridge from Vala 8 to Laranjeiras (Fig. I-4, Plate I-3, Table A-1). The levels were excavated to take hold of the same ore body, and several portals can be observed including the Maxixal level, Santa Barbara I and 2, and others. To the southwest of the above, the showings such as Santo Antonio and Três Bocas have been known, where old pits and old trenches are found. Several showings were newly confirmed this time to the southwest of the above. Beside these, the gold showing is known in AIII<sub>3</sub>psB to the northeast beyond the boundary of the area.

### 2-2 Shape and Scale of Ore Deposit

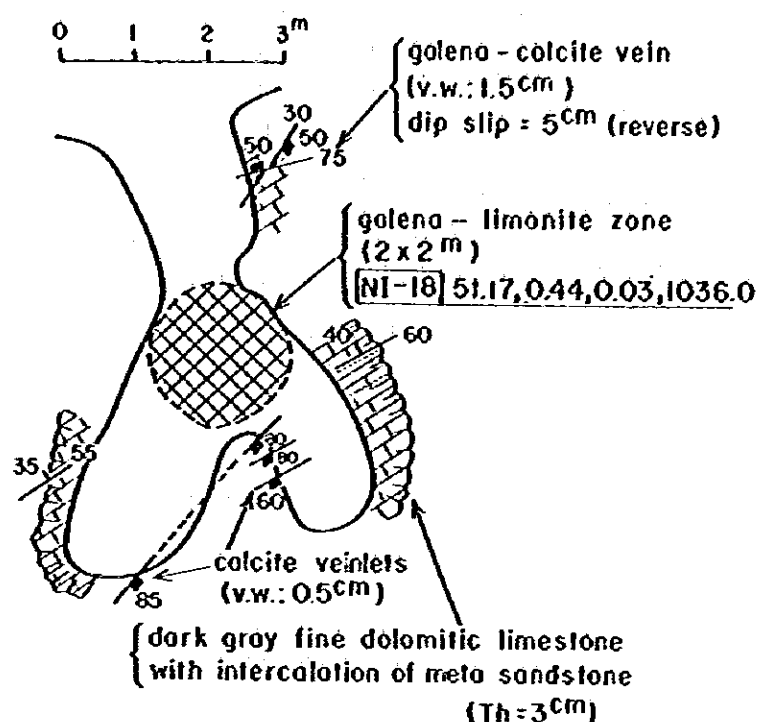
The ore deposits are emplaced in the fractures of NE-SW system consistent with the bedding plane and the steeply dipping fractures of E-W system in carbonate rocks (AIII<sub>3</sub>dolA<sub>1</sub>, AIII<sub>3</sub>dolA<sub>2</sub>) and partly in limestone (AIII<sub>3</sub>lsA). Especially the bonanzas were formed at the intersection of the two fractures, where an irregular shape of pipe or chimney is shown by repetition of swells and pinches. The direction of "chute" of bonanza accords with the line of intersection between the plane of fracture which is consistent with the bedding plane and that of the steeply dipping fracture of E-W system, which generally plunges toward the west showing the plunge of 40° to 50°.

In terms of the size of ore deposit, the width of the vein which is consistent with the bedding plane reaches up to one meter and the obliquely intersecting one reaches up to 2 m.

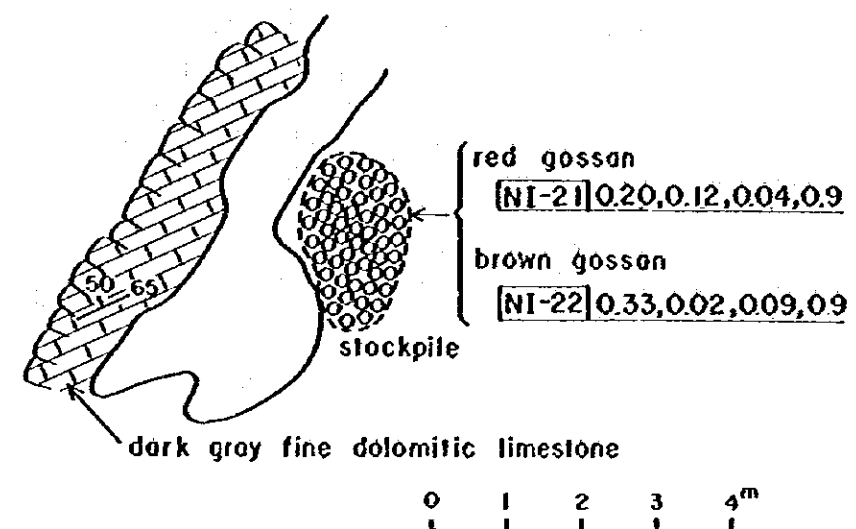
(Vala 8) (trench of west part)



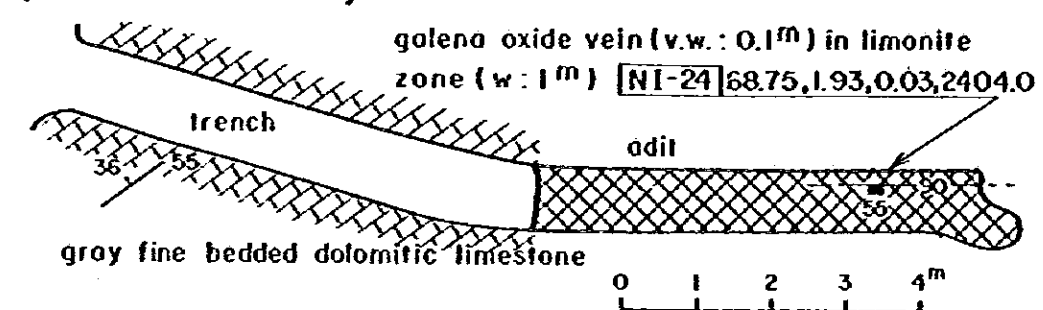
(St. Antonio de Cima) (trench)



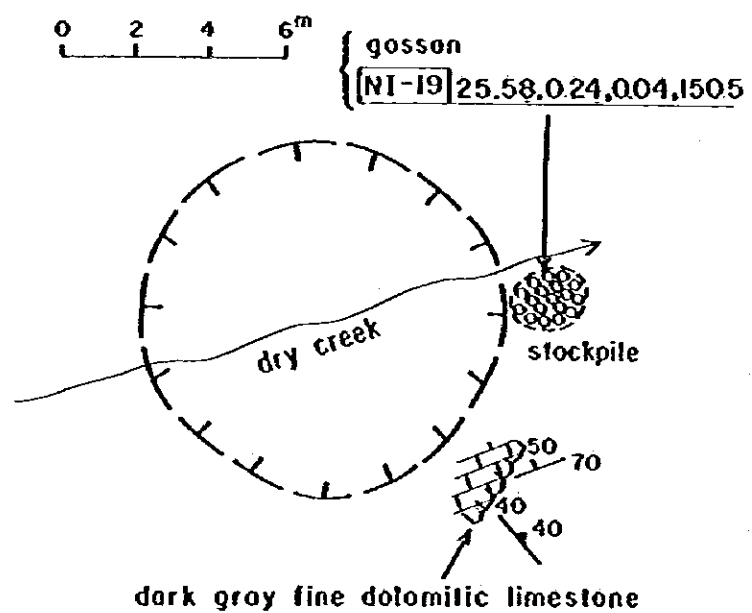
(Tres Bocas de Cima) (trench)



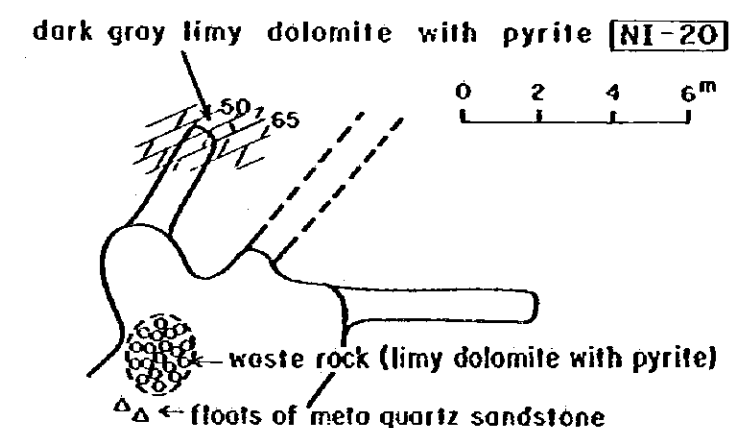
(East of Barreira) (trench and adit)



(St. Antonio de Baixo) (open pit)



(Tres Bocas de Baixo) (adit)



(Santo Oswaldo) (open pit)

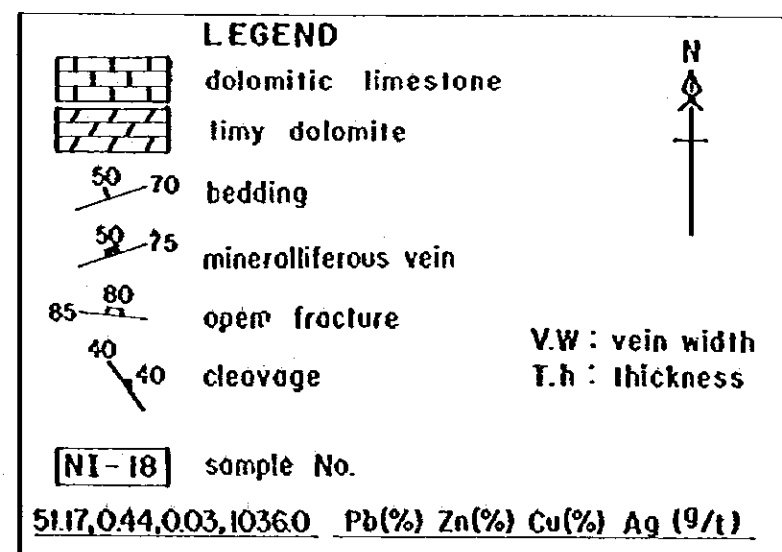
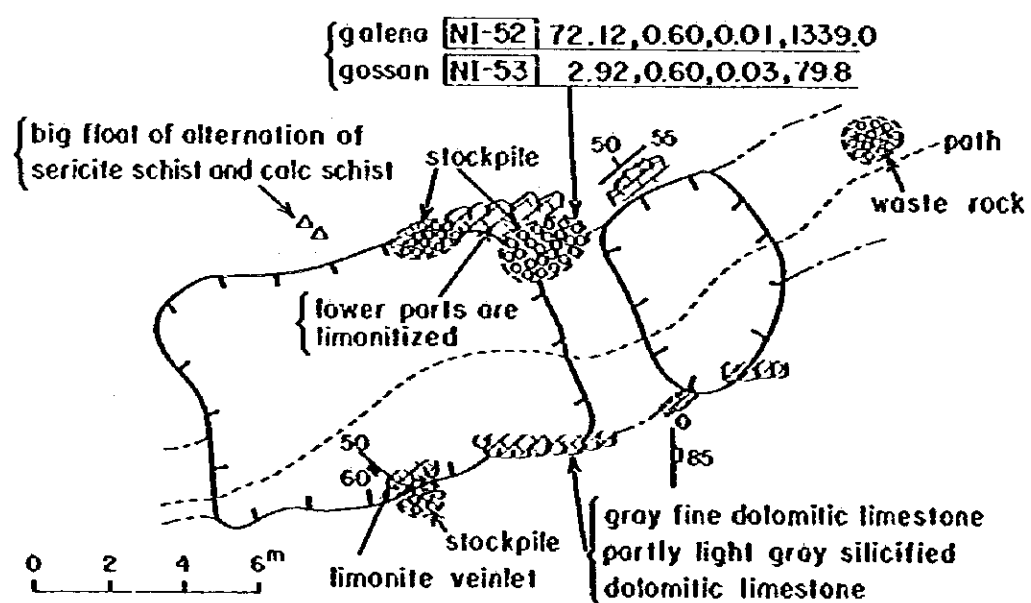


Fig. 1-1 Geological Sketch of Trench, Open Pit and Underground in Furnas Area

The lateral extension of a unit body of pipe formed at the intersection of the aboves is several tens meters and the vertical length reaches up to more than 100 m. Several showings are found, showing a tendency to be concentrated in three places such as the northeastern part of Laranjeiras, the surrounding area of Santo Antonio and Três Bocas.

### 2-3 Assemblage of Ore Minerals

Since the deposits in the survey area have been subjected to a marked oxidation, the oxide minerals are dominantly found even below the surface up to about 100 m. Megascopically, therefore, porous limonite-hematite gossan predominates on the surface, locally accompanied by galena and cerussite. In the underground, the assemblage of limonite-hematite predominates in the places near the surface, where remnants of galena, cerussite and pyrite are found in massive or lenticular form, and galena and pyrite become dominant toward the depth.

The result of macroscopic and microscopic observation of the polished sections of typical ores is as follows (Table A-3-1) :

#### NI-16 (southwestern end)

##### Macroscopic Observation

The sample consists of quartz and black silicified parts, and fine-grained galena dissemination is observed in quartz.

##### Microscopic Observation

Galena, cerussite > chalcopyrite, pyrite, anglesite

Galena occurs in close association with cerussite, showing a texture that cerussite have replaced galena. Abundant remnant of irregularly shaped fine-grained galena is observed in cerussite. Galena and cerussite are found along the cracks in quartz. On the other hand, very fine-grained subhedral to euhedral chalcopyrite and pyrite are disseminated in the black silicified part. A small amount of anglesite is also found in the silicified part.

#### NI-18 (Santo Antonio de Cima)

##### Macroscopic Observation

Zonal arrangement is observed on the surface of polished section, and it ranges from the center outward, coarse galena → black cerussite → aggregate of reddish brown goethite and gangue minerals.

##### Microscopic Observation

Galena > cerussite > pyrite, anglesite, goethite

Galena occupies the most part of the sulphide minerals accompanied with subhedral to euhedral pyrite, which is replaced by cerussite along the cleavage and the periphery.

Cerussite which is in contact with galena contains in abundance irregularly shaped galena and fine-grained euhedral pyrite. Anglesite is found in the aggregate consisting of goethite showing a texture of thin tabular and stringer.

#### NI--24A (north of Barreira)

##### Macroscopic Observation

The sample is predominated by galena, and coarse galena is surrounded by black cerussite along the periphery.

##### Microscopic Observation

Galena ( $10\ \mu\text{m} \sim 1\ \text{cm}$ )  $\gg$  cerussite, goethite  $>$  sphalerite ( $30\ \mu\text{m} \sim 2\ \text{mm}$ )  $>$  pyrite ( $20\ \mu\text{m} \sim 1.5\ \text{mm}$ ), arsenopyrite ( $5 \sim 300\ \mu\text{m}$ )  $>$  tetrahedrite ( $10 \sim 20\ \mu\text{m}$ ), anglesite

Galena is dominant, and galena 0.5 to 1 cm across forms the compact mass. Abundant irregularly corroded sphalerite and pyrite are observed in galena. Sphalerite contains fine-grained galena and euhedral or lath-shaped pyrite. Euhedral arsenopyrite is found in galena. Galena has been replaced by cerussite along the periphery, and partly along cleavage and triangular groove. Abundant relict mineral of fine-grained galena is observed in cerussite.

#### NI--25 (São José)

##### Macroscopic Observation

The sample contains massive galena, being surrounded by thin dark bands.

##### Microscopic Observation

Galena ( $500\ \mu\text{m} \sim 1.2\ \text{cm}$ )  $>$  cerussite  $>$  pyrite ( $20 \sim 200\ \mu\text{m}$ ), goethite  $>$  sphalerite ( $30 \sim 100\ \mu\text{m}$ ), hematite

Galena is dominant among the ore minerals, forming a compact mass. Irregularly corroded pyrite is found in galena in abundance, and cerussite is present along the cleavage. Galena is also replaced by cerussite which contains abundant irregularly corroded fine-grained galena along the periphery.

Hematite occurs partly as the pseudomorph of pyrite.

#### NI--52B (Santo Osvaldo)

##### Macroscopic Observation

The sample is dominant with galena.

##### Microscopic Observation

Galena  $\gg$  pyrite ( $40 \sim 400\ \mu\text{m}$ ), sphalerite, cerussite, goethite  $>$  anglesite, pyrrhotite, covellite

Galena occupies 50 % of the surface of the polished section. Cerussite replaces

galena along the periphery and fills the cracks along the cleavage. Also it contains abundant relict crystals of irregularly corroded subhedral fine-grained galena. Euhedral or subhedral pyrite is found in galena and cerussite. A small amount of sphalerite and pyrrhotite is observed in galena. Covellite is found as the aggregate which has replaced sphalerite and pyrrhotite. Goethite occurs as aggregates and veinlets, and its periphery is partly replaced by anglesite.

#### 2-4 Result of Analysis of Ore

In the survey of this year, 22 ore samples were obtained in total from the ore outcrops and the floats, which were analyzed for four components of Pb, Zn, Cu and Ag (Table I-1). The former three were analyzed by wet method and the last by atomic absorption method.

Since most of the ore outcrops had been mined out, many samples were obtained from the stockpile. Therefore, it seems that the assay result would show the higher values than the grades of crude ore, but it is possible to know a general tendency.

The lead grade is very high in the ore consisting of galena, cerussite and anglesite, showing the maximum value of 72.12% (NI-52). On the other hand, it was less than 1% in the ore consisting mainly of hematite and goethite.

It might not hastily be concluded that the new showings confirmed this time do not warrant economical operation because of low grade of assay result of lead obtained from there when taking into account the extensive oxidation at the surface of the Fumas deposit as mentioned in the previous section.

The grade of zinc is generally low excepting the maximum value of 18.57% shown in the sample NI-23. The ore mainly consisting of sphalerite and galena is partly contained in those produced from the Fumas mine, so that it is considered that there would be local concentration of zinc.

Copper grade is very low in general, showing the highest value of 0.25 (NI-41).

Silver grade is very high in the ore composed of galena, cerussite and anglesite, similar to that of lead, showing the highest value of 2404 g/t (NI-24), and it is low in the ore consisting mainly of hematite and goethite, showing only several grams per ton. Thus positive correlation is shown between the silver grade and lead grade.

Although the silver minerals can not be observed under the microscope, it is strongly possible that silver in the ore of the area is contained in galena and tetrahedrite when taking into consideration that silver is fairly high in grade such as about 30 g/t in some samples (NI-16, 40, 41) in which galena can be observed with the naked eye even if the lead grade is not so high

Table 1-1 Assay Results of Ores of Furnas Area

No.	Sample No.	Location	Occurrence	Pb (%)	Zn (%)	Cu (%)	Ag (g/t)
1	NI - 15	the western extremity	limonite-calcite vein (W: 0.1~1.0m)	0.41	0.02	0.01	4.7
2	NI - 16	do.	float of galena-quartz vein	0.43	0.02	0.04	29.1
3	NI - 18	St. Antonio de Cima	float of galena-Pb oxide	51.17	0.44	0.03	1036.0
4	NI - 19	St. Antonio de Baixo	float of gossan	25.58	0.24	0.04	150.5
5	NI - 21	Tres Bocas	do.	0.20	0.12	0.04	0.9
6	NI - 22	do.	do.	0.23	0.02	0.09	0.9
7	NI - 23	Vala 8	galena-Pb oxide vein (W: 0.15 m)	16.17	18.57	0.06	249.5
8	NI - 24	east side of Barreira	do. (W: 1.0 m)	68.75	1.93	0.03	2404.0
9	NI - 25	São José	do. (W: 0.3 m)	70.96	0.77	0.06	779.8
10	NI - 30	the eastern outside	float of gossan	2.24	0.15	0.01	23.4 (Au: 125.3)
11	NI - 33	west side of FK-10.0	do.	0.67	0.41	0.03	3.5
12	NI - 40	FA-9.0	galena-quartz vein (W: 2 ~ 5 cm)	0.57	0.02	0.03	26.8
13	NI - 41	do.	do.	0.53	0.02	0.25	23.9
14	NI - 42	FH-10.2	float of gossan	0.99	0.02	0.00	6.1
15	NI - 49	FJ-10.0	float of quartz	0.08	0.01	0.00	0.2
16	NI - 51	FB-7.7	quartz vein (W: 0.6 m)	0.09	0.01	0.00	0.3
17	NI - 52	St. Oswaldo	float of galena	72.12	0.60	0.01	1339.0
18	NI - 53	do.	float of gossan	2.92	0.60	0.03	79.8
19	NI - 57	FJK-3.5	quartz vein (W: 5 cm)	0.08	0.01	0.01	3.0
20	JG - 15	FD-8.5	galena-quartz vein (W: 3 cm)	0.07	0.02	0.00	5.9
21	JG - 19	FFG-7.0	float of gossan	0.13	0.01	0.00	1.2
22	JG - 20	do.	do.	0.16	0.01	0.03	1.4

and that silver is present in a form of isomorphous substitution in sulphide minerals such as galena and tetrahedrite as has been reported.

Consequently, the ore to warrant economic operation is Pb – Ag (–Zn) ore.

#### 2-5 Relationship between Geologic Structure and Ore Deposit

The strata of the survey area show an homoclinal structure generally striking N60°E and dipping 45°NW, in which the fault and fold on a large scale is not observed.

Taking into consideration comprehensively that the area is situated, from the standpoint of regional geologic structure, in the middle between the Calabouço syncline and the Serra Manduri anticline, both of which are of NE–SW system and that the lateral compression of NW–SE system was obtained by analysis of principal stress field of the fractures in which the ore deposits are emplaced, it is considered that the vein fractures in the survey area were simultaneously formed with the folding. A part of geotectonic history shown in the report of Phase III is cited in Fig. 1-5. It is interesting that the figure shows that the Furnas deposit is positioned at a part of limb where the AIII<sub>3</sub> member suddenly decreases its thickness from the anticlinal axis which is of one order lower than the Serra Manduri anticline located to the southeast.

The showings in the area have a tendency topographically to be concentrated to the saddle as is evidently shown in Plate 1-3, which may suggest that the structurally weak part and the position of ore deposit would be relevant.

#### 2-6 Relationship between Geologic Structure and the Result of Geophysical Survey

Taking into account the facts hitherto mentioned, the relationship between the result of geological survey and the result of electric survey (IP, SIP) is discussed in the following. These surveys were conducted in the areas which include the surrounding area of Três Bocas mineral showing and Santo Antonio mineral showing located to the southwest of the Laranjeiras deposit at the southwesternmost end of the area in which the lower part remains unexplored, where operation for exploration and mining are being performed at the Furnas mine.

The result of the electric survey revealed that apparent resistivity on each line resulted in to show a zonal arrangement from the northwestern part toward the southeast such as high resistivity, low resistivity, high resistivity and intermediate resistivity respectively. Such a zonal distribution is well consistent with the distribution of geology and the geologic structure of the area, and seems to reflect apparent resistivity of the members such as the upper part of AIII<sub>3</sub>, the middle part of AIII<sub>3</sub>, the lower part of AIII<sub>3</sub> and the AIII<sub>2</sub>.

The distribution of FE is also harmonious with the geologic structure, showing a zonal

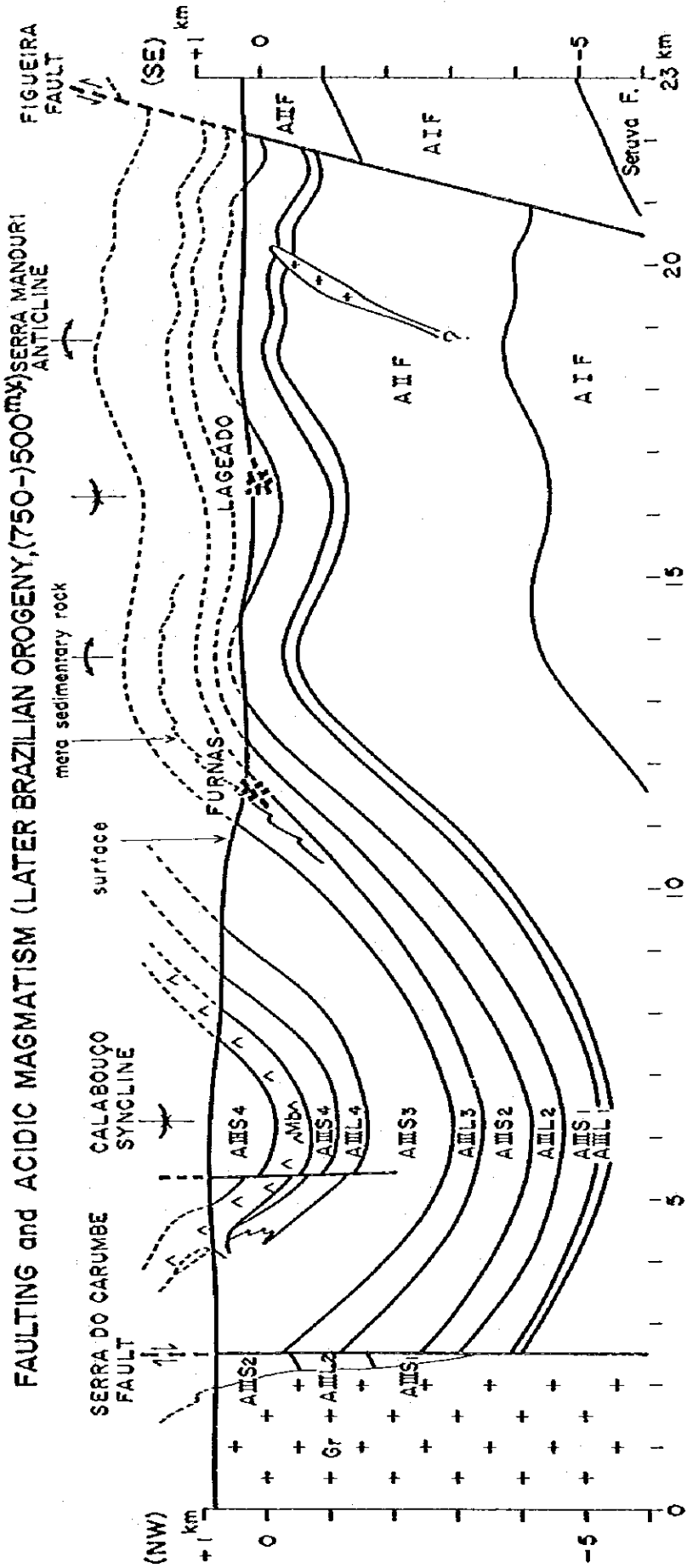


Fig. I-5 Geotectonic Profile of Phase III Surveyed Area



arrangement from the northwest toward the southeast such as low FE, high FE, low FE and high FE respectively in a rough way. Among these, the high FE zone in the central part is likely to have been caused by a strong IP effect of pyrite dissemination in pelitic dolomite and graphitic sericite schist intercalated in the middle part of the AIII<sub>3</sub> member, and the high FE zone in the southern part seems to have been caused by a strong FE effect of film-like graphite and pyrite dissemination contained in sericite schist in the AIII<sub>2</sub> member.

On the other hand, no marked FE anomaly was detected in the lower part of the AIII<sub>3</sub> member, which is the lead ore-bearing horizon. The reason for this is considered to be as follows: the various cause made difficult to detect FE anomaly, such as that the size of ore deposit was too small, that the host rock was non-polarizable and of high resistivity and that high FE anomalies in the hanging wall and the footwall of the ore horizon showed an effect of interference.

## 2-7 Future Exploration

Since the ore bearing horizon of the Furnas deposit and the deposits of the same kind has been made clear, it is considered to be an effective method of exploration to extract the promising mineralized zone by carrying out detailed soil geochemical survey or rock geochemical survey in the area the ore horizon might be distributed.

Because it became clear that the ore horizon of the Furnas deposit continues to the areas beyond the boundary of the survey area, it is desirable to conduct detailed geological survey and geochemical survey.

## PART II GEOPHYSICAL SURVEY

## CHAPTER I OUTLINE OF GEOPHYSICAL SURVEY

### 1-1 Purpose of Survey

By the geological survey in Phase III, the possible existence of veinlets and network type deposits has been expected in the southern extension of the Furnas Mine. On the basis of the results, the Spectral Induced Polarization (SIP) and Induced Polarization (IP) methods were performed in Phase IV survey in order to clarify the possible existence of the concealed ore deposits in the Furnas survey area.

### 1-2 Survey Area

The survey area, which has the extent of 1.5 km x 1.5 km, is situated in about 20 km east of Apiai city.

### 1-3 Survey Period

Field survey	Oct. 28, 1983 – Feb. 7, 1984
Analysis and report making	Feb. 8, 1984 – May 30, 1984

## CHAPTER 2 SIP AND IP METHODS

### 2-1 Survey Method

#### 2-1-1 Survey Method

The existence of the induced polarization phenomenon has been well known theoretically and experimentally and IP method has been conventionally used for mineral exploration, and SIP method has been recently utilized for mineral discrimination. Both methods stand upon the same phenomenon which resembles the discharge of a capacitor or the variation of the impedance of a RC circuit. There are two operating techniques in IP method: time domain and frequency domain. In this survey, frequency domain method with 3 Hz and 0.3 Hz was adopted.

In SIP method, induced polarization phenomenon is measured as a spectral characteristic of frequencies ranging from 0.125 Hz to 8 Hz, which enable us to distinguish the geology, ore type and so on.

Specifications and instruments are shown on Table II-1.

**Table II-1 Specifications and Instruments**

	SIP survey	IP survey
Line length	4.5 km	15.0 km
Line interval	450 m – 750 m	150 m
Electrode spacing	100 m	100 m
Electrode configuration	Dipole-dipole	Dipole-dipole
Space factor	n = 1 – 5	n = 1 – 5
Auxiliary survey	Laboratory measurement of 28 samples	In-situ measurement at 13 localities
Instruments	Transmitter FT-4 Receiver GDP-12	Transmitter CHT-7802 Receiver CHR-7801 Receiver CHR-7802

Schematic Diagram of SIP measurement is shown in Fig. II-2.

#### 2-1-2 Survey Line

Eleven survey lines were planned and set using a pocket compass and measuring tape to cross perpendicularly the geological structure, and three communication lines for SIP survey were also set parallel to the survey lines 25 m apart from each Line of FA, FD and FI. Electrode stations are named 0, 1, ..., 14, and 15 from the south end of each line. A table of survey lines is shown on Table II-2.

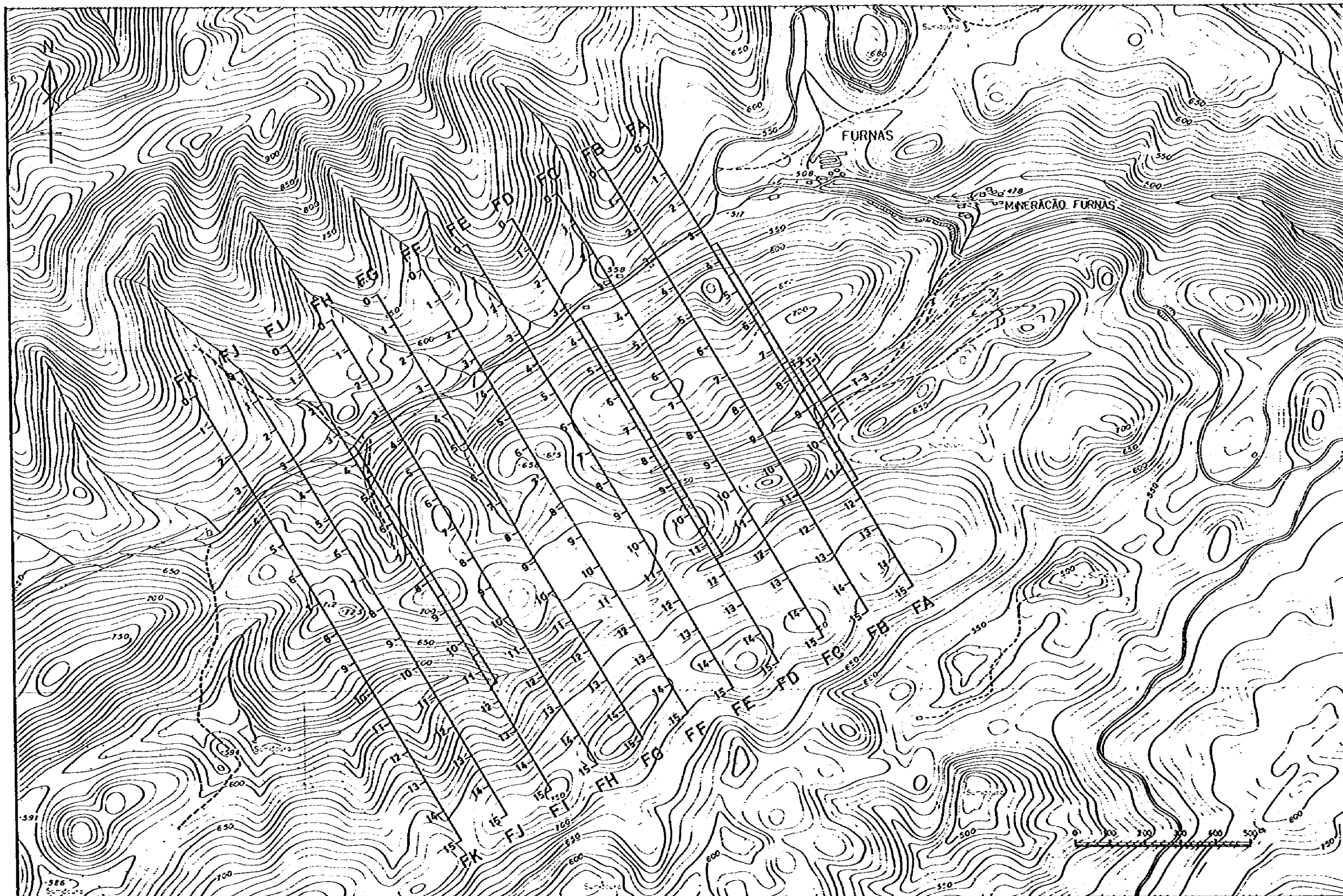


Fig. II-1 Location Map of IP & SIP Survey Lines

Table II-2 List of Survey Lines

Line Name	SIP survey		IP survey	
	Line Length (km)	Observation Point	Line Length (km)	Observation Point
FA	1.5	49	1.5	55
FB			1.5	55
FC			1.5	55
FD	1.5	49	1.5	55
FE			1.5	55
FF			1.5	55
FG			1.5	55
FH			1.5	55
FI	1.5	49		
FJ			1.5	55
FK			1.5	55
<b>Total</b>	<b>4.5 km</b>	<b>147 points</b>	<b>15.0 km</b>	<b>550 points</b>

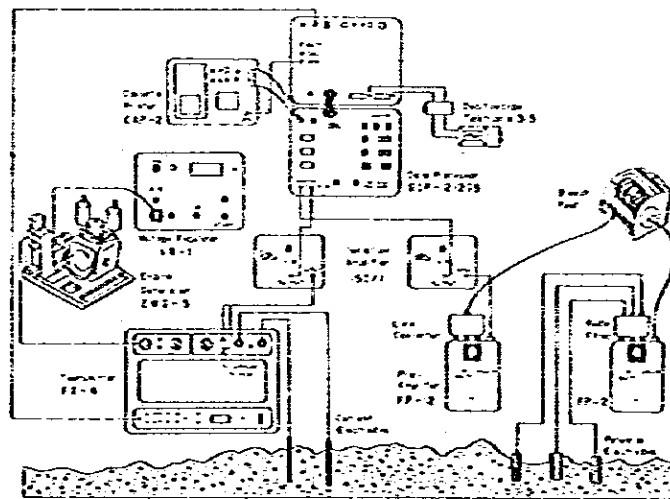


Fig. II-2 Schematic Diagram of SIP Measurement

2-1-3 Procedure for Data Analysis

The analysis was done following the flow chart shown in Fig. II-3.

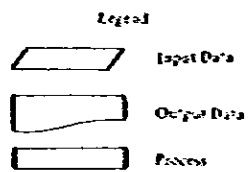
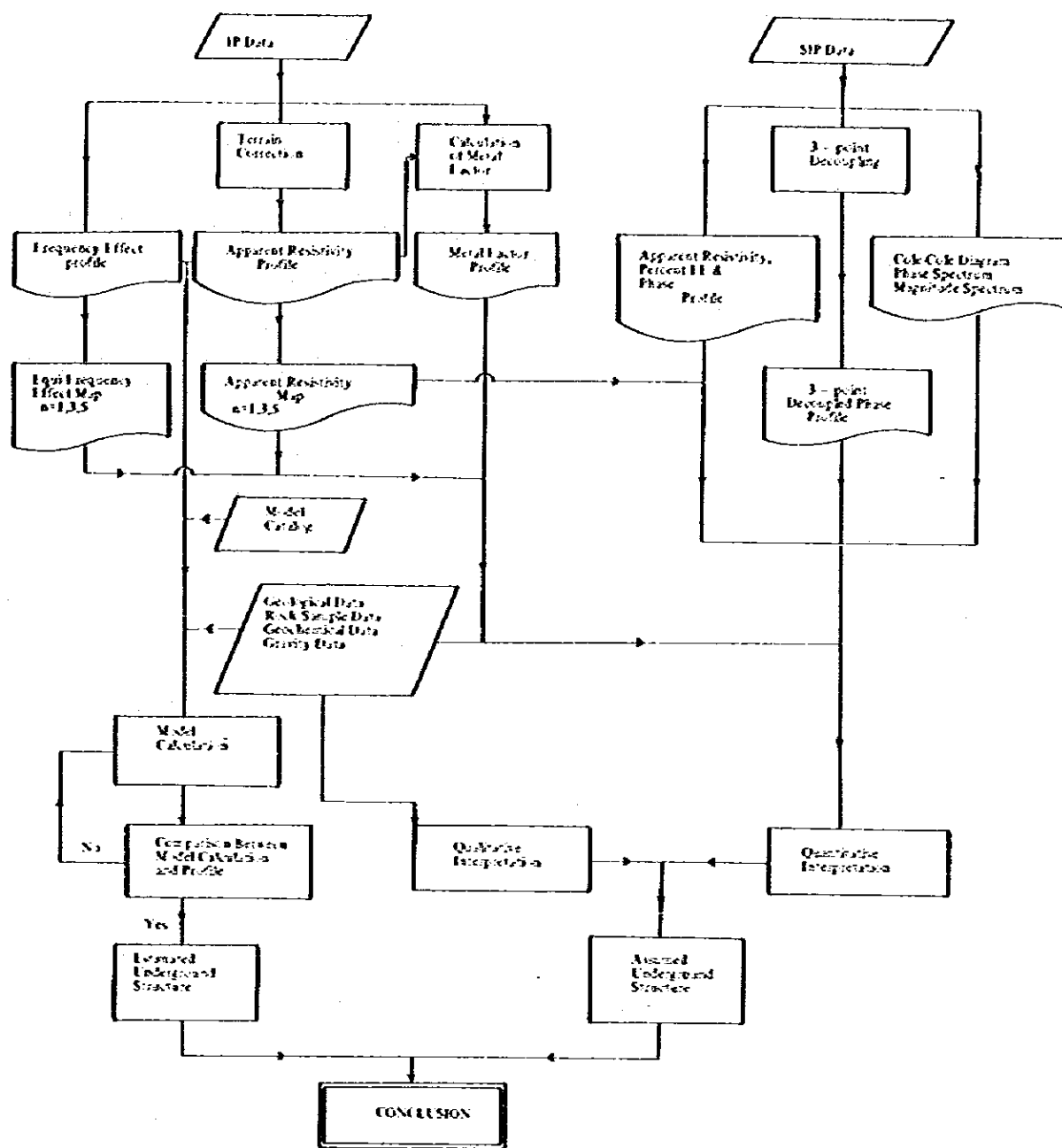


Fig. II-3 Flow Chart of IP & SIP Data Analysis

## 2-2 Results of SIP Method

SIP measurement was performed on Lines FA, FD and FI. Among them, IP measurement was also made in Lines FA and FI. Line FA was set to cross over the deposits under exploitation and other two lines set in the vicinity of the most promising area for deposits.

### 2-1-1 Pseudosection

Seven kinds of pseudosection were presented: apparent resistivity (AR), raw phase, 3-point decoupled phase (3PDP), percent frequency effect (PFE), phase spectrum, cole-cole diagram and magnitude spectrum.

#### (1) AR pseudosection (Fig. II-4)

The section shows the AR measured in 0.125 Hz. The overall distribution of resistivity shows high-low-medium-high values from the north to the south. The resistivity pattern agrees well with the geological structure. High resistivity of more than 2,500  $\Omega\text{m}$  is detected north of No. 3, low resistivity of less than 1,000  $\Omega\text{m}$  between No. 3 and No. 7, and relatively high resistivity of more than 1,000  $\Omega\text{m}$  south of No. 7. The high resistivity may reflect compact rocks.

#### (2) Raw phase pseudosection (Fig. II-5)

The values exceeding  $-20$  mrad are interpreted as an anomaly. Two remarkable anomalies are observed between No. 3 and No. 8, and between No. 12 and No. 14 on each line. They are most widely distributed on Line FI. The indications of more than  $-30$  mrad within both anomalies may correspond centers of those. On Line FA, both indications dip northward. On the other hand, on Lines FA and FI, an indication between No. 3 and No. 8 dips northward, while one between No. 12 and No. 14 dips nearly vertically. The anomalies between No. 12 and No. 14 on Lines FA, FD and FI show a similar pattern and are diagnostic.

#### (3) 3PD pseudosection (Fig. II-6)

Three frequencies of 0.125 Hz, 0.375 Hz and 0.625 Hz were utilized to introduce the phase in extremely low frequency. The contour pattern is quite similar to the raw phase 0.125 Hz.

#### (4) PFE pseudosection (Fig. II-7)

PFE is calculated out by using 0.125 Hz and 1.0 Hz. Two anomalies of more than 3% are observed between No. 2 and No. 8 and No. 12 and No. 14. These anomalies are expected to continue to the depths of between No. 8 and No. 11. The center of anomaly of more than 5% may directly reflect the anomalous source. Though this anomalous source stretches to the depths dipping northward from the surface on Lines FA and FD, it disappears on Line FI. But the anomaly dipping southward, which isn't detected on Lines FA and FD, is detected near No. 3 - No. 5 on Line FI. On the other hand, the anomalies, which are detected around No. 12 - No. 14 on each



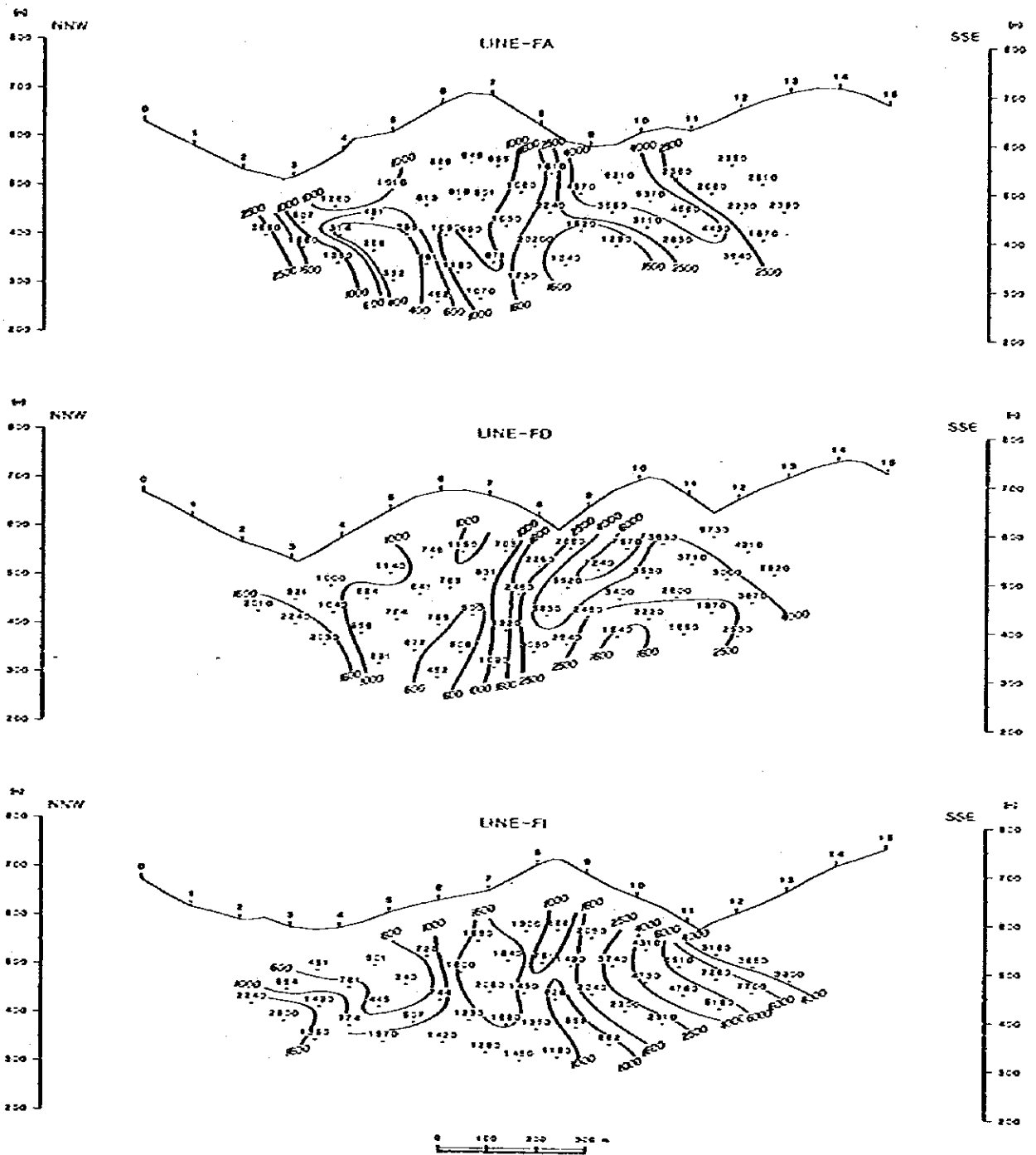
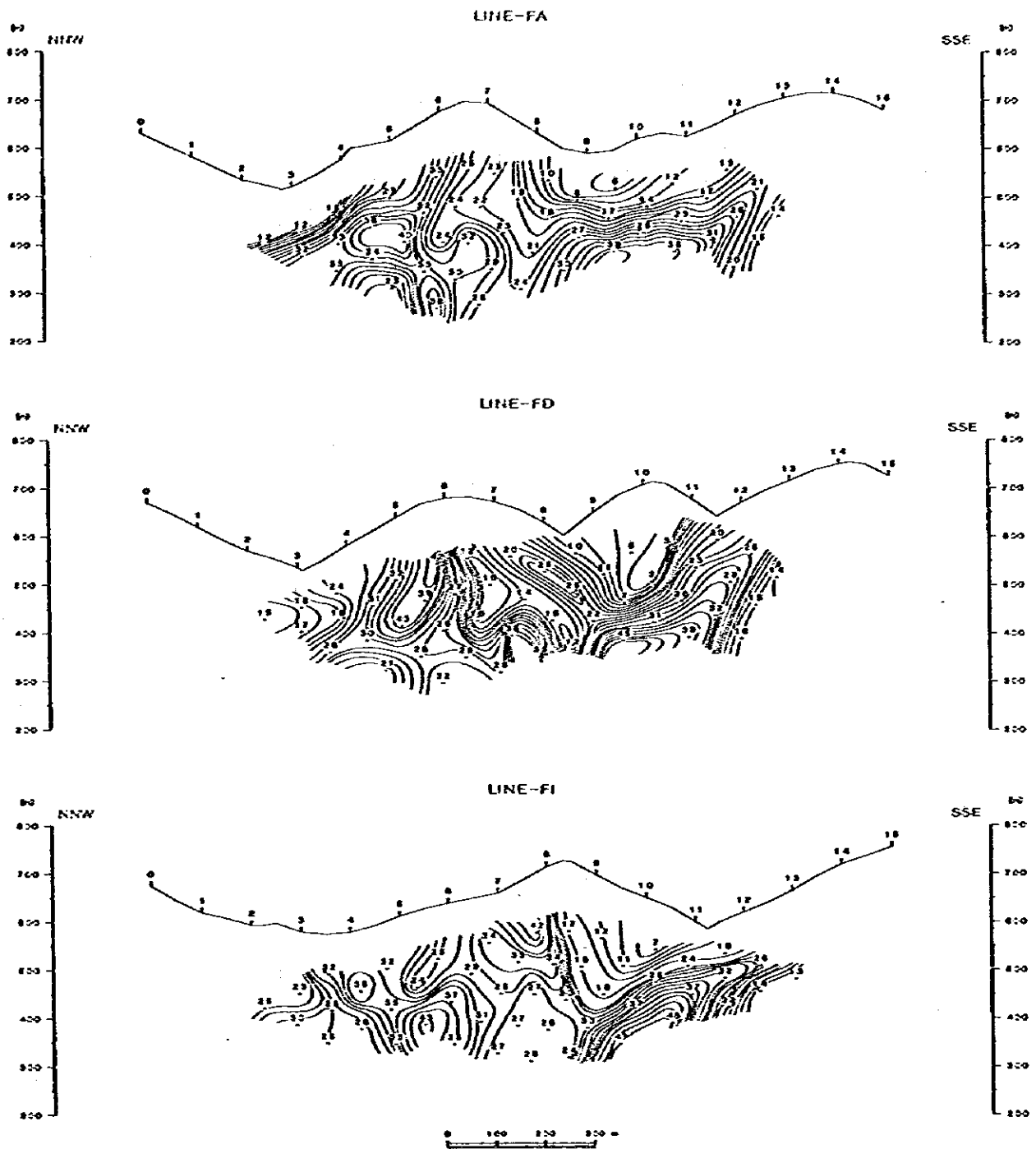
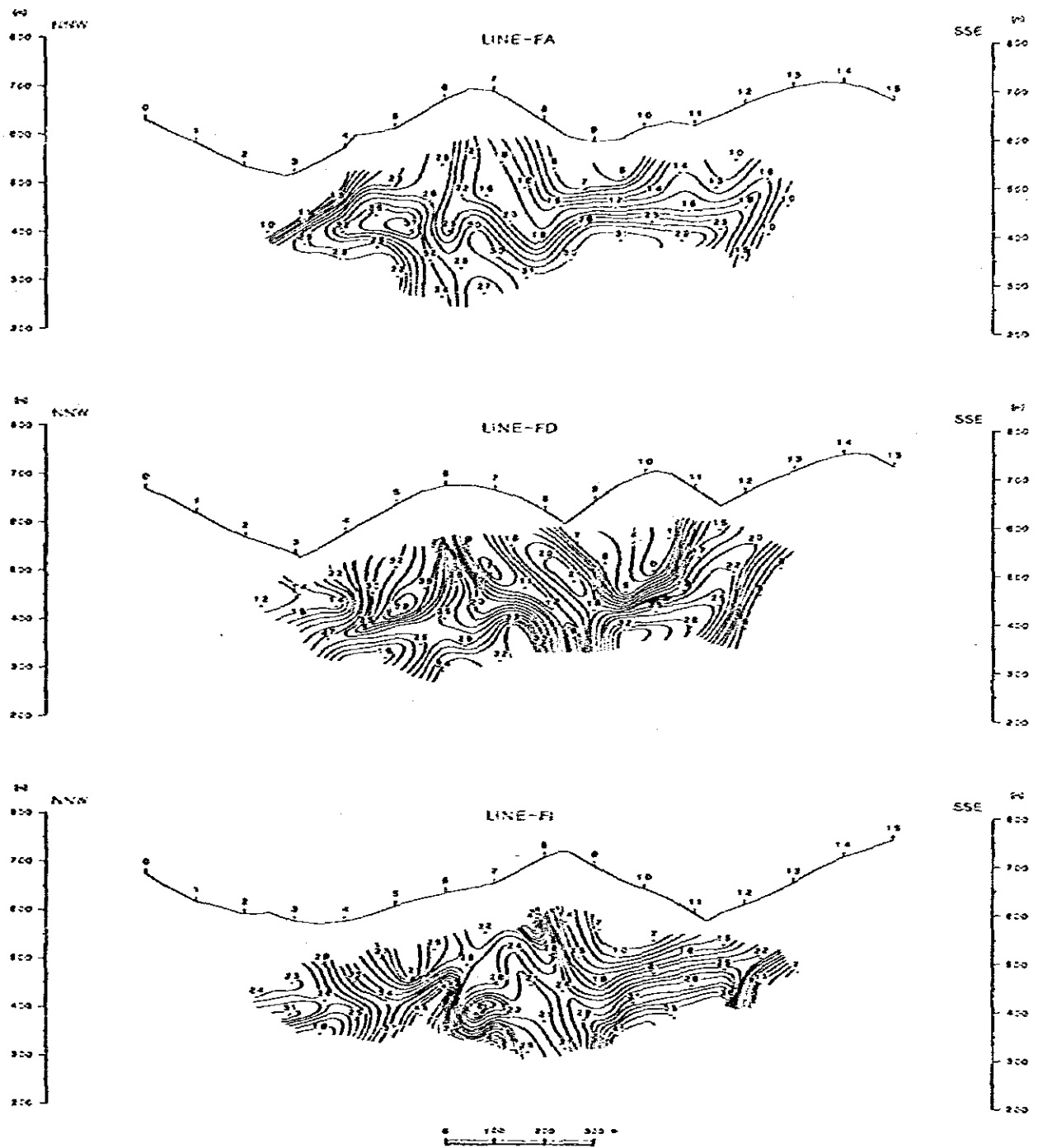


Fig. II-4 SIP Pseudosection of Apparent Resistivity(0.125Hz)  
(Line-FA, FD, FI)



**Fig. II-5 SIP Pseudosection of Raw Phase(0.125Hz)  
(Line-FA, FD, FI)**



**Fig. II-6 SIP Pseudosection of 3-Point Decoupled Phase  
 (0.125-0.375-0.625Hz)(Line-FA, FD, FI)**

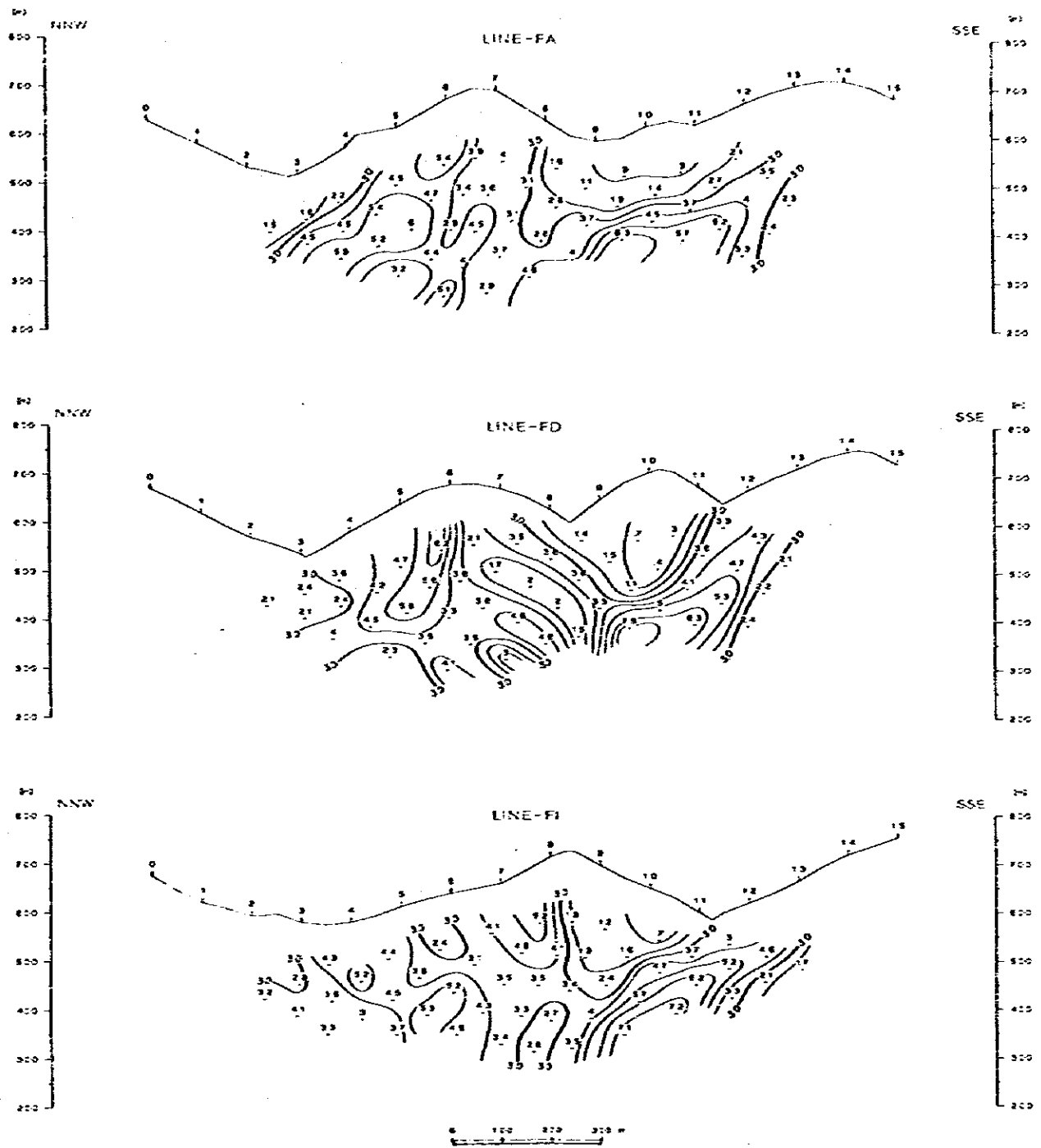


**Fig. II-7 SIP Pseudosection of Percent Frequency Effect (0.125-1.0Hz)(Line-FA, FD, FI)**

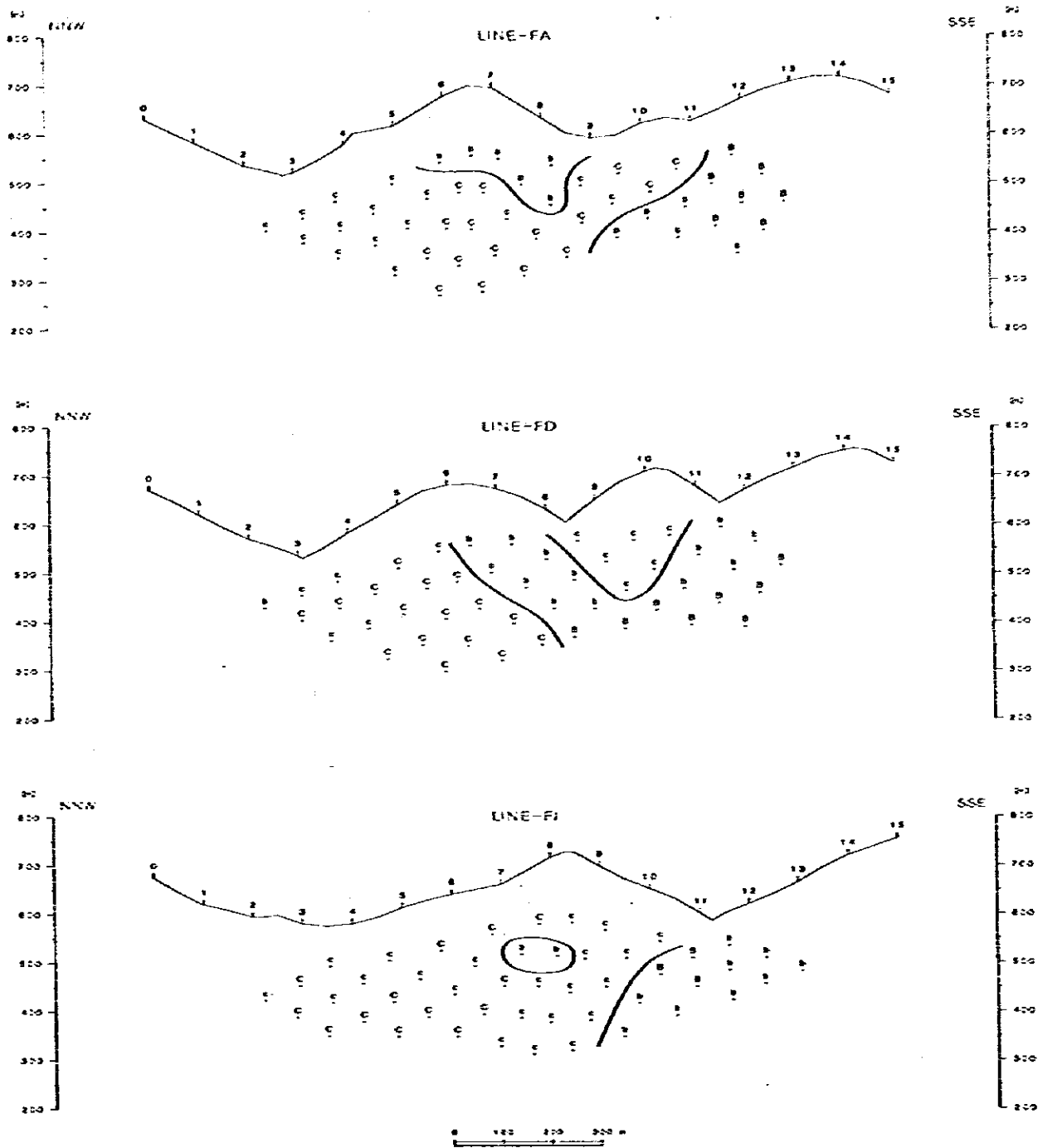


**Fig. II-8 Classification of Phase Spectral Type**

line, have almost same shapes. It is understood that the IP effect by this anomalous source is as intensive as that detected on Lines FA and FD.

**(5) Phase spectrum (Fig. II-9-1 ~ 3)**

In general, it can be said that an IP anomaly accompanied by high resistive rocks has less influence of electro-magnetic coupling. The detected spectra of 0.125 Hz and 2 Hz on each line reflect high resistivity rocks, so that it shows gentle increase under a little influence of electro-magnetic coupling. The spectra detected at the northern side of each line show nearly constant in the range from 0.125 Hz to 5 Hz. These spectra indicate inverse V shape extending to the depth, and center of each spectra is around No. 5.

On the other hand, the spectra detected at the southern side of each line have intensive IP effect stretching to the depths from the surface dipping northward.

The phase of these spectra increase as the frequencies increase, so they must be affected by electro-magnetic coupling, which indicates the existence of low resistivity rock. This type of spectrum is called "B" type. Other anomalous spectra are detected at n=1-2 around No. 9-No. 11 on each line, and are also influenced by electro-magnetic coupling.

**(6) Magnitude spectrum (Fig. II-10-1 ~ 3)**

As the characteristics of the two anomalies mentioned above, it is eminent that the magnitude sharply decreases as the frequency increases. As for the decreasing rate of the magnitude, the northern anomaly is a little smaller than that of the southern one, and also the magnitude has a characteristic tendency to increase around 8 Hz. This tendency is observed broadly in the northern side of No. 8.

**(7) Cole-Cole diagram (Fig. II-11-1 ~ 3)**

Three frequency patterns are detected. The first one is that an imaginary component sharply increases at around 8 Hz as the frequency increases. The next one is that a real component is nearly constant and an imaginary component also increases at low frequency range. The last one is that an imaginary component increases gradually as the frequency increases. The first one is detected on each line around No. 4 -- No. 8.5 and it stretches to the depths from the surface dipping northward. The next one is detected on each line at n=1-2 around No. 9 -- No. 11. The last one is detected on each line around No. 11 -- No. 14 and it stretches to the depths from the surface.

**2-2-2 Laboratory Measurement**

An electrical property measured at the surface does not necessarily indicate a real property of rock. Although the rock samples are sometimes collected from overburden and/or weathered

rock, it is important to know the real property of rock for interpretation. Accordingly, 28 rock samples were collected at the locations shown in Fig. II-12, and measurement of resistivity, PFE and phase were made for these samples by SIP method. Block diagram of laboratory measurement is shown in Fig. II-13, and Table II-3 shows the results. Also phase spectra of some rock samples are shown in Fig. II-14 ~ 16.

- (1) Specimens from L<sub>3</sub>PsA, S<sub>2</sub>Ps and L<sub>3</sub>dolB show high PFE, and resistivity of L<sub>3</sub>PsA is low to medium, and L<sub>3</sub>dolB varies from low to high, and S<sub>2</sub>Ps is medium.
- (2) Resistivity of specimens taken from L<sub>3</sub>S<sub>3</sub>, L<sub>3</sub>dolC, and L<sub>2</sub> varies a little and is relatively low.
- (3) Medium to high PFE of L<sub>3</sub>PsA, S<sub>2</sub>Ps and L<sub>3</sub>PsB seem to be due to graphite in schist, because they scarcely bear sulphide.
- (4) Medium to high PFE of L<sub>3</sub>dolB is due to pyritization in the specimen.
- (5) A spectral type of specimen taken from L<sub>3</sub>dolB is similar to that of field data observed at the northern of each line.
- (6) A low resistivity of specimen from S<sub>2</sub>Ps is due to weathering.
- (7) A spectrum in dolomitic limestone shows nearly a constant phase between 0.125 Hz and 0.625 Hz and increases in phase at the high frequency range from 1 Hz to 40 Hz, and decreases at higher frequency range.

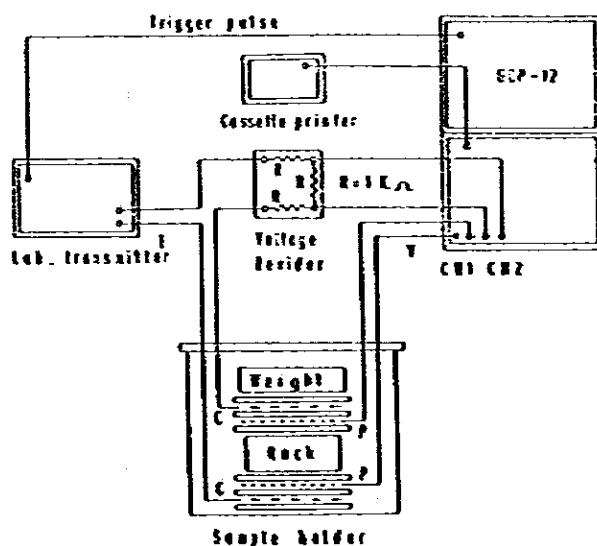


Fig. II-13 Block Diagram for Laboratory Measurement

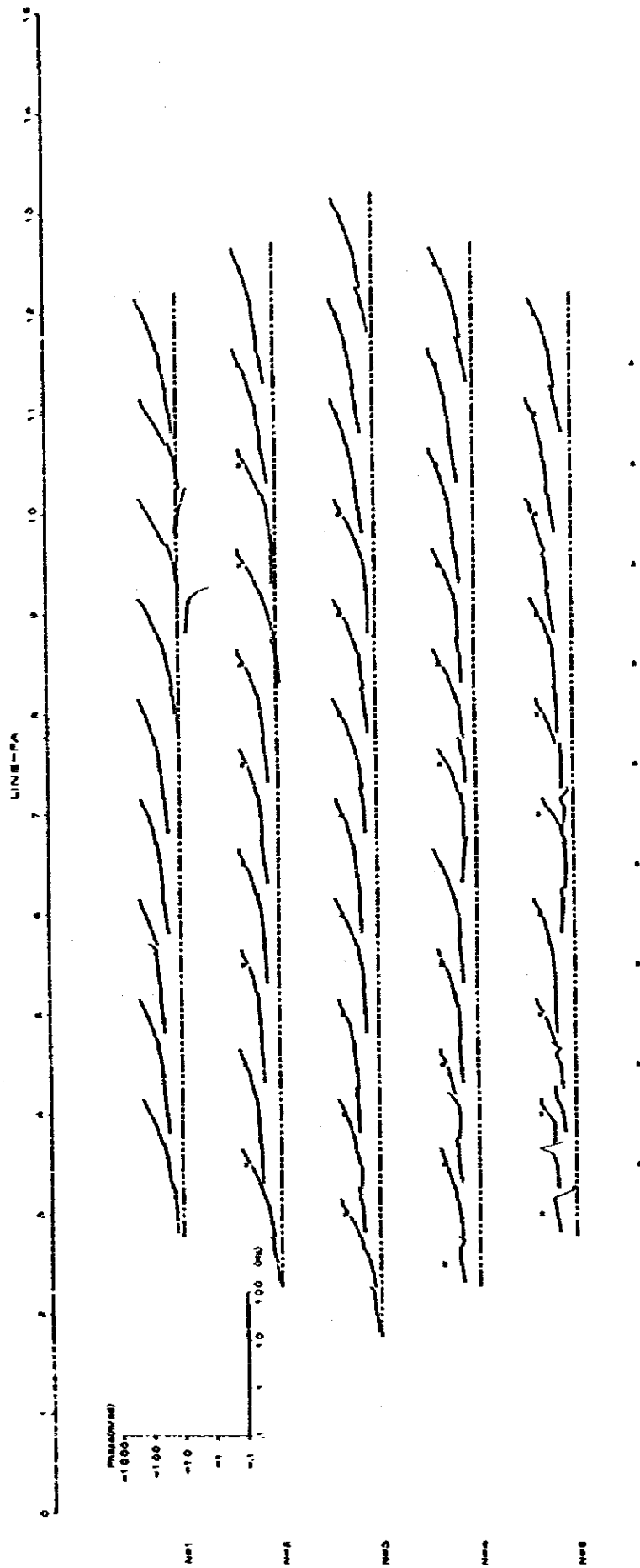


Fig. II-9-1 Phase Spectrum (Line-FA)



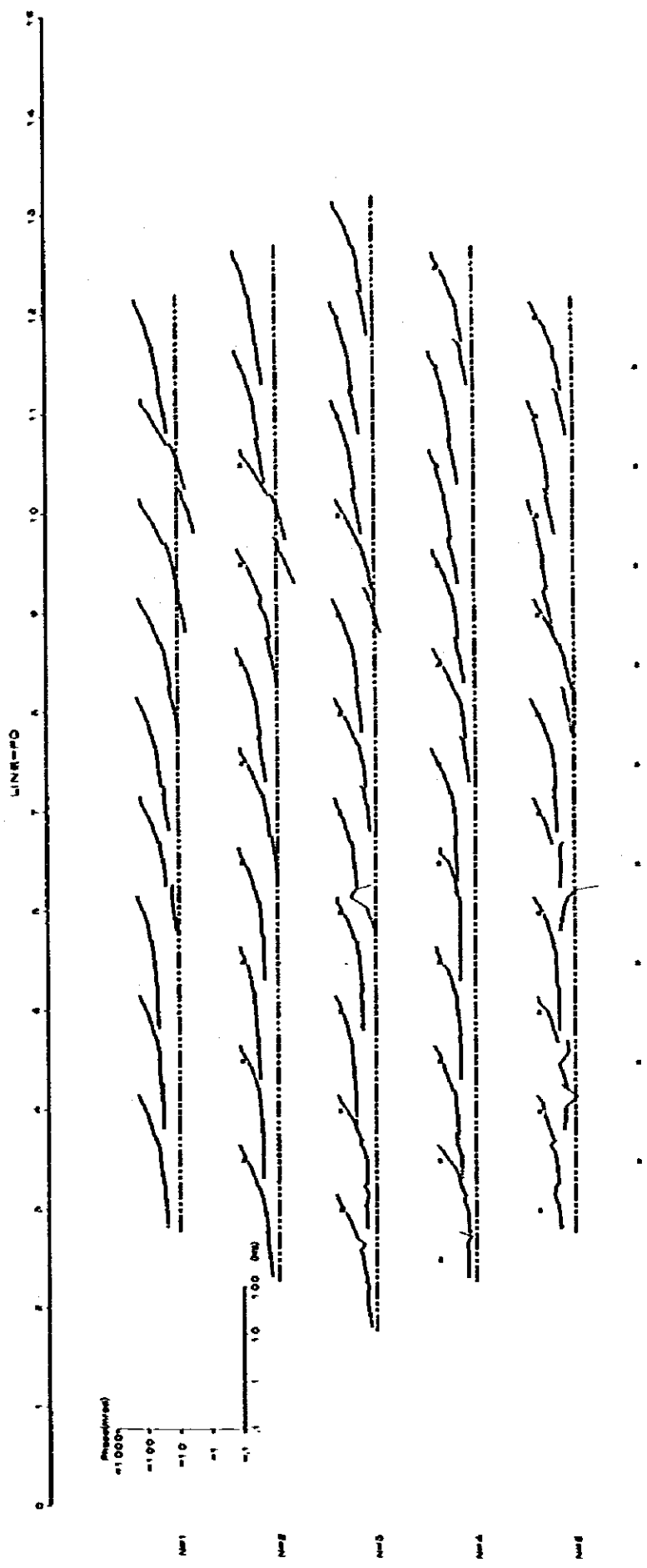


Fig. II-9-2 Phase Spectrum (Line-FD)

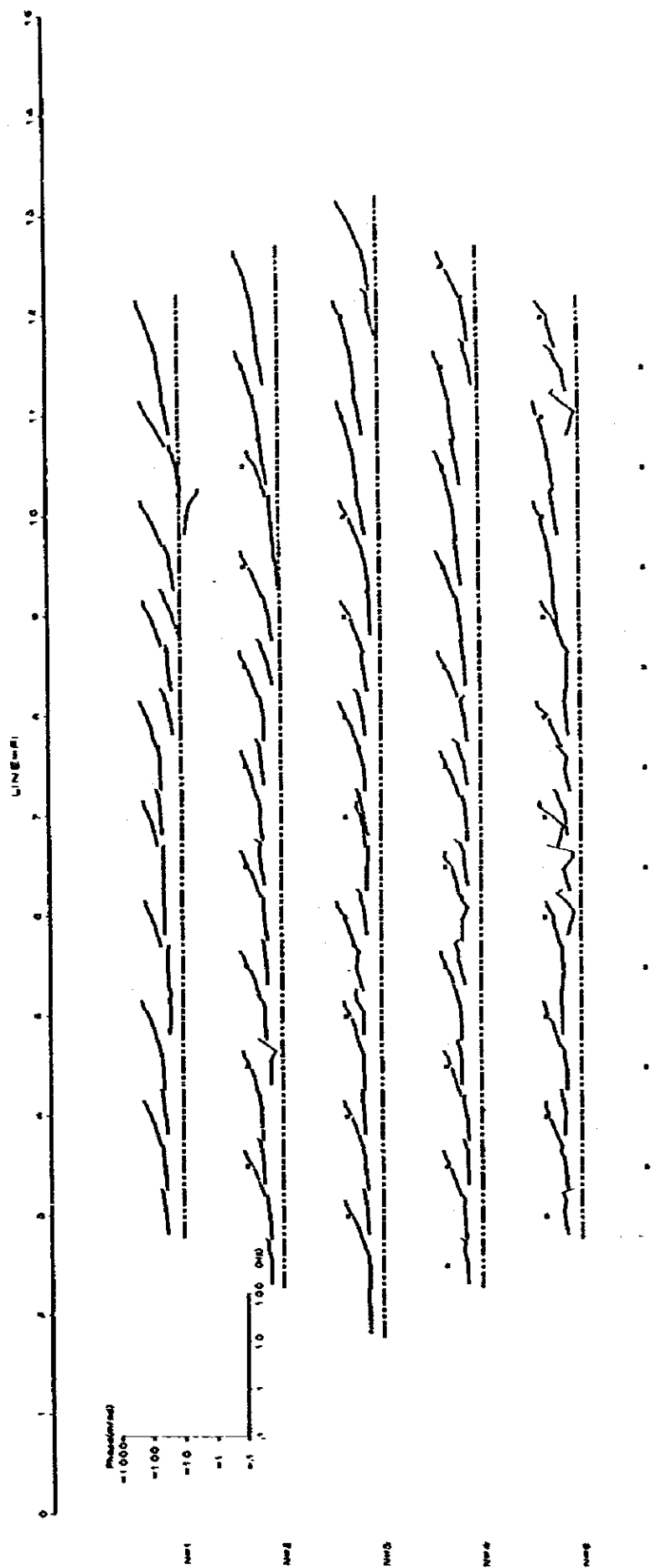


Fig. II-9-3 Phase Spectrum (Line-FI)

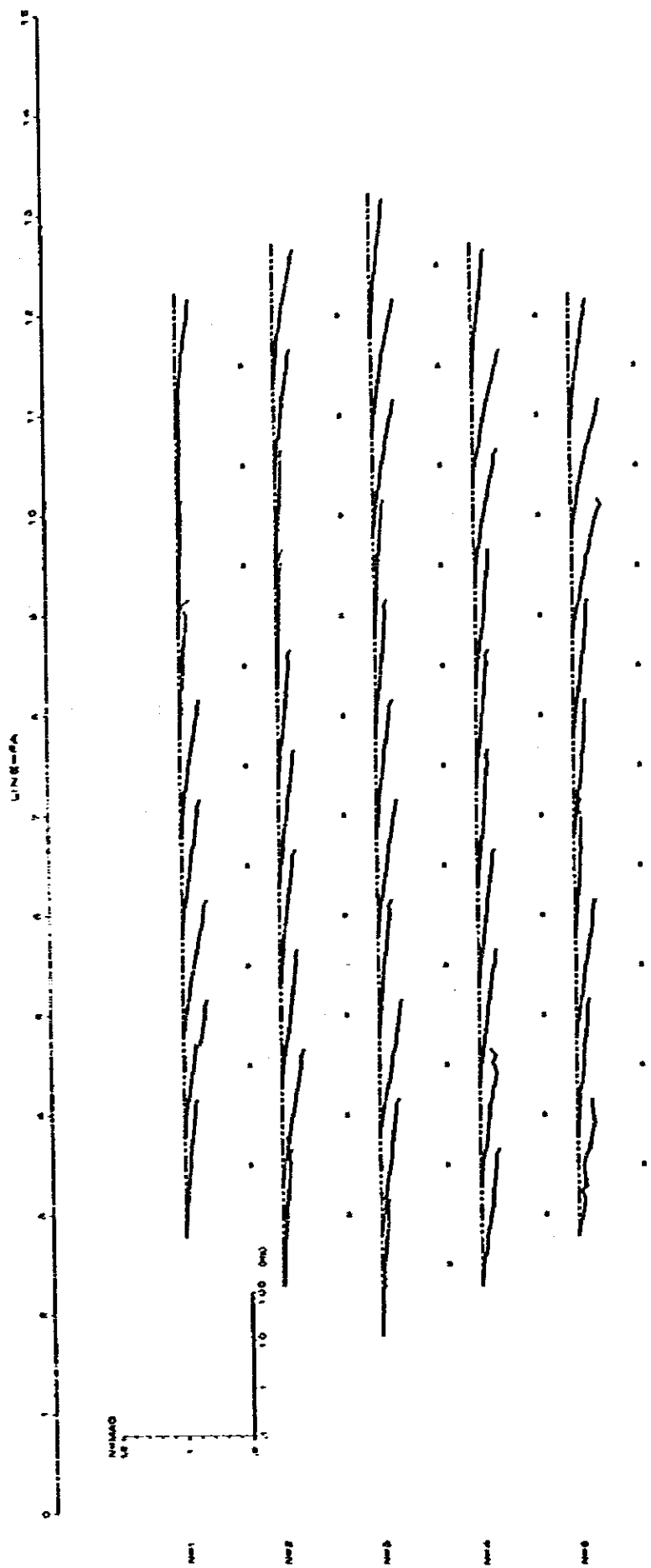


Fig. II-10-1 Magnitude Spectrum (Line-FA)

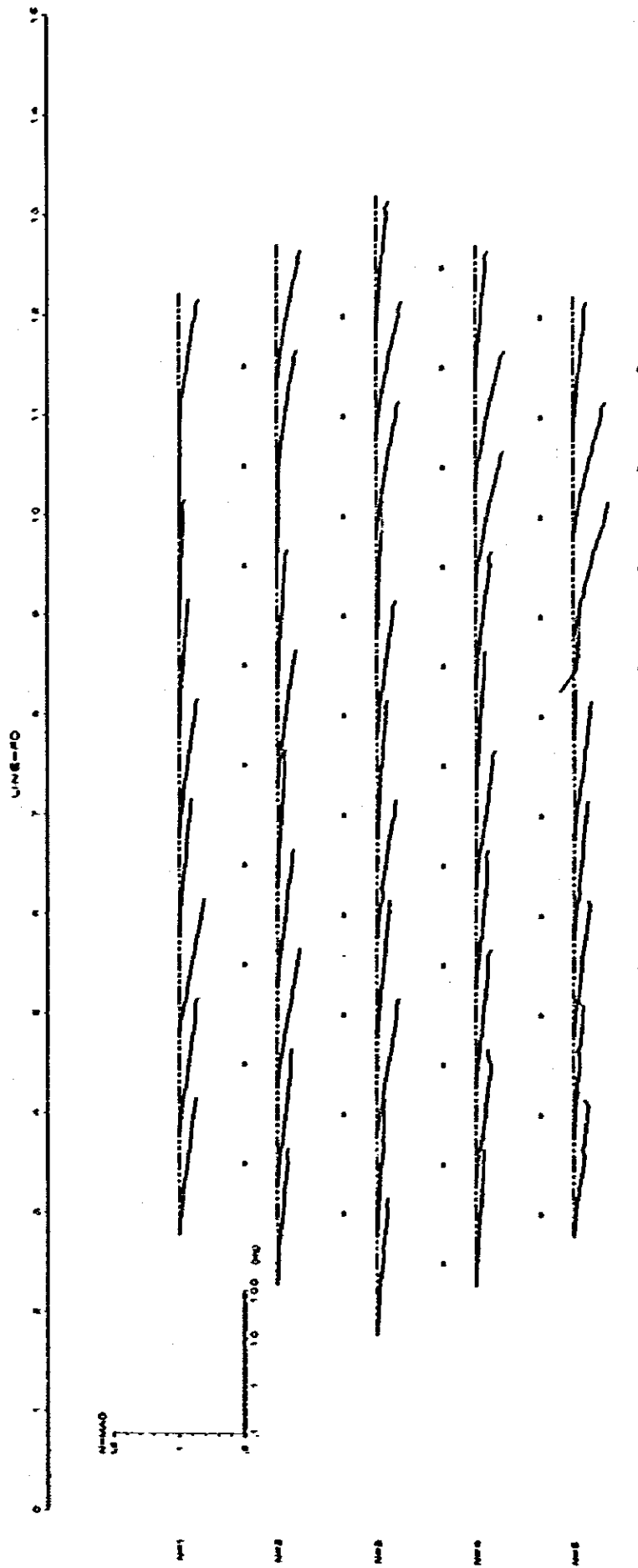


Fig. II-10-2 Magnitude Spectrum (Line·FD)

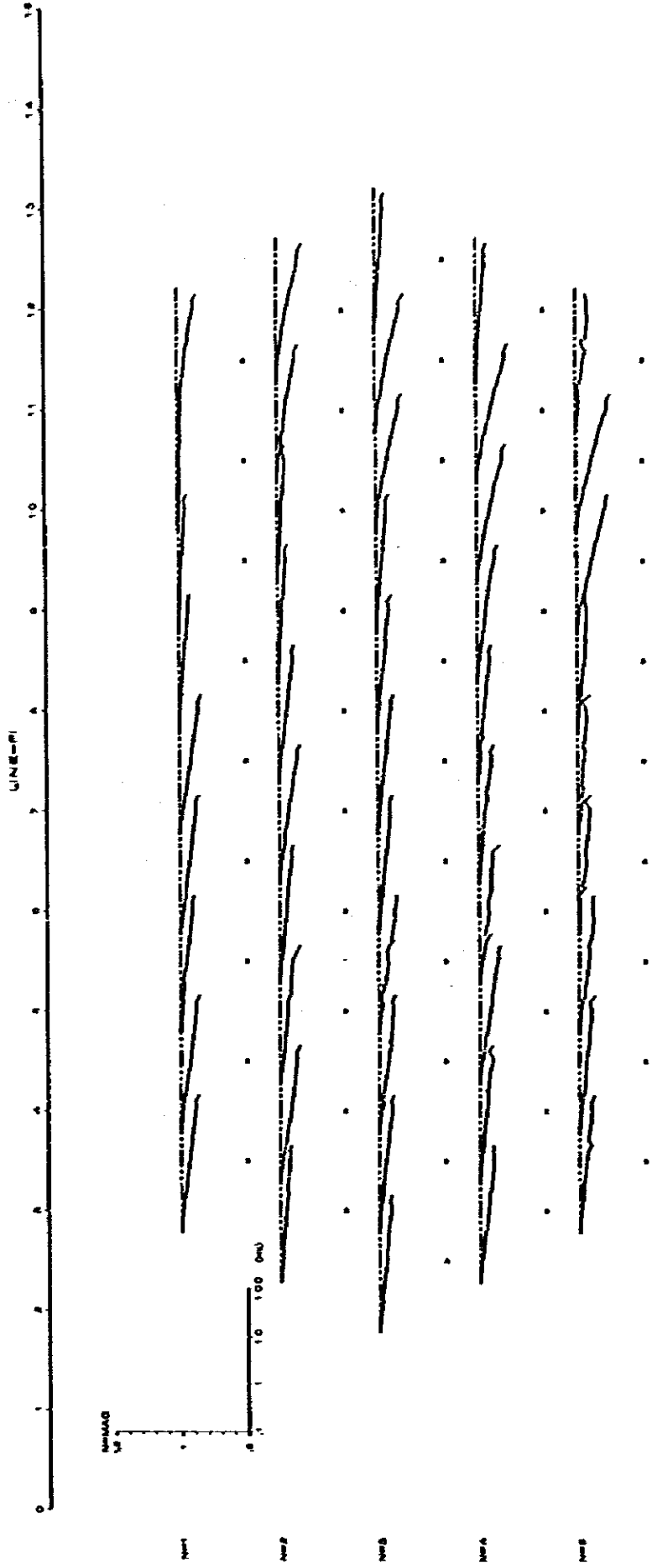


Fig. II-10-3 Magnitude Spectrum (Line-FI)

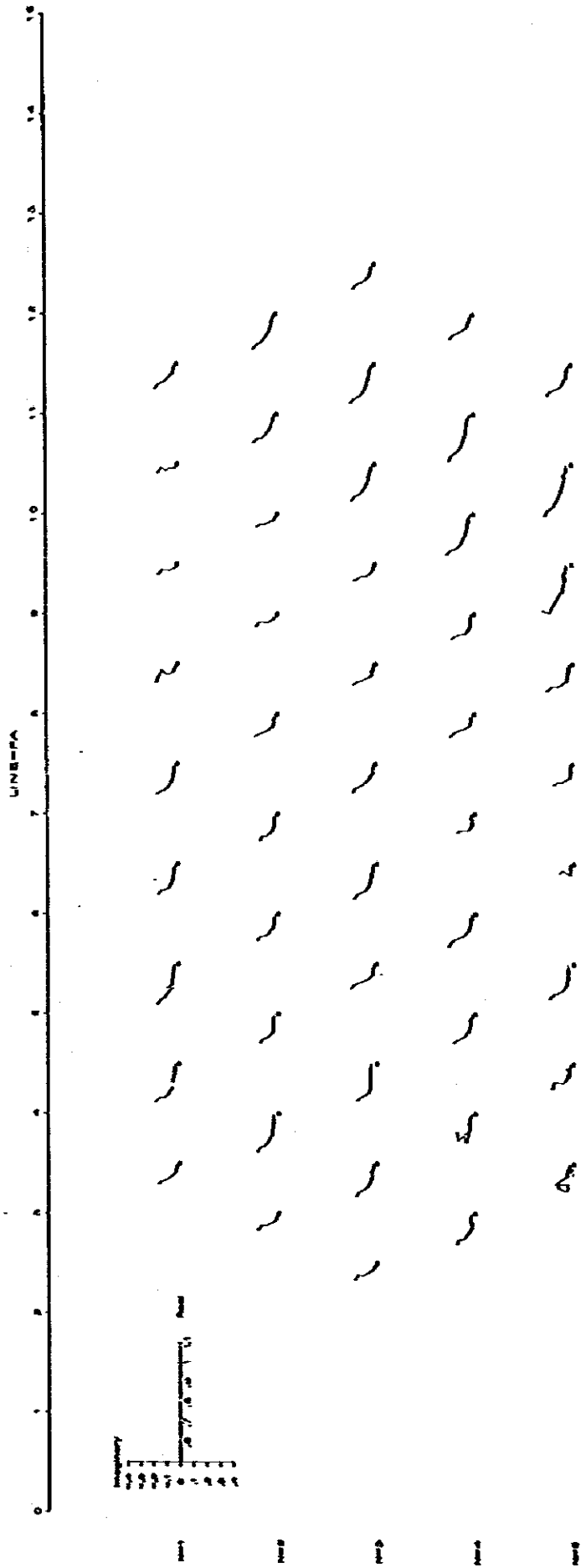


Fig. II-11-1 Cole-Cole Diagram (Line-FA)

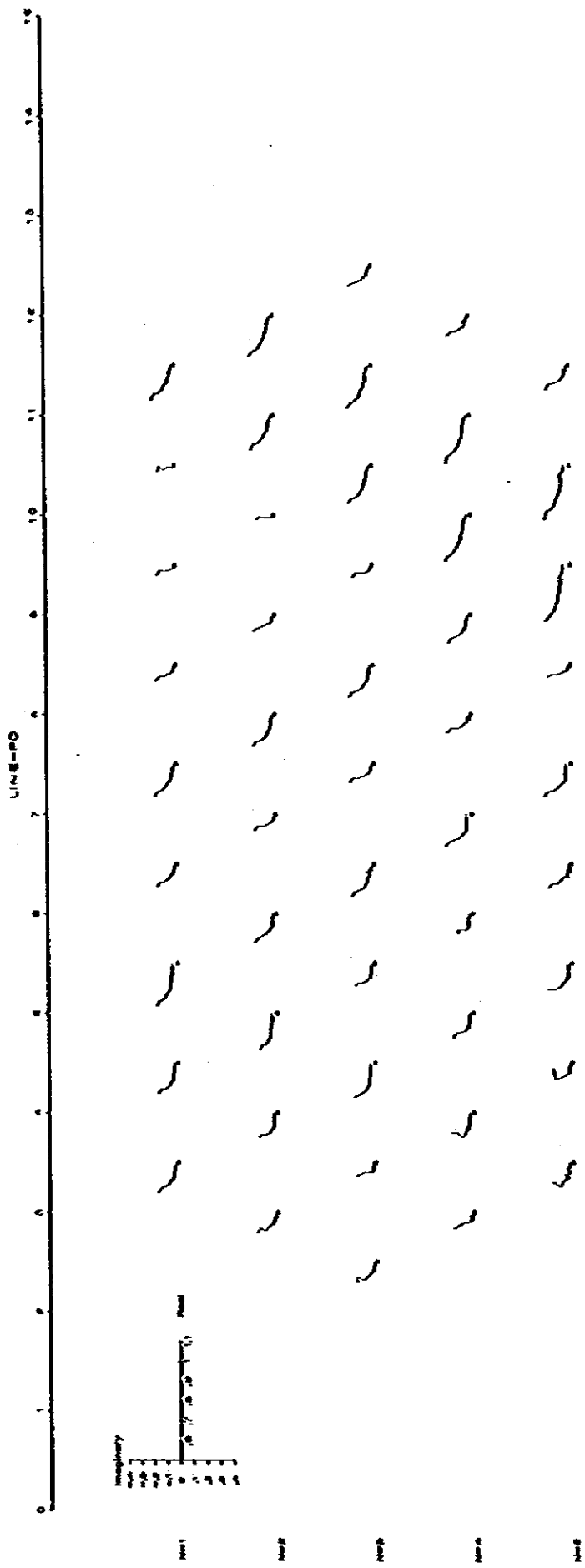


Fig. II-11-2 Cole-Cole Diagram (Line-FD)

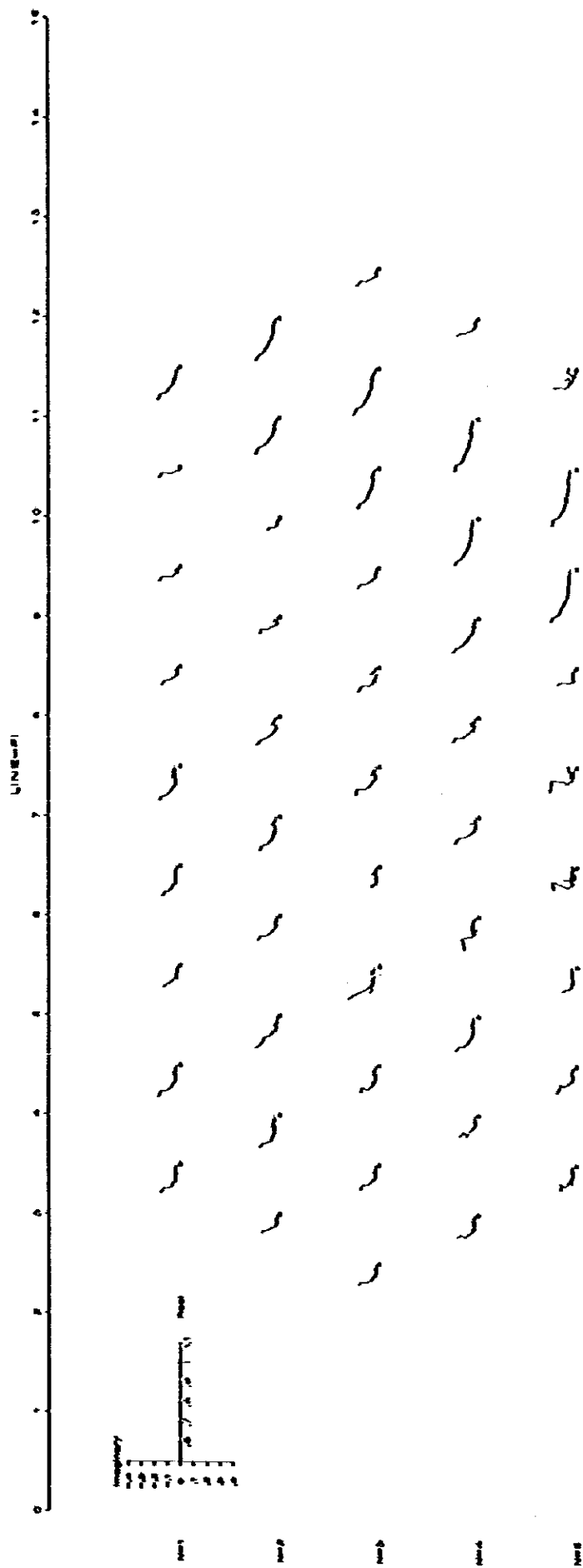


Fig. II-11-3 Cole-Cole Diagram (Line-FI)



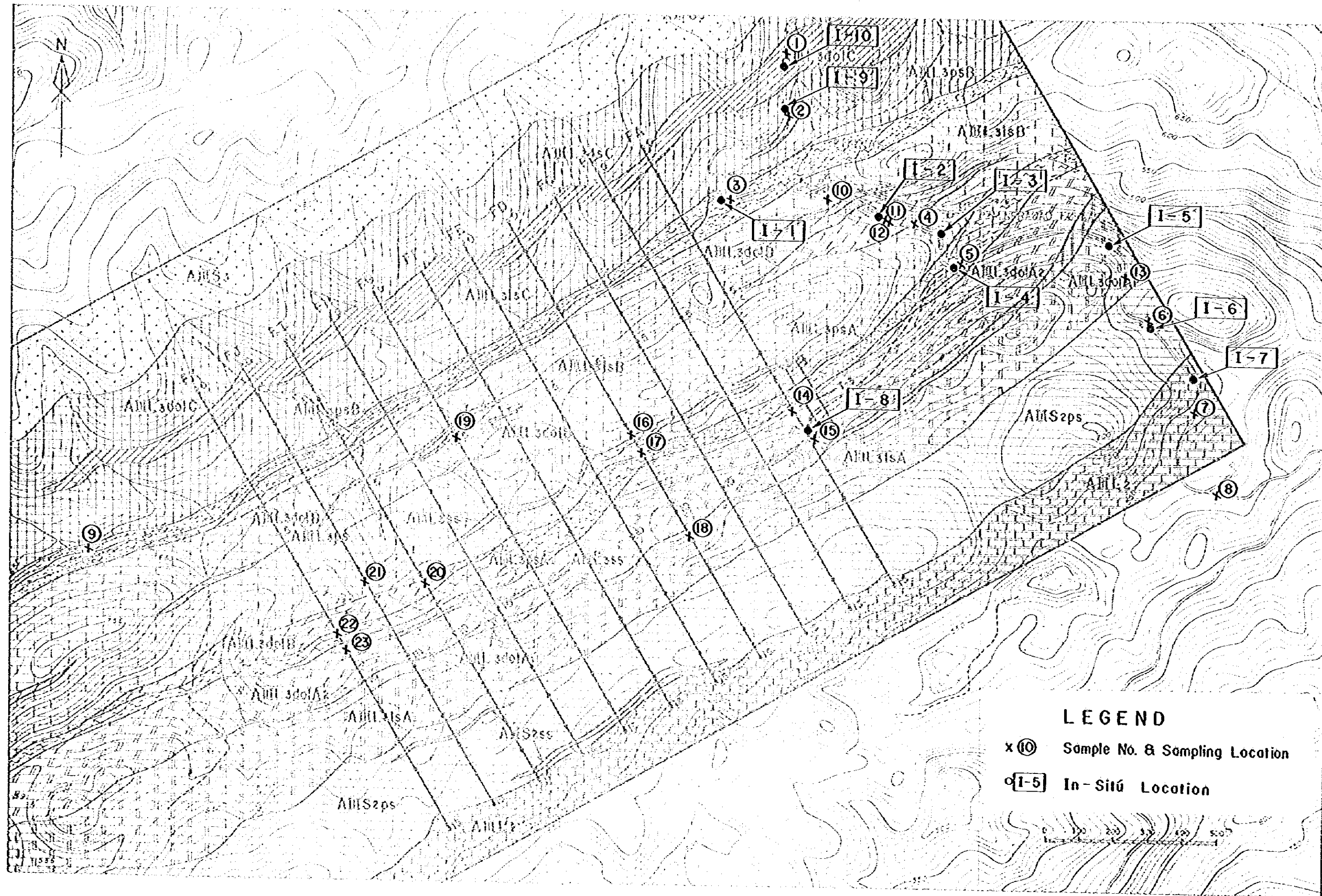


Fig. II-12 Location Map of Collected Rock Samples

Table II-3 Results of Laboratory Measurement in Rock Samples

Sample No.	Name	Rock Name	Formation	PRE (%)	A R. ( $\Omega$ m)	Raw Phase Shift (-mrad)	Spectral Type
1	ES- 1	Dolomitic limestone	L <sub>3</sub> dol C	0.2	162	0.1	C
2	ES- 2	Limestone banded	L <sub>3</sub> ls C	0.8	6490	5.3	C
3	ES- 4	Meta siltstone	L <sub>3</sub> Ps B	1.9	815	11.3	B
4	ES- 5	Dolomitic limestone	L <sub>3</sub> ls B	0.1	4540	0.5	C
5	ES- 6	Quartz sericite schist Graphite sericite schist	L <sub>3</sub> Ps A	5.5	2350	29.3	B
6	ES- 7	Sericite schist	S <sub>2</sub> Ps	4.5	1390	29.6	B
7	ES- 9	Sericite-calcite-graphite schist	L <sub>2</sub>	1.1	625	6.1	B
8	ES-10	Limestone	L <sub>2</sub>	0.3	20000	2.2	B
9	ES-11	Phyllite	L <sub>3</sub> Ps B	4.5	3350	28.7	C
10	ES-14	Dolomitic limestone	L <sub>3</sub> ls B	0.6	12600	4.2	B
11	ES-15	Calcare dolomite with pyrite	L <sub>3</sub> dol B	5.4	1450	5.4	C
12	ES-16	Calcare dolomite with pyrite	L <sub>3</sub> dol B	2.9	362	15.9	C
13	ES-18	Limestone	L <sub>3</sub> ls A	1.3	10500	8.3	B
14	FA-9	Dolomitic limestone	L <sub>3</sub> dol A <sub>2</sub>	0.7	10500	3.7	B
15	FA-10	Dolomitic limestone	L <sub>3</sub> dol A <sub>2</sub>	1.9	37000	15.5	B
16	FD-7.5	Dolomitic limestone	L <sub>3</sub> ls B	0.7	9090	2.9	B
17	FD-8	Limestone with pyrite	L <sub>3</sub> dol B	7.5	4560	7.5	B
18	FD-10.9	Limestone	L <sub>3</sub> ls A	2.6	70500	2.6	B
19	FG- 5	Phyllite	L <sub>3</sub> Ps B	3.2	283	18.0	C
20	FI- 8.3	Calcare dolomite with pyrite	L <sub>3</sub> dol B	2.8	9590	16.3	C
21	FJ-7.5	Dolomitic limestone	L <sub>3</sub> dol B	6.9	16700	6.9	C
22	FK-5.5	Dolomitic limestone	L <sub>3</sub> dol A <sub>2</sub>	2.4	23400	14.9	C
23	FK-9	Dolomitic limestone with pyrite	L <sub>3</sub> dol A <sub>2</sub>	2.2	33000	13.5	C
24	Ore-1	Sphalerite		150	17	160	C
25	Ore-2	Galena		165	28	165	C
26	Ore-3	Galena		231	17	831	C
27	Ore-4	Galena		337	21	781	C
28	Ore-5	Galena		210	50	210	C

Rock Name	Resistivity ( $\Omega$ m)		FFE (%)	
	Observed	Average	Observed	Average
Ps (Schist)	283 ~ 3,350	1,210	1.9 ~ 5.5	3.92
ls (Limestone)	4,540 ~ 70,500	11,700	0.1 ~ 2.6	1.02
Dol (Dolomite)	162 ~ 37,000	5,360	0.1 ~ 7.5	3.28
Ore	17 ~ 50	26.6	165 ~ 337	224.6

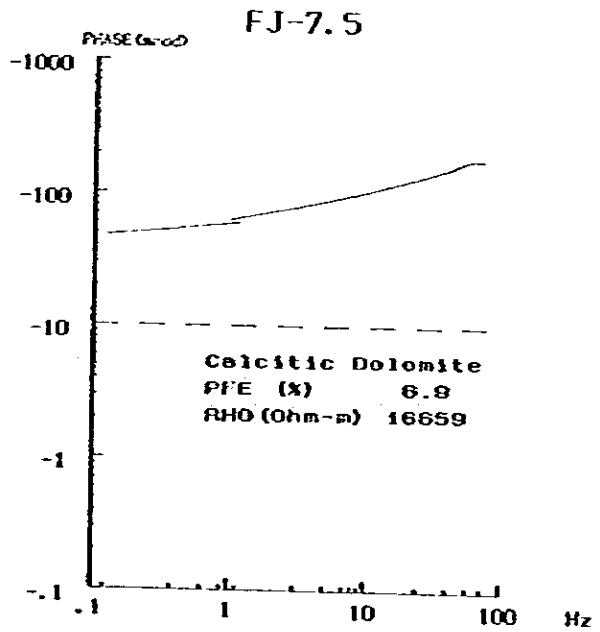
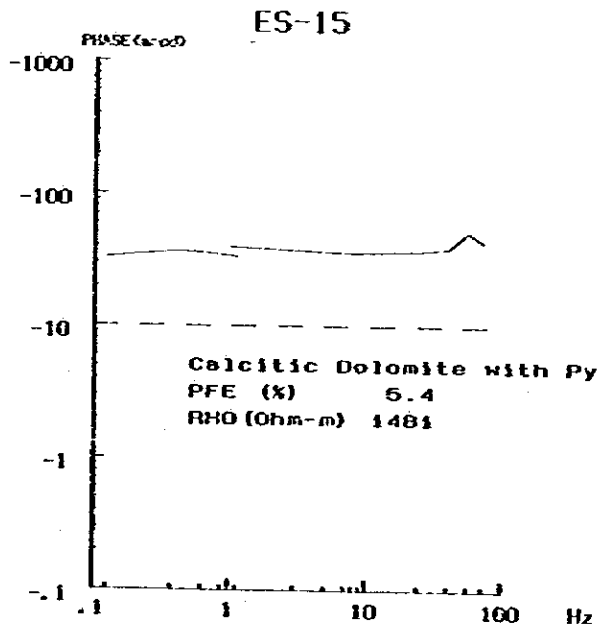
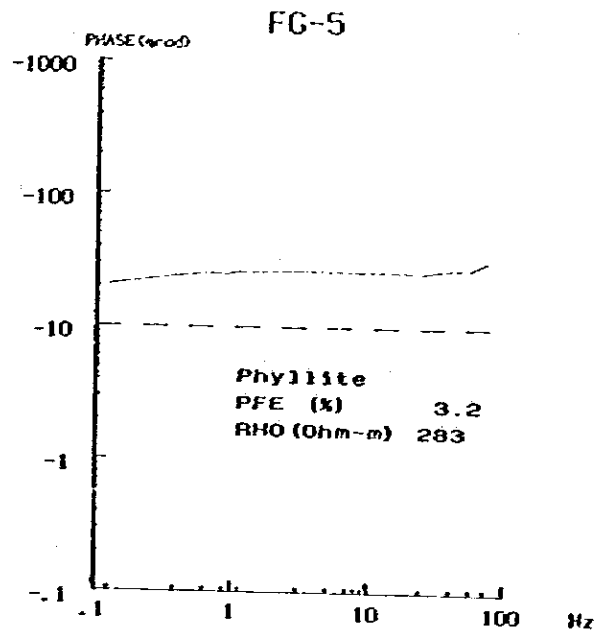
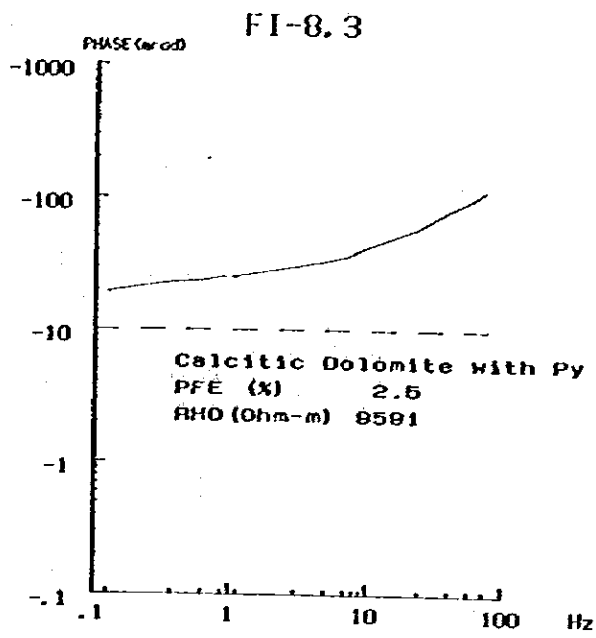
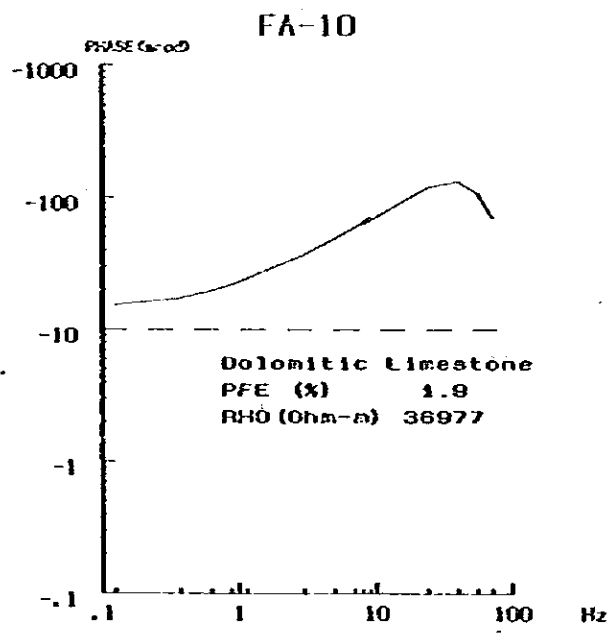
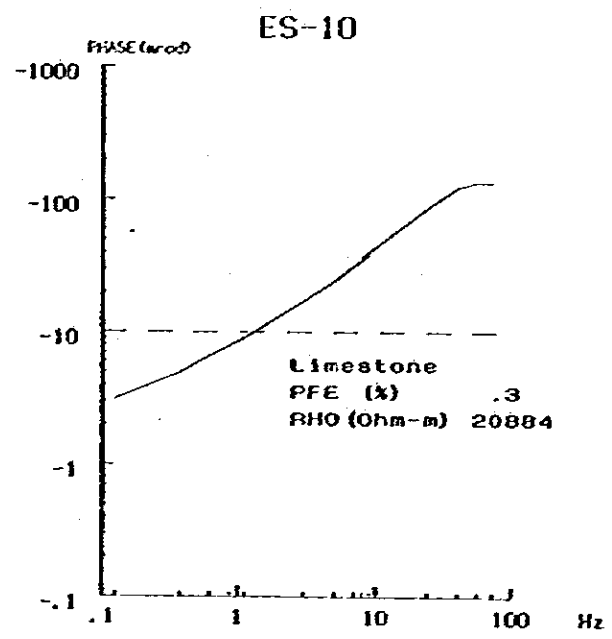
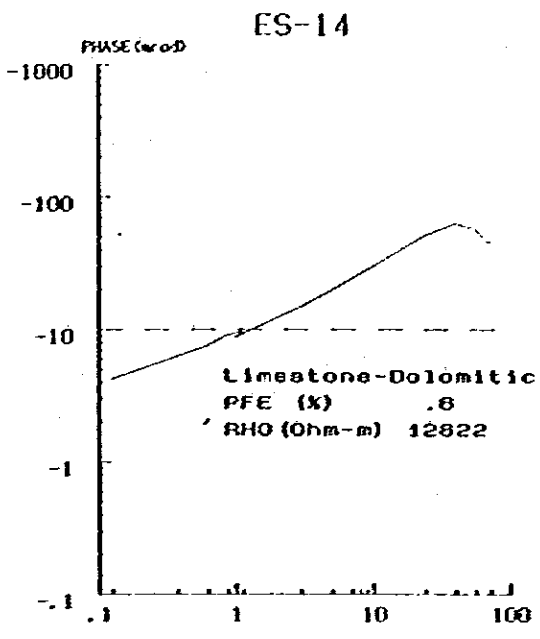


Fig. II-14 Typical Phase Spectral Type of Dolomite



**Fig. II-15 Typical Phase Spectral Type of Limestone**

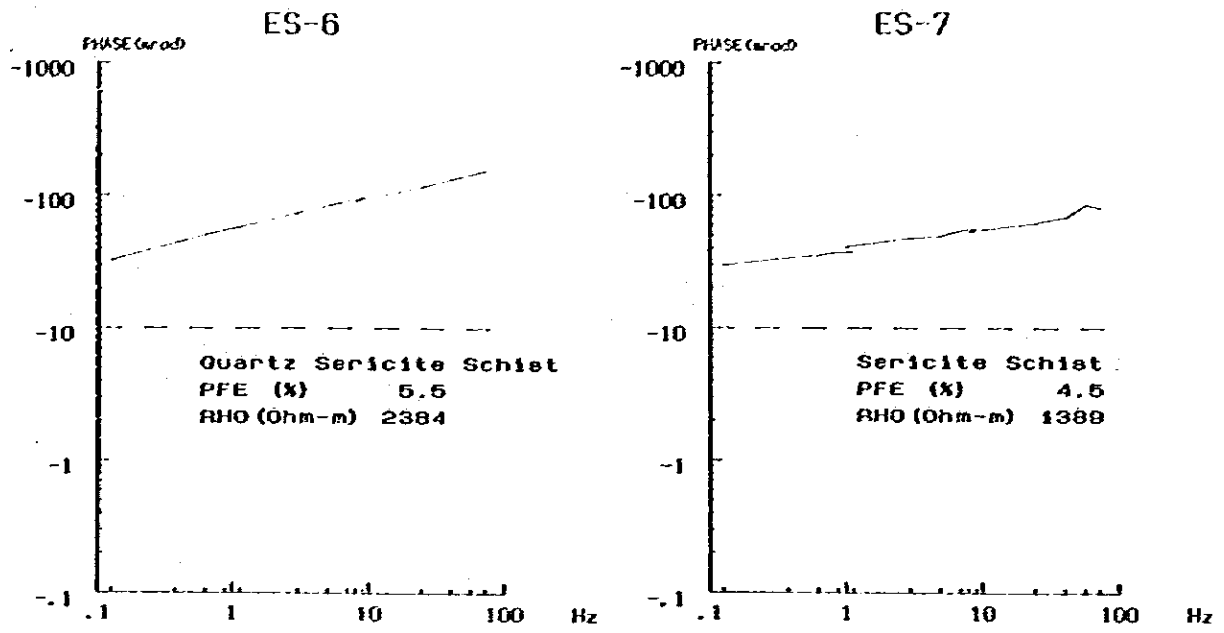


Fig. II-16 Typical Phase Spectral Type of Sericite Schist

### 2-3 Results of IP Method

Pseudosections of percent frequency effect (PFE) and apparent resistivity (AR) on each line are shown along with the geological sections on Fig. II-17-1 ~ 11.

AR is topographically corrected by means of a computer. The ranges of observed data of PFE and AR after the correction are shown on Table II-4.

Table II-4 Ranges of observed PFE and AR

Line Name	PFE (%)	AR ( $\Omega$ m)
FA	0.7 ~ 10.0	248 ~ 6,390
FB	0.1 ~ 9.3	471 ~ 10,100
FC	0.7 ~ 10.4	470 ~ 4,880
FD	0.8 ~ 8.9	426 ~ 7,610
FE	0.4 ~ 9.7	438 ~ 4,520
FF	0.6 ~ 10.3	424 ~ 11,300
FG	-0.2 ~ 10.0	151 ~ 11,400
FH	0.6 ~ 10.7	267 ~ 8,890
FI	0.7 ~ 10.0	481 ~ 7,700
FJ	0.1 ~ 11.5	371 ~ 9,590
FK	-0.3 ~ 10.9	178 ~ 31,800

PFE on Line FI was calculated using its values of SIP in 0.375 - 3 Hz. Fig. II-18-1 ~ 2 are correlation maps of PFE and AR of between IP and SIP methods by the overlapped measurement on Lines FA and FD. This indicates that the coefficients of PFE and AR of conventional IP are 1.2 times and 0.989 times as big as those of SIP.

### 2-3-1 Pseudosection

AR is classified in three groups by judging visually from the resistivity contour pattern: high AR more than 2,500  $\Omega\text{m}$ , medium AR between 1,000  $\Omega\text{m}$  and 2,500  $\Omega\text{m}$ , and low AR less than 1,000  $\Omega\text{m}$ .

A contour pattern on each line is similar each other and high AR is detected north of No. 3 and between No. 8 and No. 13, and low AR can be commonly detected between No. 3 and No. 8 on each line.

PFE is classified into three groups by judging visually from the contour pattern: high PFE more than 5%, medium PFE between 3% and 5%, and low PFE less than 3%. PFE more than 3% are called and IP anomaly. PFE contour pattern on each line is similar each other.

Distinct anomalies are detected in two areas: one is distributed from the area between No. 12 and No. 14 on each line of  $n=1$  to the area between No. 10 and No. 12 on  $n=5$ , and this anomaly is called "Anomalous zone A". Another is seen between No. 3 and No. 8, and this is called "Anomalous zone B". The anomalous part of more than 5% in "Anomalous zone B" is not distributed in the whole area, and its contour pattern has a little difference on each line. Background values of less than 3% are seen in the south of "Anomalous zone A" and north of "Anomalous zone B", and in the area between anomalous zones A and B.

### 2-3-2 Plan Map

The contour pattern is dominant to the normal direction of survey lines and correlates closely with the geological strike, especially on plan map of  $n=1$ .

Low AR less than 1,000  $\Omega\text{m}$  on  $n=1$  is zonally seen between No. 4 and No. 8 extending over all the lines. This low resistivity zone is named "L".

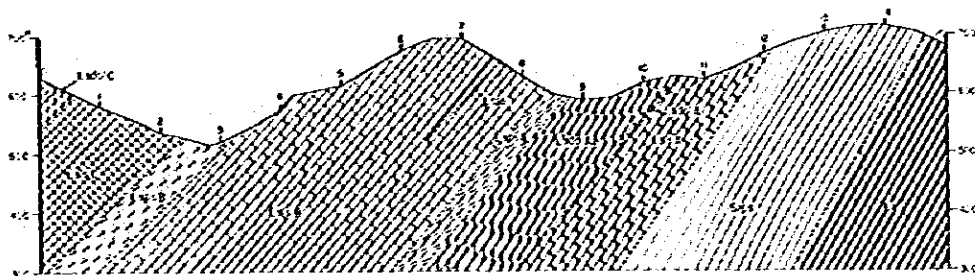
As the apparent resistivity value in "L" still decreases on  $n=3$  and 5, it can be said that the conductive rock continues to the depths.

High AR more than 2,500  $\Omega\text{m}$  is obtained extending from No. 8 to No. 12 on Lines FA--FD, FI and FK. Another high AR is distributed between Lines FE and FI. This resistive zone is called "H". In addition, a narrow belt-shaped resistive zone exceeding 4,000  $\Omega\text{m}$  is distributed along the central parts in "H" as follows: between No. 9 and No. 10 of Lines FA--FD, between No. 11 and No. 12 of Lines FE--FH, and between No. 10 and No. 11 of Lines FI--FK. On the plan map of  $n=3$ , this resistive zone shifts 100 m to the north between Lines FA and FE, and in turn 100 m to the south on Lines FG--FK.

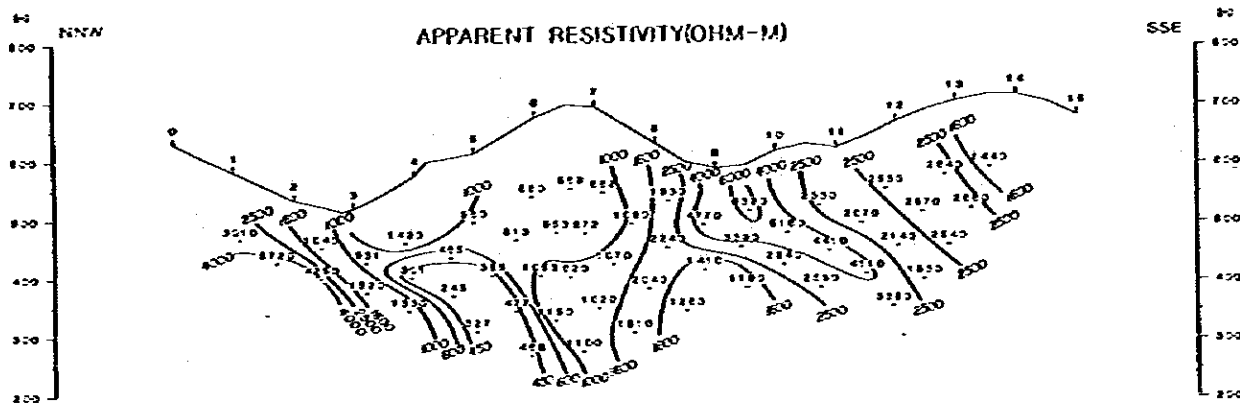
The PFE contour is also dominant to the normal direction of the survey lines.

The distinct anomalous parts of more than 5% of PFE are seen south of No. 12 and

GEOLOGICAL SECTION



APPARENT RESISTIVITY(OHM-M)



PERCENT FREQUENCY EFFECT (%)

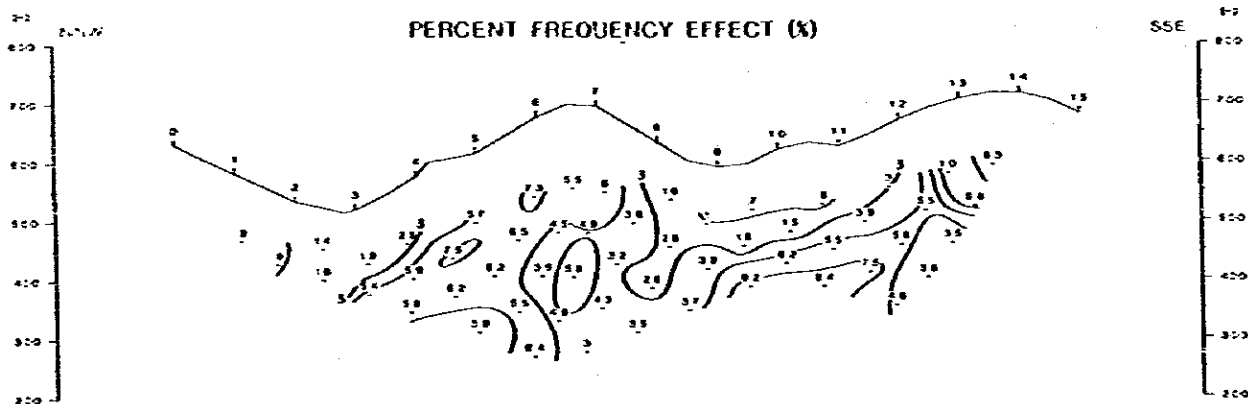


Fig. II-17-1 IP Pseudosection (Line-FA)



GEOLOGICAL SECTION

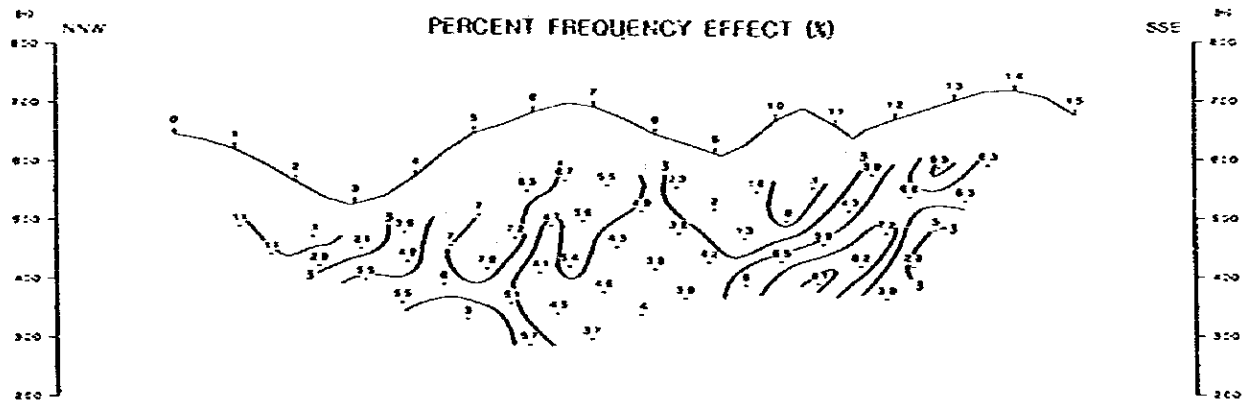
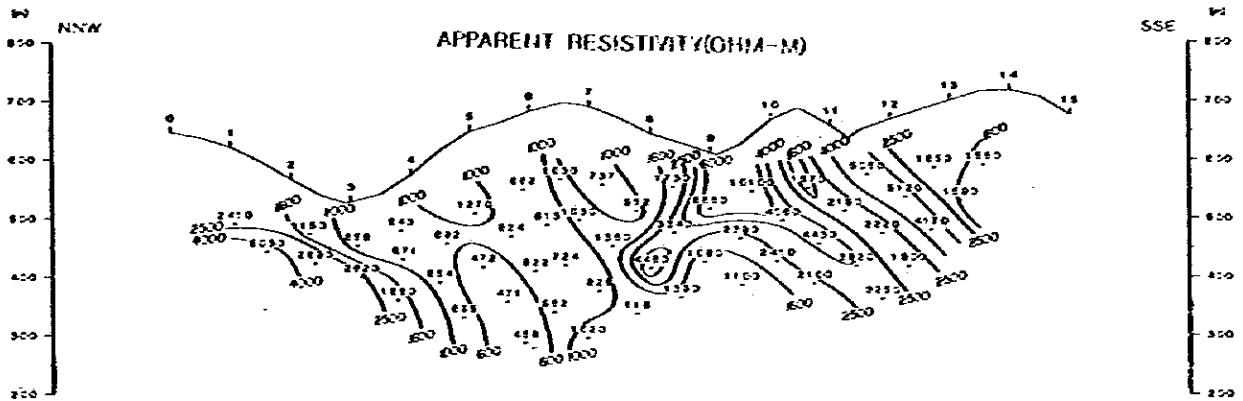
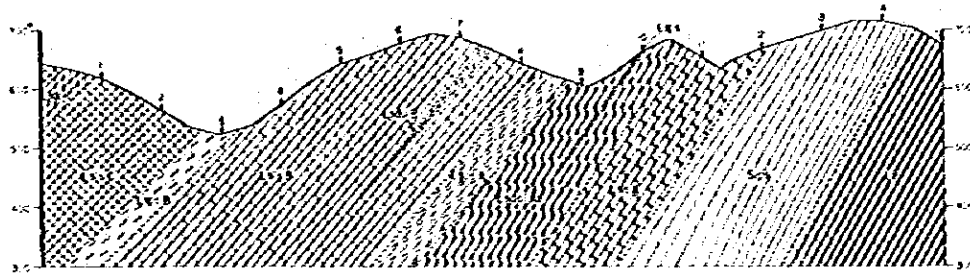


Fig. II-17-2 IP Pseudosection (Line-FB)

GEOLOGICAL SECTION

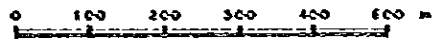
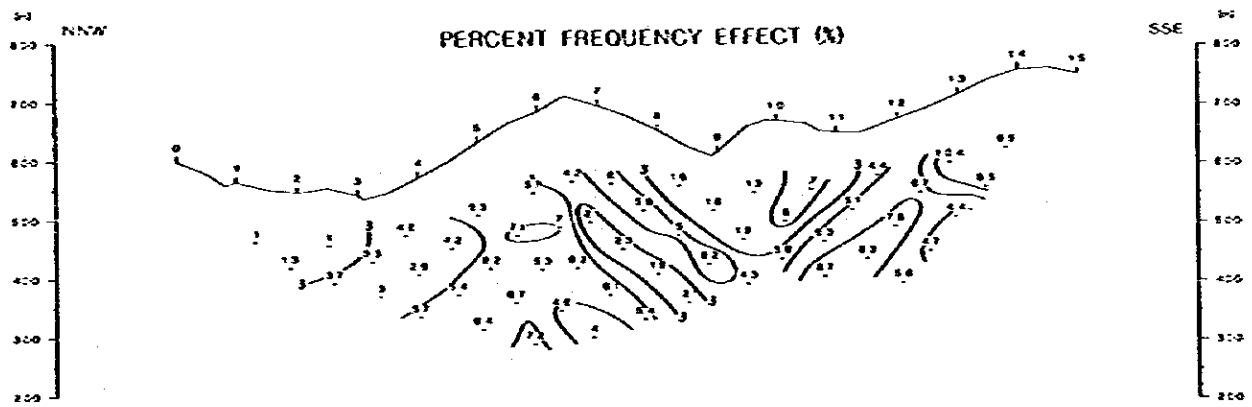
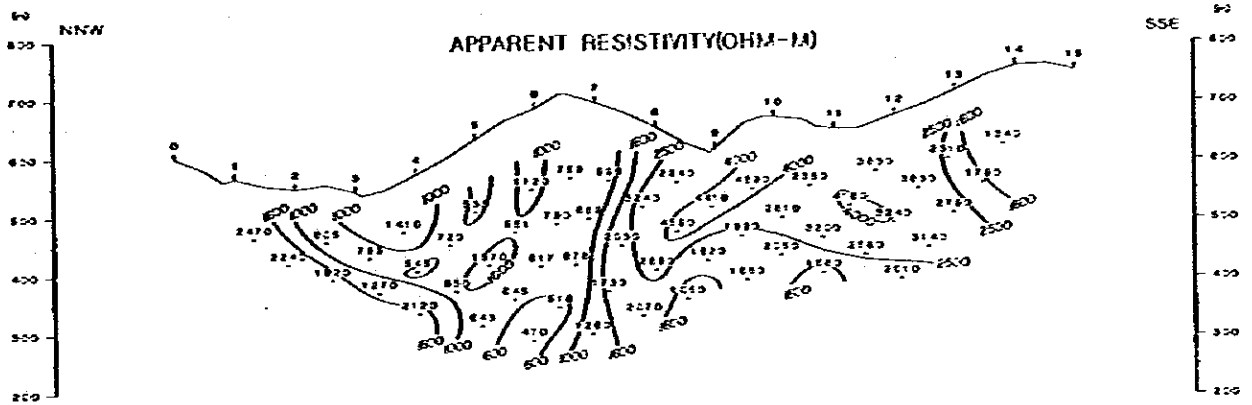
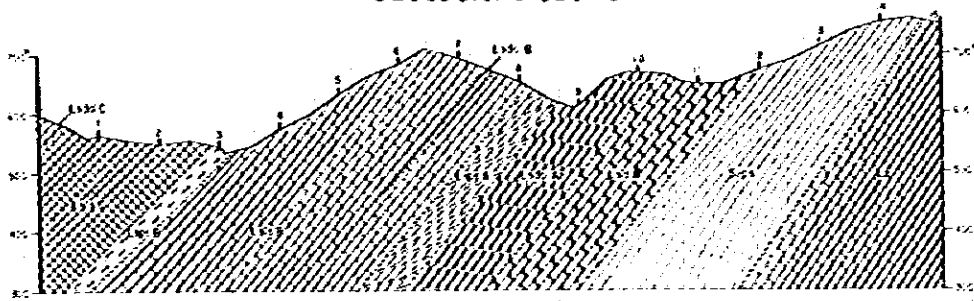
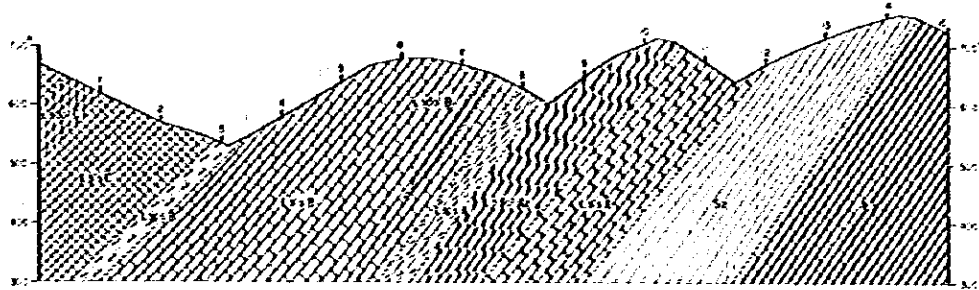
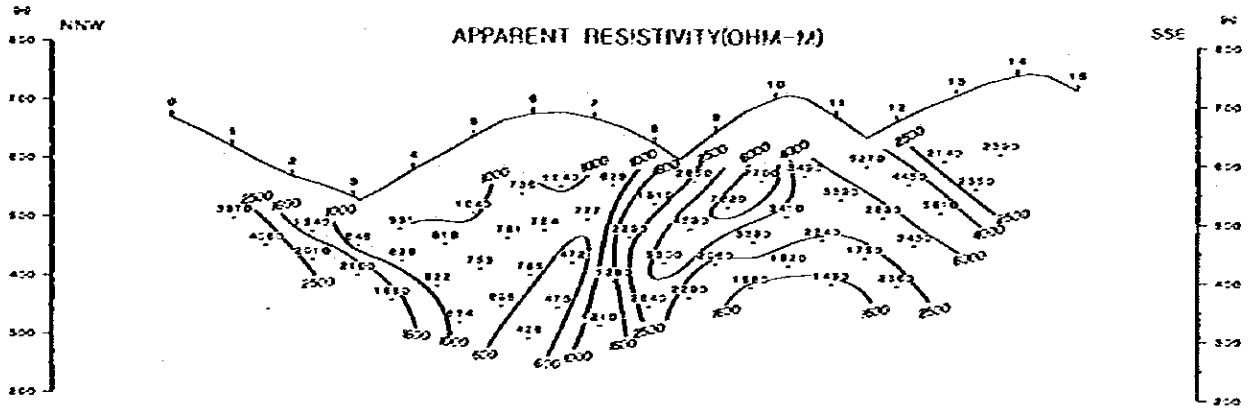


Fig. II-17-3 IP Pseudosection (Line-FC)

GEOLOGICAL SECTION



APPARENT RESISTIVITY(OHM- $m$ )



PERCENT FREQUENCY EFFECT (%)

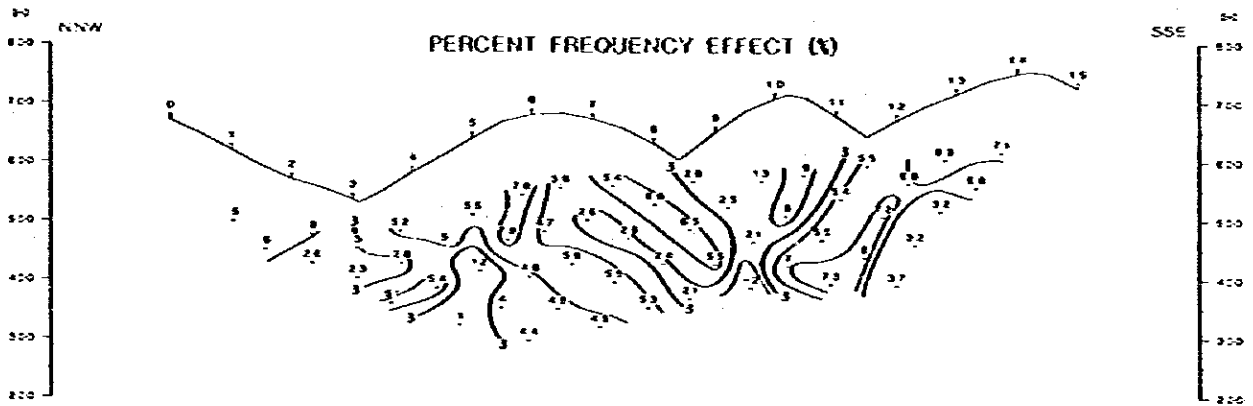


Fig. II-17-4 IP Pseudosection (Line-FD)

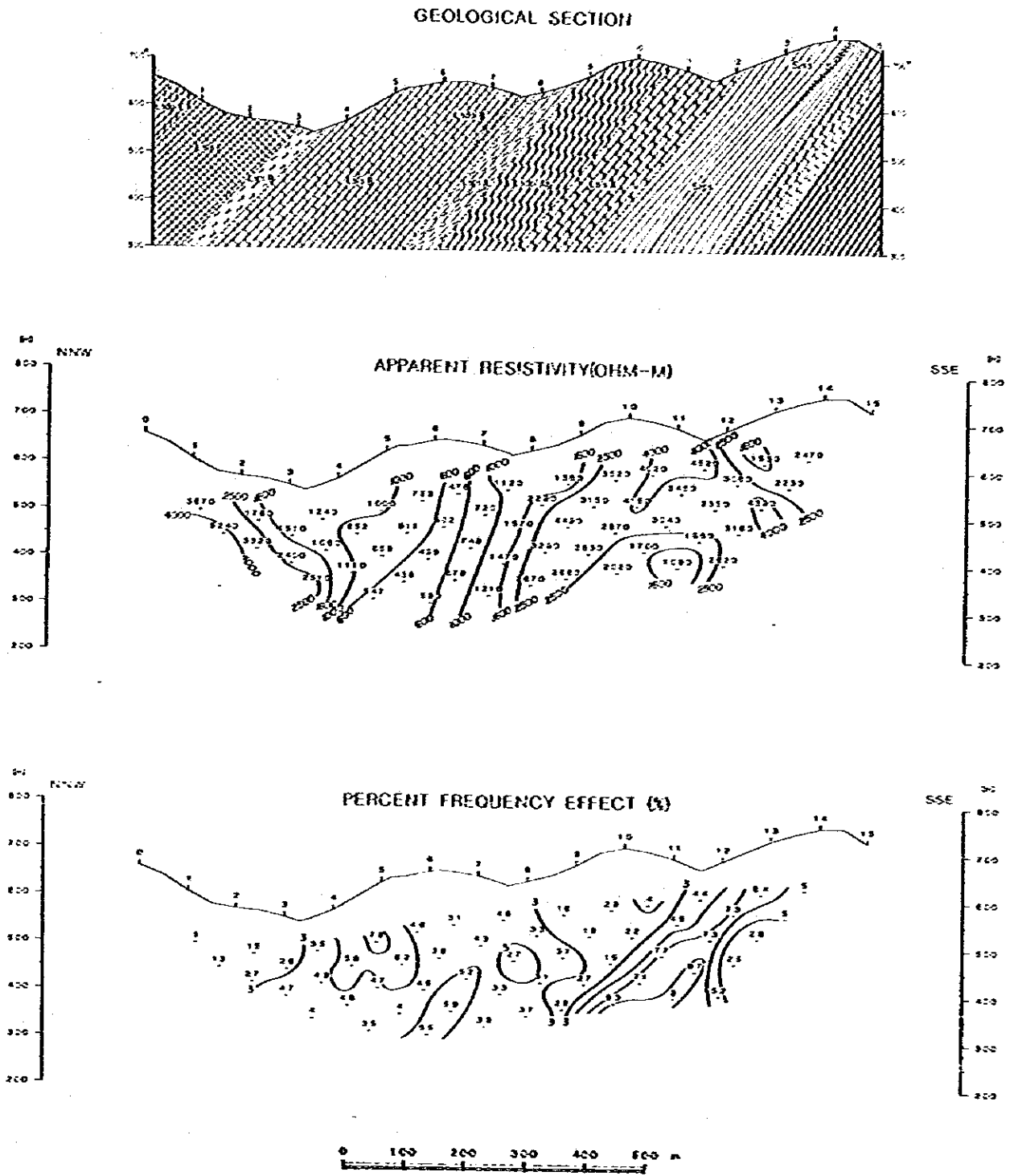
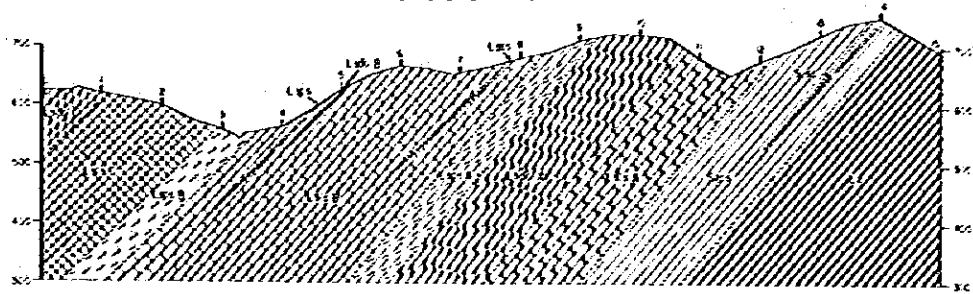
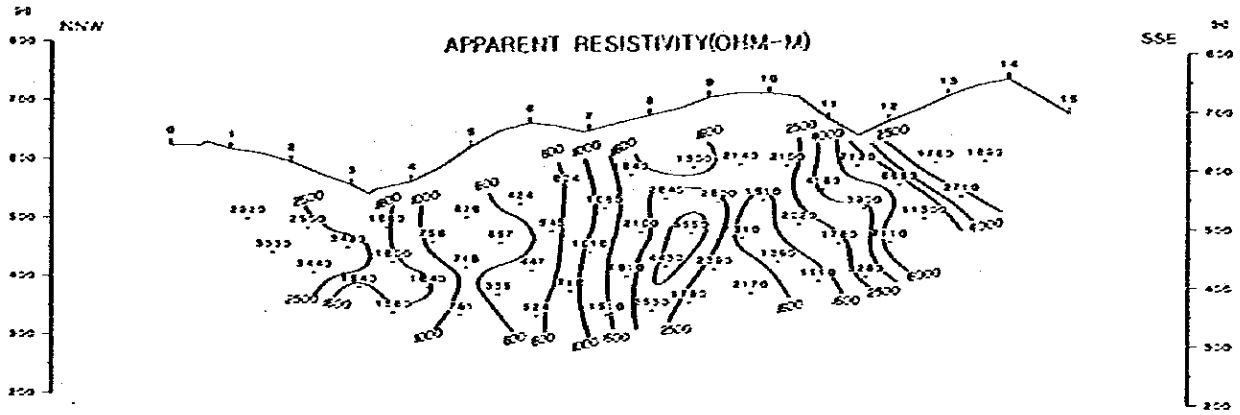


Fig. II-17-5 IP Pseudosection (Line-FE)

GEOLOGICAL SECTION



APPARENT RESISTIVITY(OHM-M)



PERCENT FREQUENCY EFFECT (%)

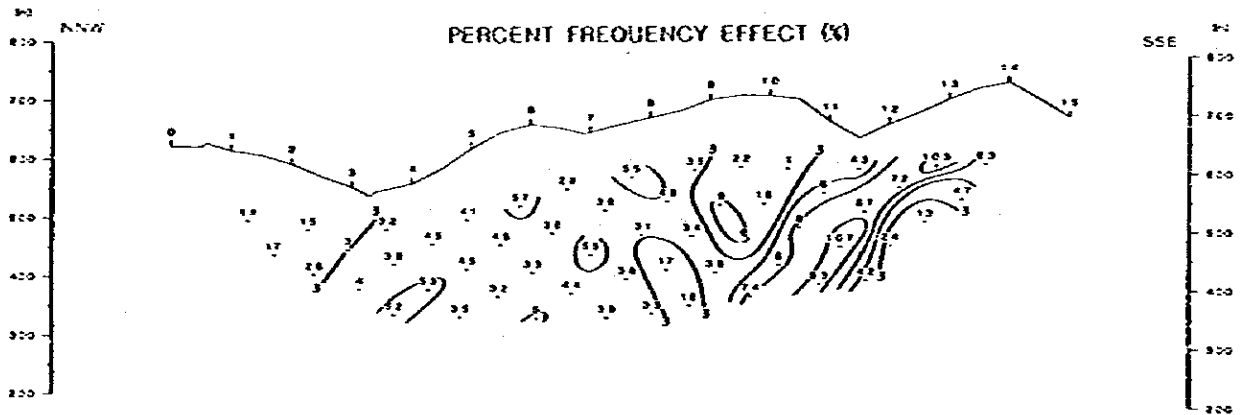


Fig. II-17-6 IP Pseudosection (Line-FF)

GEOLOGICAL SECTION

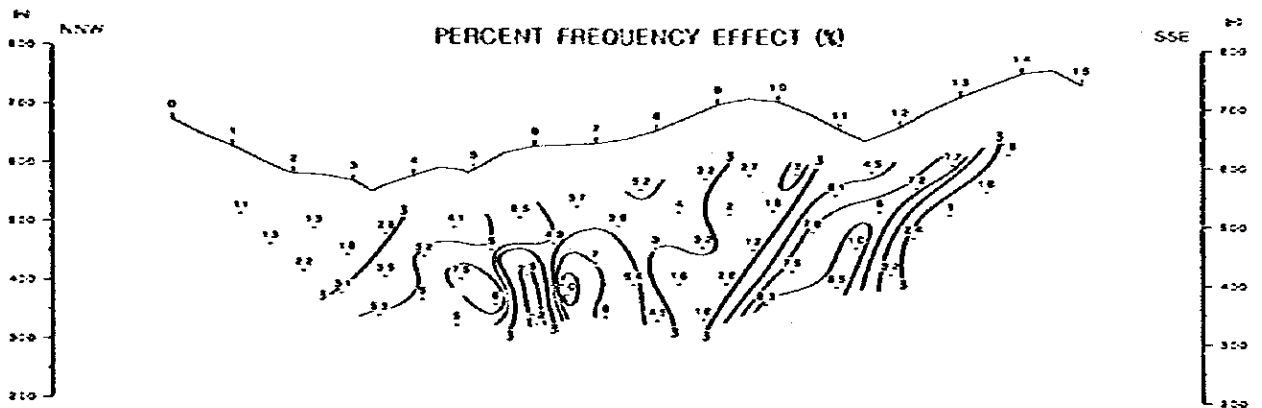
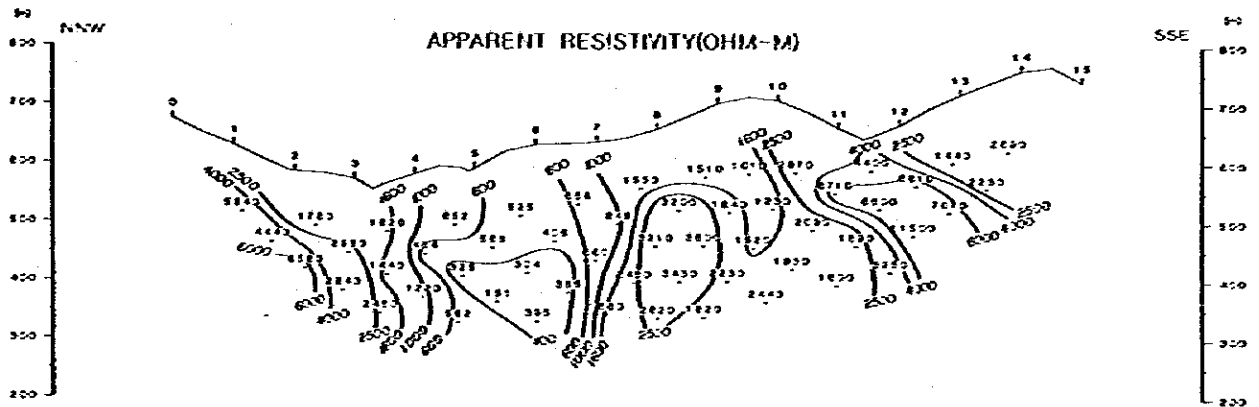
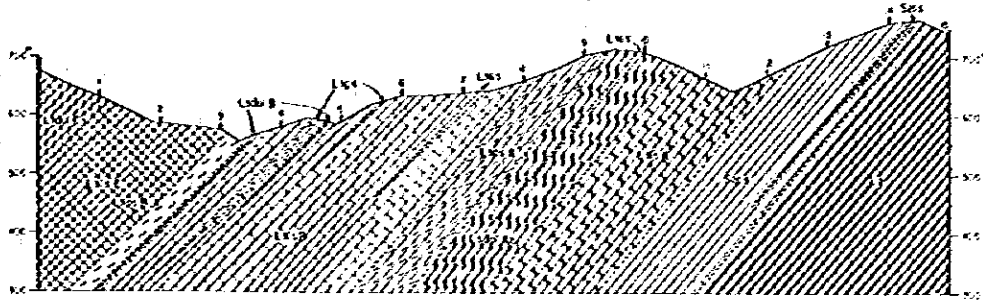
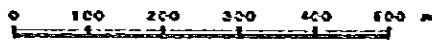
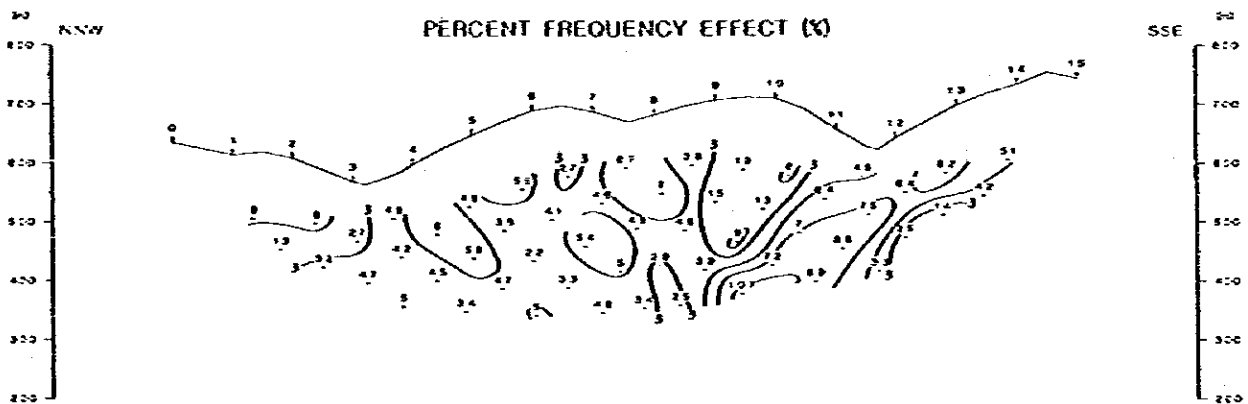
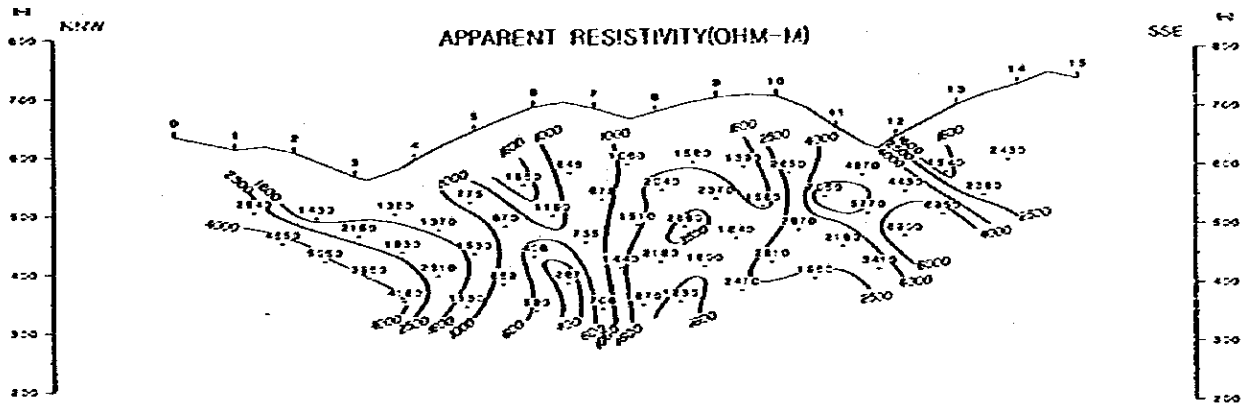
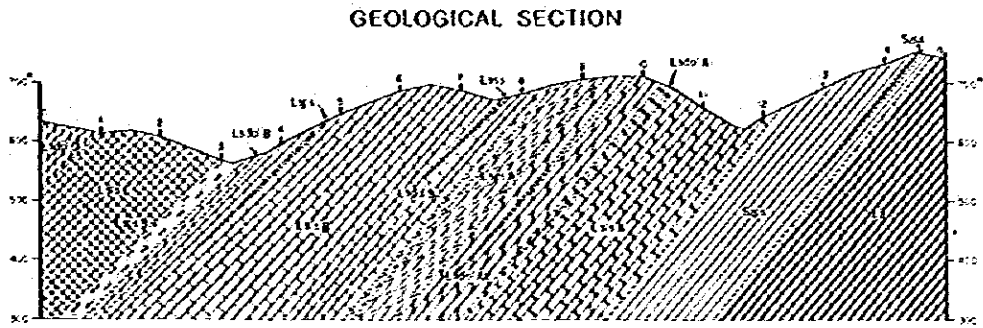
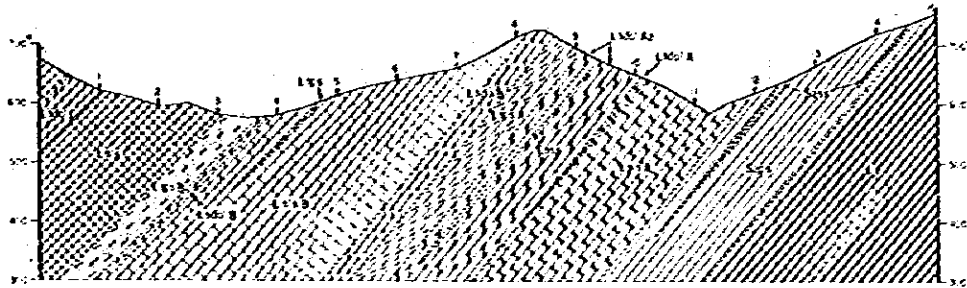


Fig. II-17-7 IP Pseudosection (Line-FG)

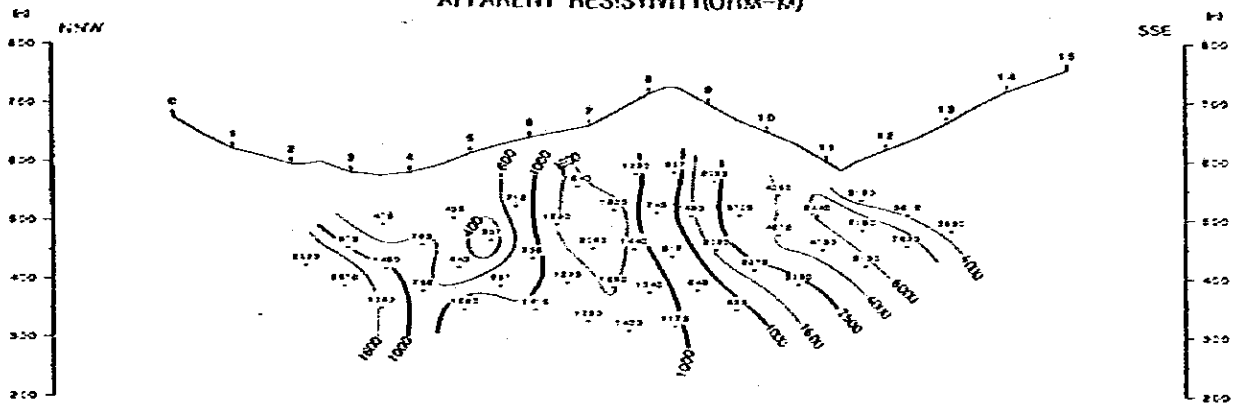


**Fig. II-17-8 IP Pseudosection (Line-FII)**

GEOLOGICAL SECTION



APPARENT RESISTIVITY(OHM-M)



PERCENT FREQUENCY EFFECT (%)

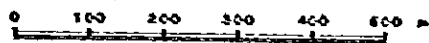
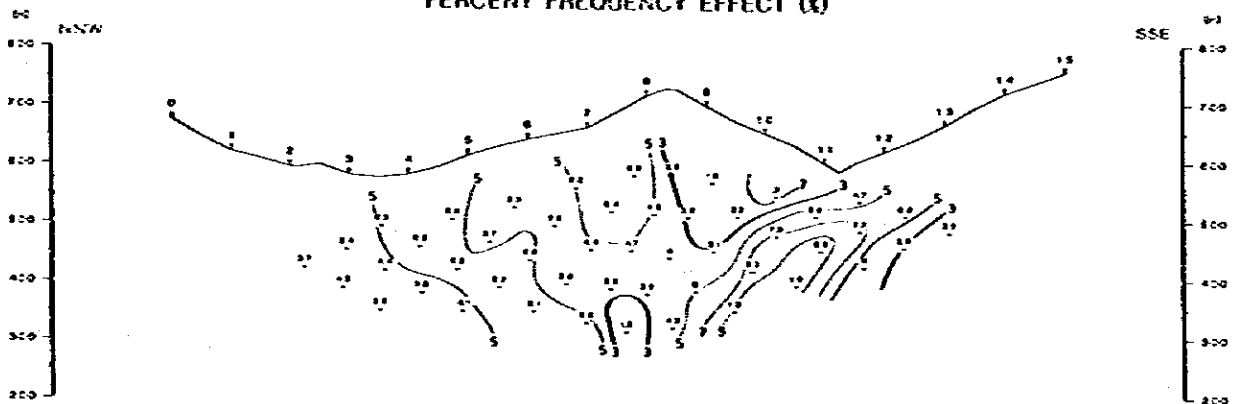
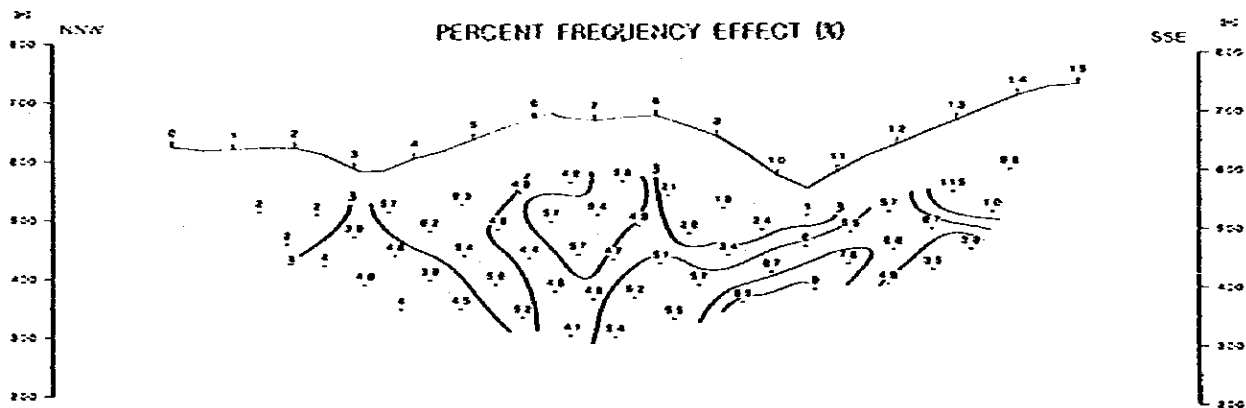
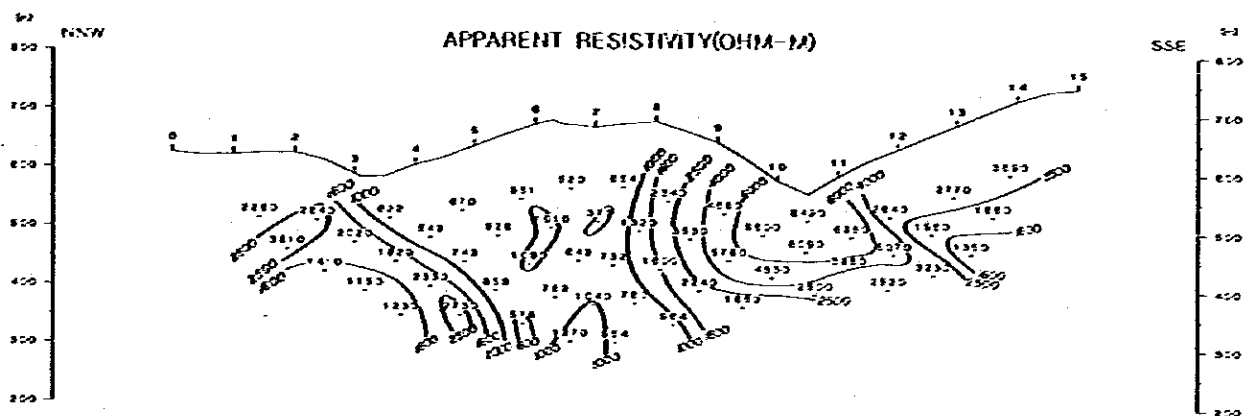
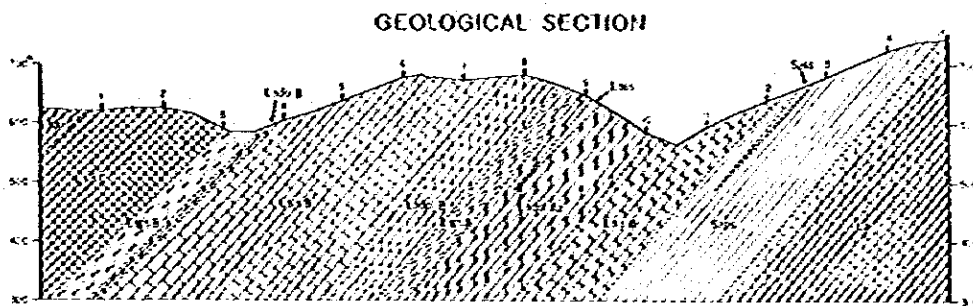


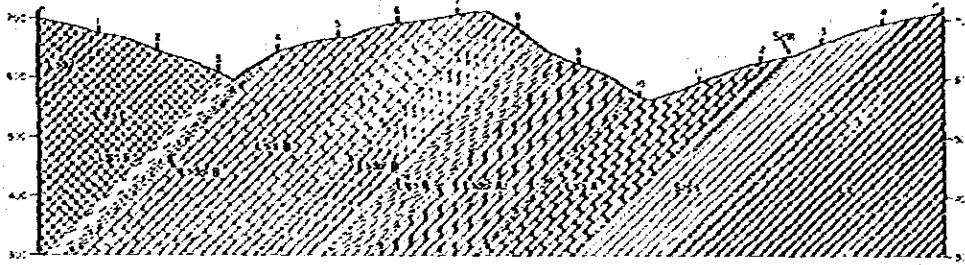
Fig. II-17-9 IP Pseudosection (Line-F1)



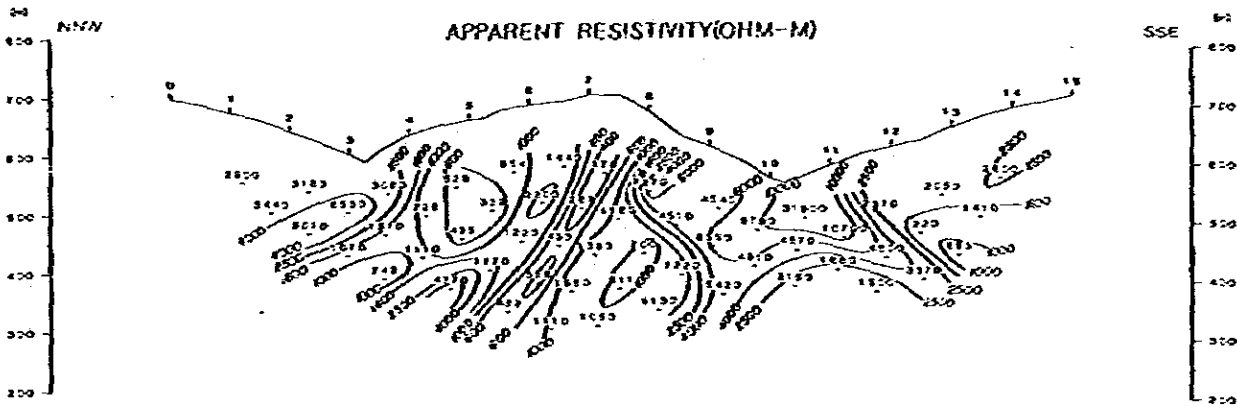


**Fig. II-17-10 IP Pseudosection (Line-FJ)**

GEOLOGICAL SECTION



APPARENT RESISTIVITY(OHM-M)



PERCENT FREQUENCY EFFECT (%)

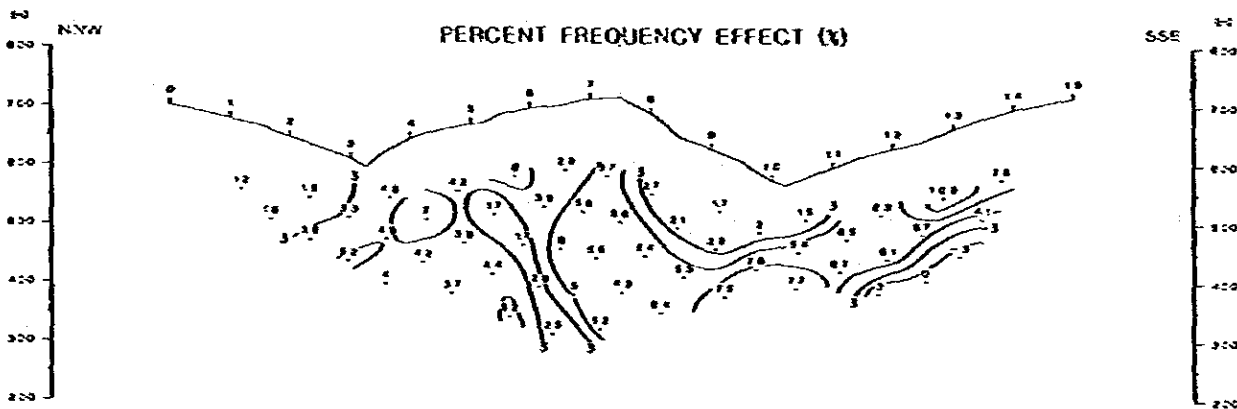


Fig. II-17-11 IP Pseudosection (Line-FK)

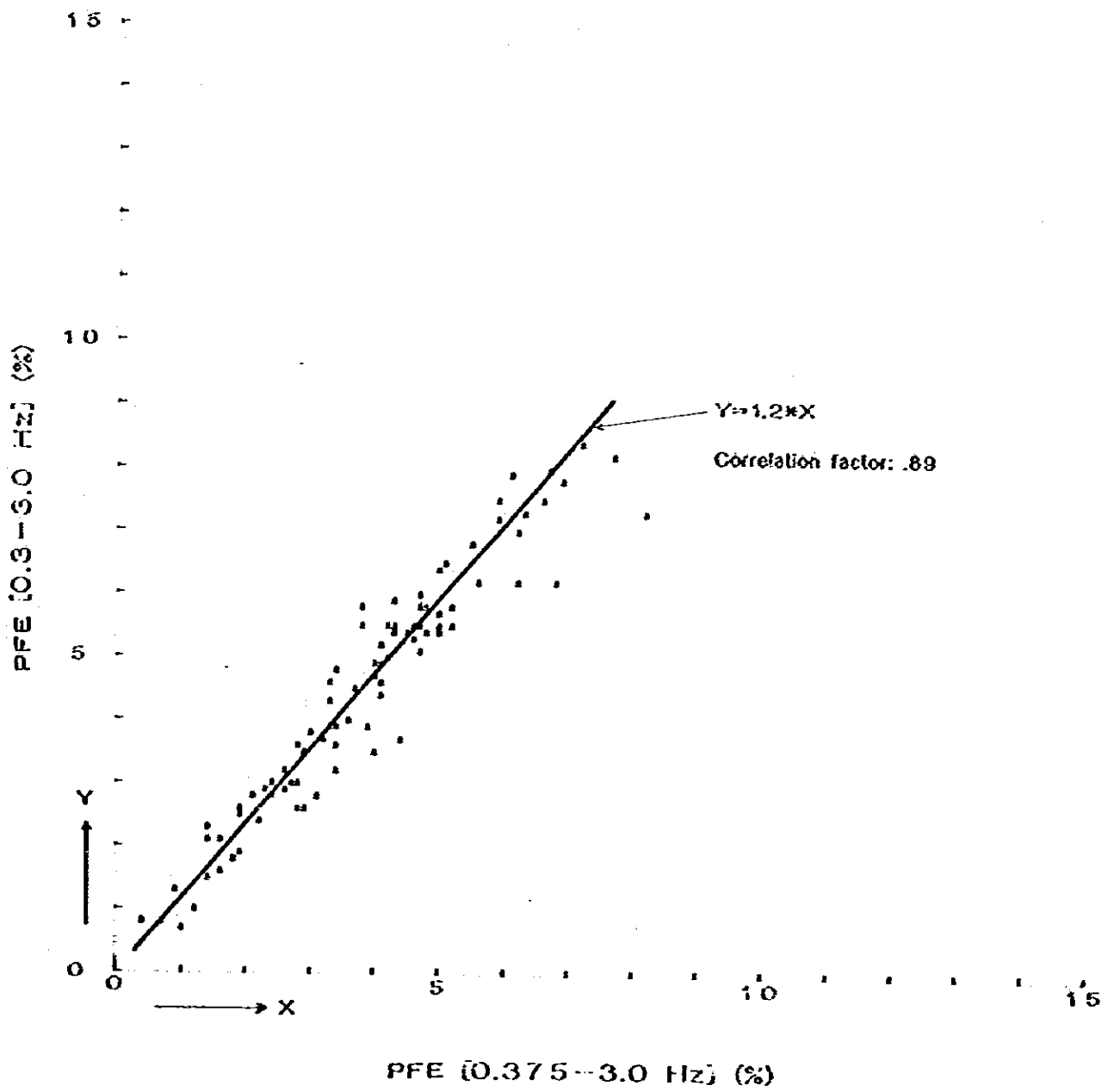


Fig. II-18-1 Correlation of PFE(0.3-3.0Hz) with PFE(0.375-3.0Hz)

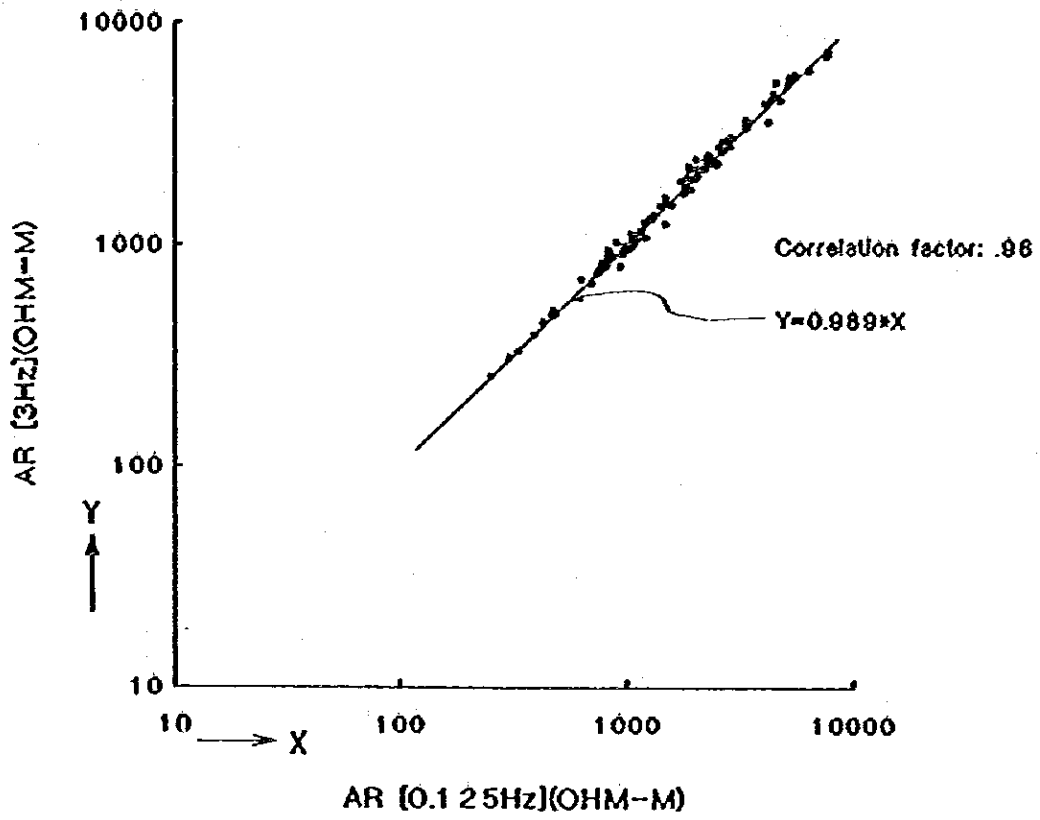


Fig. II-18-2 Correlation of AR (0.125Hz) with AR (3.0Hz)

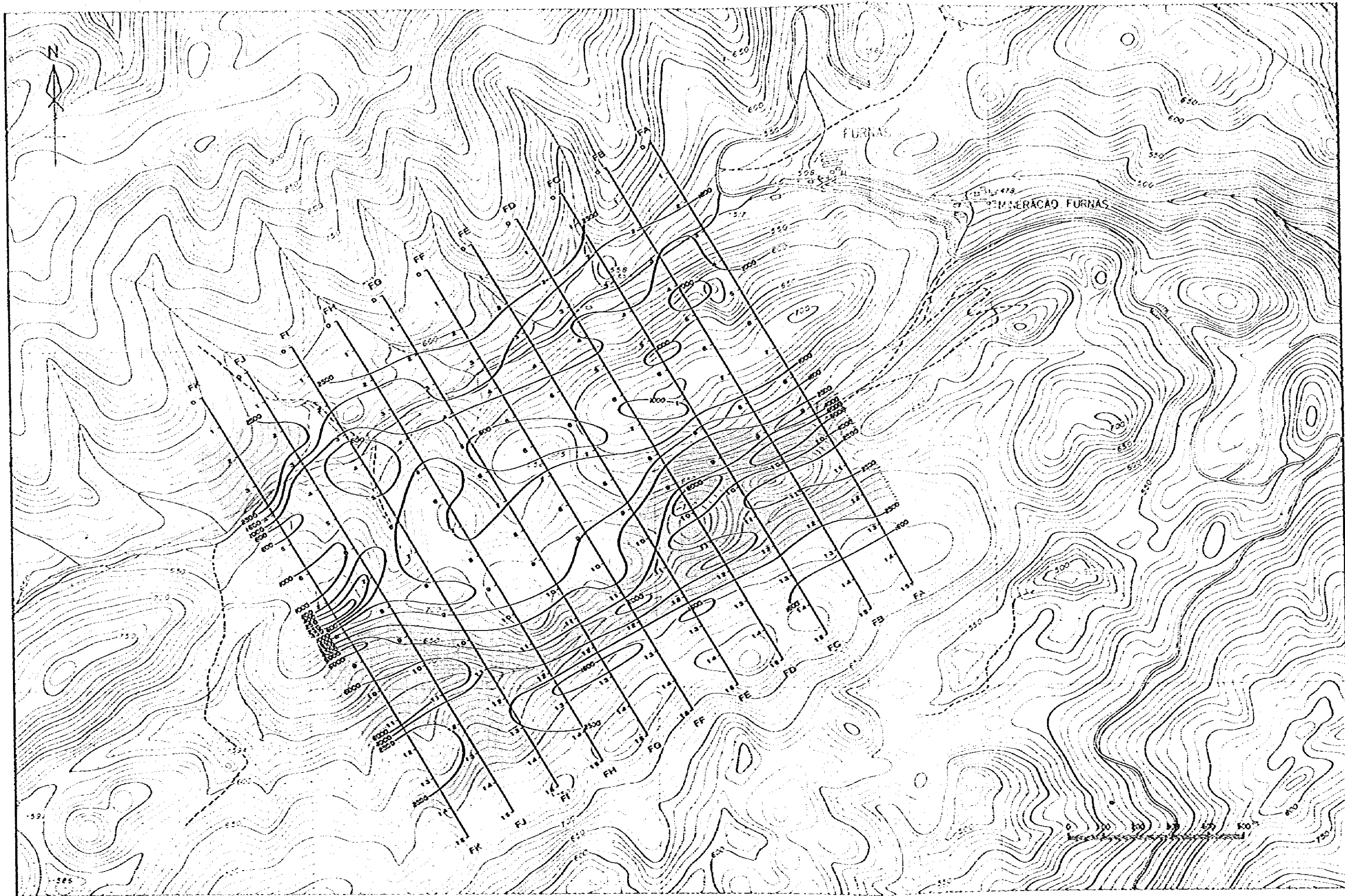


Fig. II-19-1 Plan Map of Apparent Resistivity(N=1)

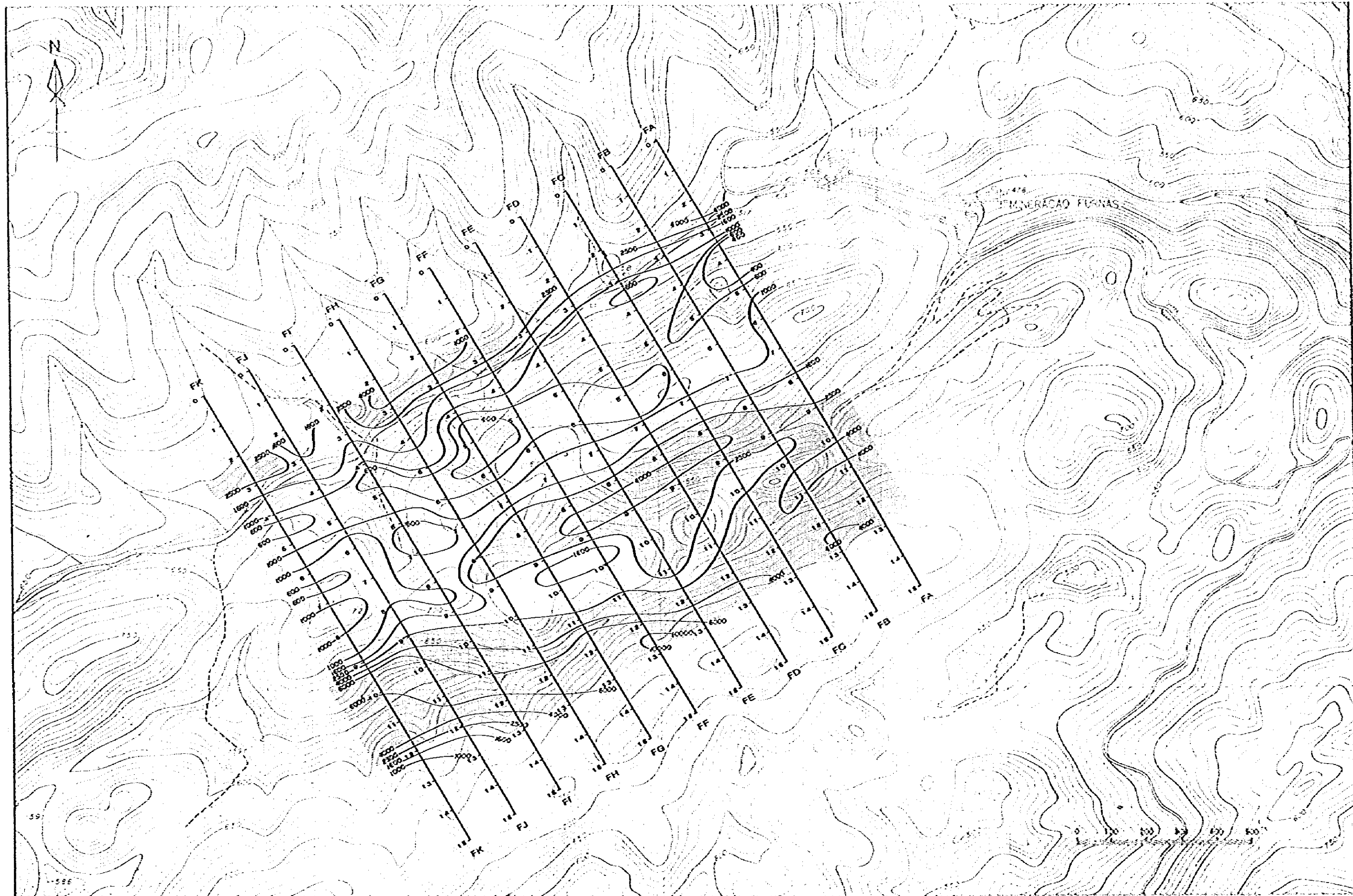


Fig. II-19-2 Plan Map of Apparent Resistivity(N=3)

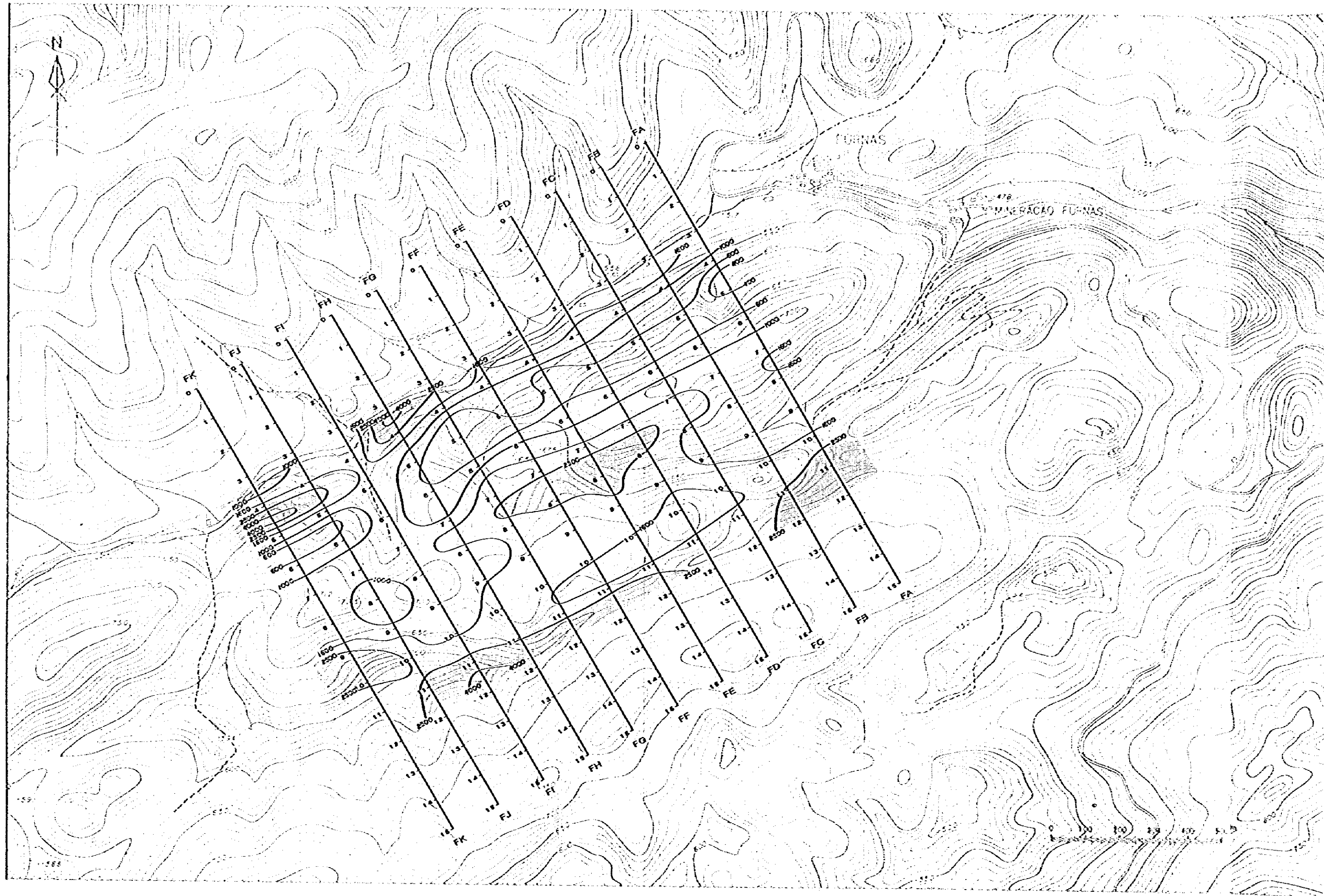


Fig. II-19-3 Plan Map of Apparent Resistivity(N=5)

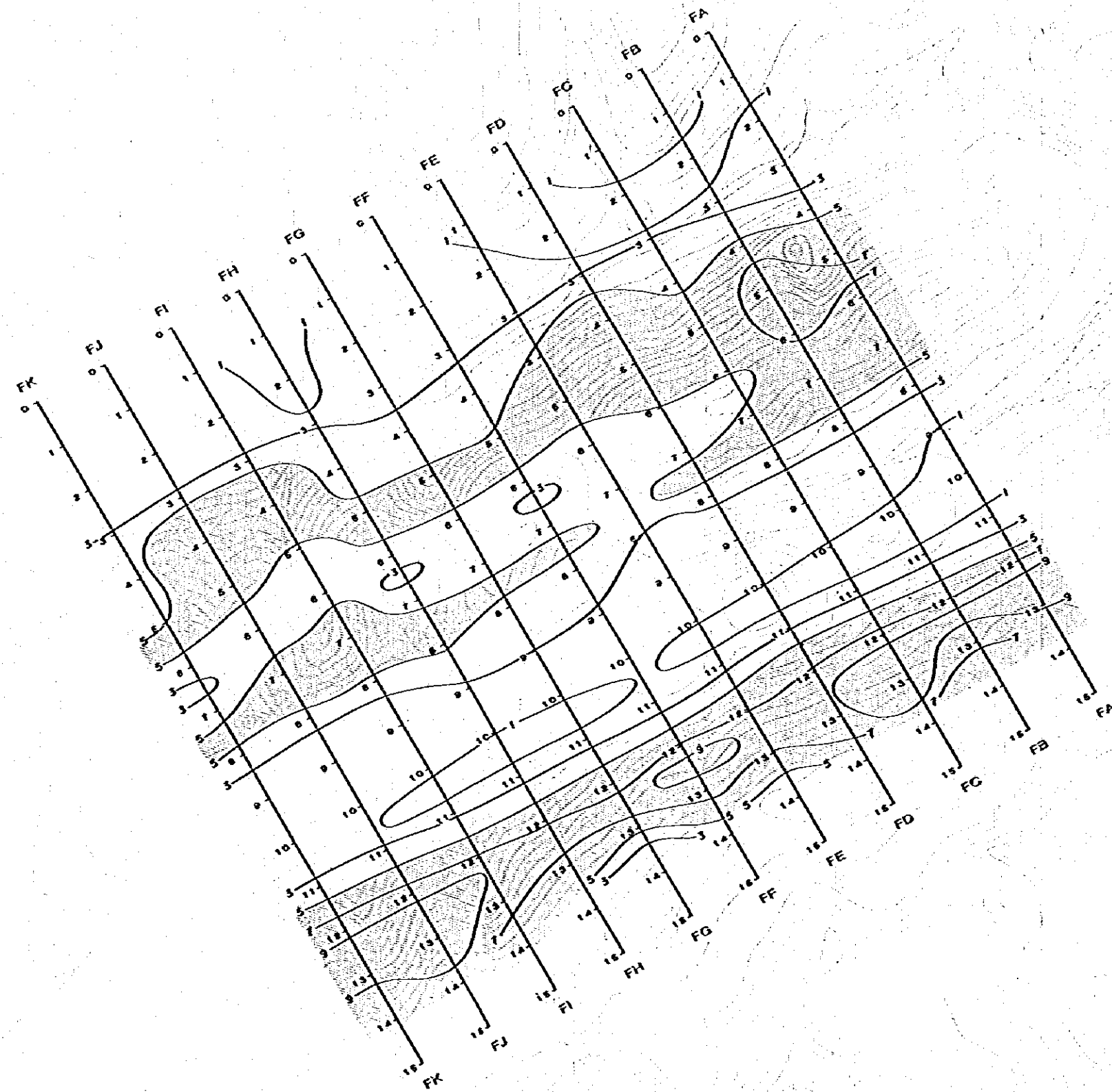


Fig. II-20-1 Plan Map of Percent Frequency Effect (N=1)



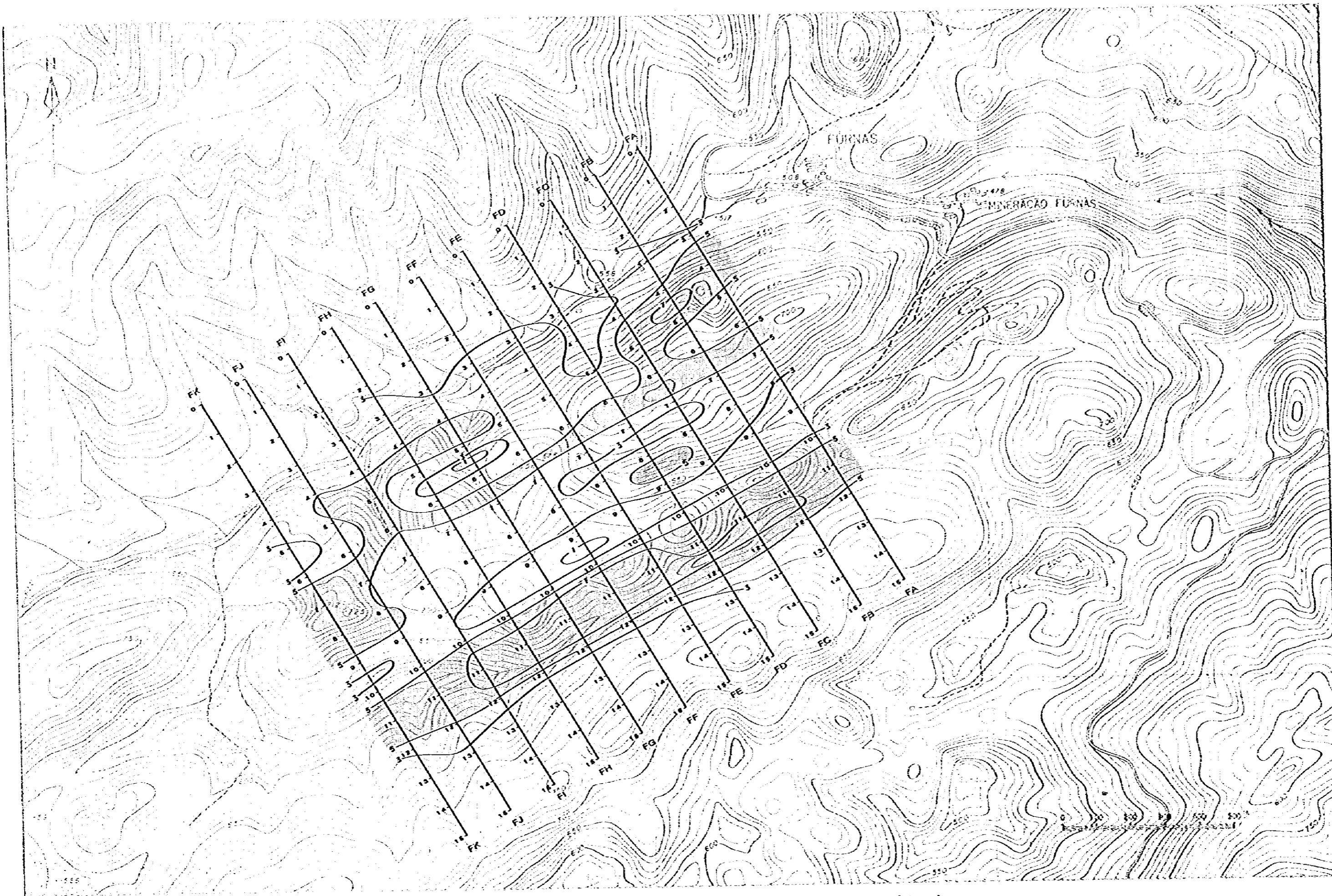


Fig. II-20-2 Plan Map of Percent Frequency Effect (N=3)

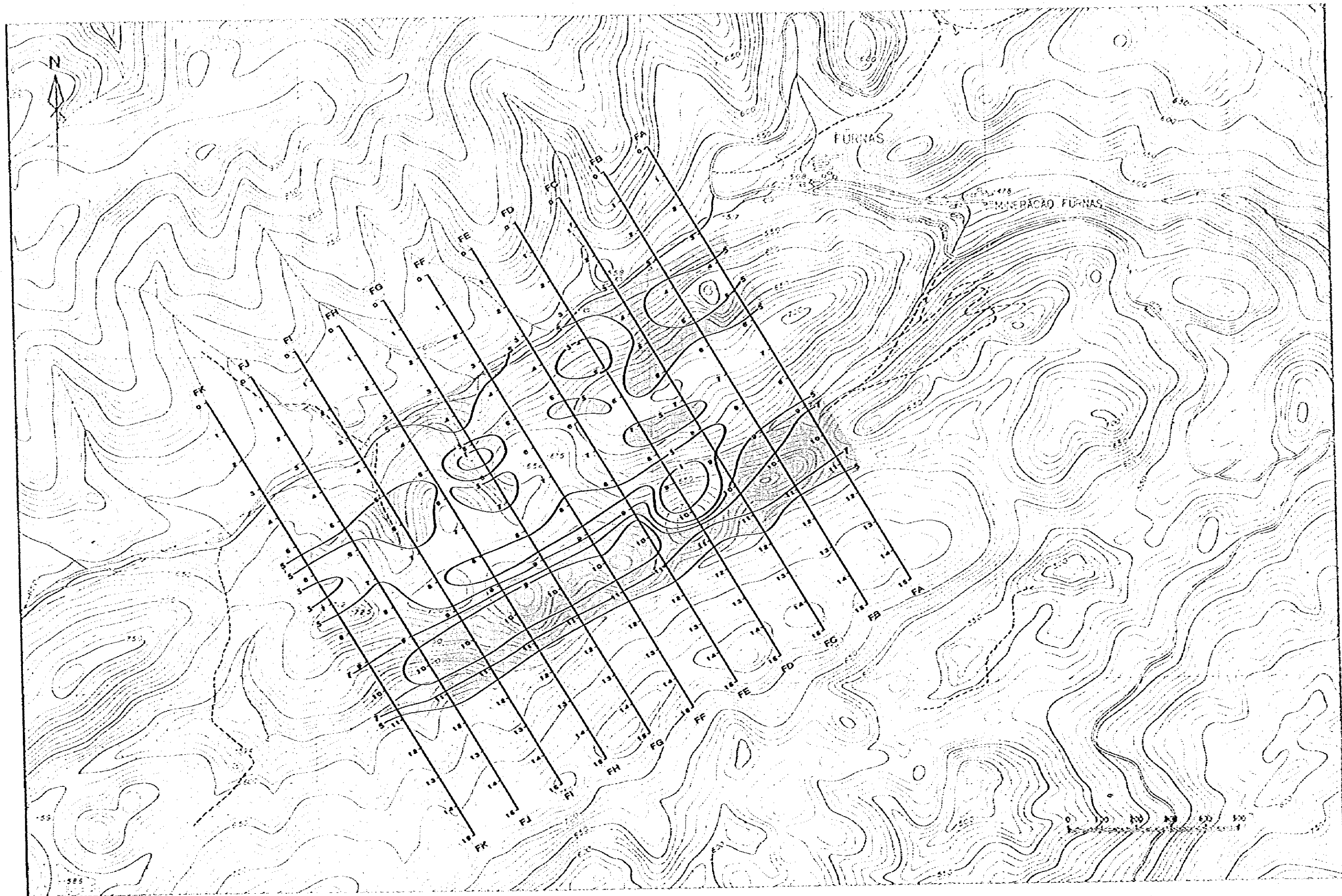


Fig. II-20-3 Plan Map of Percent Frequency Effect (N=5)